A KINETIC STUDY OF MEDIUM CONSISTENCY CHLORINATION

A Thesis Submitted By

Barbara J. Burns

B.S. 1981, University of Maine, Orono

M.S. 1986 Lawrence University

in partial fulfillment of the requirements for the degree of

Doctor of Philosophy from the

Institute of Paper Science and Technology

Atlanta, Georgia

March 1996

For my Dad,

who gave up his dream for his family.

ABSTRACT

As the technology of pulp bleaching has evolved, the pulp and paper industry is turning away from chlorine based bleaching agents. The driving force for this behavior has come from marketing and regulatory pressures to reduce or eliminate chlorine because of perceived long term effects of bleach plant effluents on the environment. To respond to the market place, the pulp and paper industry has increased its dependence on non-chlorine containing bleaching agents such as oxygen, ozone, and hydrogen peroxide. Both oxygen and ozone are gaseous reactants that have low solubility in water. Because of the low solubility, the mass transfer of oxygen and ozone into the pulp suspension is the most important step in their reaction with pulp fibers.

Because of equipment size and capital cost sensitivities, medium consistency (8-15%) solids processing of pulp is becoming the standard. In medium consistency systems, the volume of gas applied and its dispersion are important in determining the efficiency of the reaction. The mixing technology that has evolved to meet the demands of the trend utilizes a highly turbulent mixing zone to ensure complete commingling of the pulp and bleaching agent. Little information in the literature is available that describes the efficiency of mass transfer and its effect on the reaction rate for this technology.

In this thesis, the initial phase of pulp chlorination is used as a model system to determine the rate-limiting step for the gas-solid reaction. The chlorine-lignin system was chosen, because the reaction has been extensively studied in the past, and chlorine gas is highly soluble in water in

comparison to oxygen and ozone. For this thesis, a flow through, high shear medium consistency mixer was built and used to study the mass transfer of chlorine into three systems: an inert pulp suspension, inert pulp suspension with a fast liquid phase reaction, and an unbleached pulp suspension.

For the three systems, the inert pulp suspension had the lowest mass transfer coefficient while the liquid phase reaction had the highest (approximately twice that for the first case). The mass transfer coefficient for the solid phase reaction case was halfway between the other two. As expected , the chlorine application rate had the largest impact on the mass transfer coefficient, increasing the coefficient 4 times for the case with solid reaction when the chlorine application rate increased from 0.24% to 2.70% on pulp, 7 times for the case without reaction, and 16 times for the case with a fast liquid phase reaction.

The effect of the level of turbulence in the reactor on the mass transfer coefficient was only slightly greater than the effect of temperature. On average the mass transfer coefficient doubled over the rotor speed and temperature experimental range.

For the solid phase reaction case, the overall reaction rate constant was relatively insensitive to temperature indicating that the reaction rate was not the limiting step.

TABLE OF CONTENTS

TABLE OF CONTENTS CONT.

TABLE OF CONTENTS CONT.

LIST OF FIGURES

LIST OF FIGURES CONT.

LIST OF FIGURES CONT.

LIST OF TABLES

LIST OF TABLES CONT.

INTRODUCTION

After pulping, kraft pulp fibers can be bleached to full brightness in a multistage bleaching process. The bleaching process typically employs two types of bleaching agents in series to achieve the desired final pulp properties. In the first step of the bleaching process, the pulp is reacted with bleaching agents resulting in the depolymerization and removal of most of the residual kraft lignin. The bleaching agents generally used for delignification are oxygen, ozone, chlorine, and chlorine dioxide. In the second step of the bleaching process, the pulp is reacted with bleaching agents which destroy the remaining color bodies, thus brightening the pulp. The most common brightening agents are chlorine dioxide, sodium hypochlorite, and hydrogen peroxide.

Removal of lignin from the fiber occurs in two phases. In the rapid first phase, the bulk of the bleaching agent is consumed by the residual kraft lignin. This rapid phase is followed by a slow phase in which the remaining bleaching agent is consumed. The typical consumption of bleaching agent as a function of reaction time is shown in Figure 1 (1). Although this example is for chlorination, curves of similar shape are seen for the reactions of lignin in oxygen, ozone, and chlorine dioxide systems. Of the three gaseous delignifying agents, chlorine has been the most extensively studied and will be used as the representative delignification system in the ensuing discussion.

The steep slope of the initial part of the curve in Figure 1 indicates that the initial mixing of chlorine in the pulp suspension is extremely important to the chlorination process. Rydholm (2) has stated that

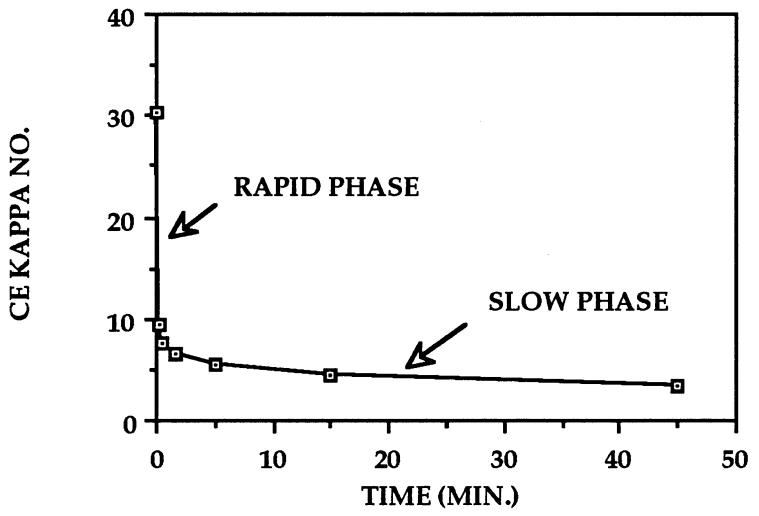

Figure 1. Consumption of chlorine as a function of time (1).

"because of the rapid reaction, instantaneous uniform distribution of chlorine is necessary to avoid over-chlorination of some parts of the pulp and insufficient chlorination of the remainder." In a well-mixed chlorination system, fine chlorine gas bubbles are uniformly dispersed in the pulp-water suspension. In a poorly-mixed system, the gas dispersion in the pulp-water suspension can be nonuniform which can lead to a nonuniform reaction with lignin.

In a low consistency system, the chlorine gas can dissolve in the liquid phase quickly, since there is enough water in the pulp suspension to dissolve the applied chlorine gas (3). The dispersion of chlorine in fiber-water suspensions resulting from conventional mixing techniques (such as static or peg mixers) usually gives good bulk or large scale mixing. More recently, the use of high shear mixers has resulted in good local or small scale mixing (4).

During the reaction period, variations in bulk chlorine concentration decrease as the chlorine molecules diffuse from regions of high chlorine concentration to regions deficient in chlorine. The rate of diffusion of the chlorine molecule is consistency dependent, but for low consistency systems it can be as high as one centimeter per hour (5).

As the consistency of the system increases, the reaction proceeds at a faster rate for a given chlorine charge. The reaction time required for low consistency systems is typically 60 minutes of retention time while that for medium consistency is typically 15 minutes at 30 °C. The faster reaction rate for the medium consistency system is probably due to the higher chlorine concentration in the bulk fluid, and the shorter diffusion distances for the chlorine as compared to the low consistency system. The higher chlorine concentration results in a larger driving force for both the reaction rate and diffusion rate. (The mass of water in a 4% consistency system is 3.3 times larger than that for a 12% consistency system. Assuming that all the applied chlorine can dissolve in the liquid phase, the resulting chlorine concentration at a constant chlorine charge is 3.3 times greater for the medium consistency system than that for the low consistency system.)

Even though the reaction rate increases with increasing consistency, other physical properties of the system decrease as a function of consistency. One such property is the diffusion coefficient of the chlorine in the fiber-water system. The diffusivity of chlorine at medium consistencies drops to approximately one third of its value at low consistencies (5).

As the consistency of the system increases, the gas phase remains in the system for a longer period of time, because the mass of applied gas is

greater than the solubility capacity of the free water in the system (3). Free water is defined as the water in the system that is not contained in either the lumen or the fiber wall.

If the initial dispersion of the gas into the pulp suspension is poor, the bubbles which do not initially dissolve in the liquid phase may coalesce into larger bubbles before they are consumed. As the bubble size increases, the mass transfer rate of chlorine into the liquid phase decreases because of the reduction in interfacial area.

At medium consistencies, 8 - 15%, conventional mixing technologies usually result in poor mixing. In cases where the bulk mixing is considered good, the local chlorine concentration can vary by as much as ±40% (4).

For low consistency systems, chlorine concentration gradients within a five millimeter radius of a point in the system will be evened out during the 60 minute reaction time. For a medium consistency system, concentration gradients within a 0.4 millimeter radius will be evened out during the 15 minute reaction time. Assuming that these radii are indicative of the scale of mixing required for a uniform reaction in the system, the scale of mixing required for the medium consistency system is 12.5 times smaller than that required for the low consistency system (5).

To achieve the uniformity of chemical concentration required by medium consistency pulps to consume lignin uniformly, a change in mixing technology was required. The new technology was developed by Gullichsen (6). This mixing technology used an intense shear field to disrupt the fiber

network into small pulp flocs. When bleaching chemicals are added to the pulp suspension, they were quickly mixed with the fiber suspension.

It is anticipated that both the nature and the intensity of the shear field will affect the dissolution rate of gaseous species into pulp-water suspensions, and ultimately the subsequent reaction with lignin. As the industry gravitates more and more toward medium consistency systems utilizing high shear mixing technology, the question of how the performance of these mixers affects the transfer of gas into the liquid phase and the subsequent desired reactions arises. When a gas is introduced into a system where it can react with either the liquid phase or the solid phase, it must travel from the gaseous phase to a reaction site. In doing so, several processes must occur in series, such as diffusion of the gas from the bulk gas phase to the liquid interface, crossing the liquid interface, and diffusing to a reaction site. Since these processes occur in series, the slowest step will control the overall process. The objective of this thesis is to determine the rate-limiting step for the initial phase of pulp chlorination when chlorine is introduced to the system as a gas.

BACKGROUND

MIXING TECHNOLOGY

Danckwerts (7) defined mixing as a process which breaks an additive into "blobs" which are uniformly distributed throughout the mixture. Once the "blobs" are distributed (macroscale uniformity), the diffusion process completes the mass transfer process to yield molecular scale uniformity throughout the mixture. The objective of convective mixing is to maximize "blob" surface areas, and to minimize the distance between regions of high additive concentration to reduce the amount of diffusion required for molecular uniformity. Convective mixing increases the opportunity for diffusion to occur, while it reduces the distance that the additive must traverse to obtain molecular uniformity.

For a 2% consistency system, Liebergott et al. (8) investigated the effect of degree of mixing intensity on pulp chlorination. In their experiments, the pulp and chlorine were initially mixed followed by either zero mixing, gentle agitation created by rolling the reaction vessel, or vigorous agitation created by a single shaft, dual turbine impeller. Except for the case of zero mixing, they did not investigate mixing times shorter than 30 seconds. They concluded that increasing the agitation beyond the level necessary to initially disperse the reactants uniformly throughout the pulp mixture would not result in a higher conversion of lignin as shown by the decrease in chlorinated-extracted lignin content as a function of time in Figure 2.

In the absence of mixing or with short mixing times, the

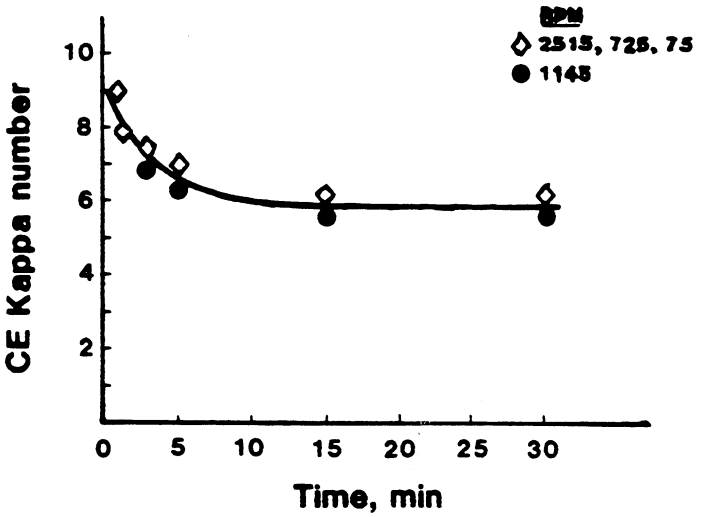

Figure 2. The effect of mixing intensity on the extent of chlorination for a low consistency pulp (8).

chlorine did not diffuse far enough to ensure uniform reaction in the time available. However, when the chlorine was uniformly distributed, the effect of the diffusion rate was minimized.

In another mixing study, Reeve and Earl (9) studied the effect of high shear mixing on the relative efficiencies of chlorinating low and medium consistency pulps. In the experiment, they used a batch, laboratory, high shear mixer. For the low consistency pulp system, chlorine was added to

the pulp suspension as a solution. For the medium consistency pulp system, chlorine gas was added to the pulp suspension. In the experiment, Reeve and Earl (9) found that an increase in consistency from 3 to 10% resulted in a decrease in chlorinated-extracted lignin content as shown in Figure 3. The increase in the delignification efficiency was probably due to the higher chlorine concentration in the liquid phase for the medium consistency pulp at a constant chlorine charge. For all levels of applied chlorine, the use of the batch mixer resulted in a lower chlorinated-extracted Kappa number than that for the hand-mixed samples.

Reeve and Earl (9) also measured the efficiency of mixing in the batch, high shear mixer by spiking a sample of bleached pulp with several dyed fiber flocs. To determine the extent of floc break-up, the number of intact fiber flocs at the end of the mixing period was compared to the initial number of flocs. They observed that after five seconds of intense mixing, some of the dyed flocs were not completely disrupted. The diameter of the intact dyed flocs was reduced on average from 3 millimeters to 1 millimeter during the mixing period. Since many of the dyed fibers were incorporated into undyed flocs, it was probable that during the intense mixing, small flocs move past one another and in passing exchange loose fibers.

The amount of mixing which is required to get the highest reaction efficiency is dependent on the ratio of chemical reaction rate to the mixing rate. If the chemical reaction rate is significantly slower than the mixing rate, then the system will become homogeneous in reactant concentration before the chemical reaction has proceeded to a great extent. For this case, the overall bleaching rate is controlled by the effective reaction rate, and a further increase in the mixing rate beyond that required for the initial

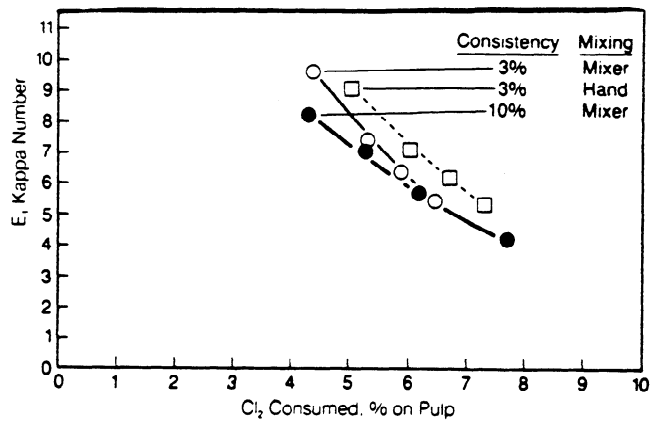

Figure 3. Chlorinated-extracted Kappa number as a function of applied chlorine and mixing intensity (9).

dispersion would not improve the pulp bleaching. Oxygen delignification in static, and high shear mixers appears to fall in this category (10).

For the case where the reaction rate and the mixing rate are about the same, both phenomena determine the observed reaction rate, and final pulp quality. Thus if the mixing rate increases so that the mixing rate becomes insignificant, this case becomes similar to the reaction rate limited case (10).

For the case where the reaction proceeds much faster than the mixing rate, the efficiency of pulp bleaching is determined by the mixing rate. In this case, a faster mixing rate would improve the pulp bleaching.

Chlorination and ozonation fall into this category. Because of the dependence of the overall reaction rate on mixing, technological improvements in mixing can improve the final pulp quality (9, 10, 11).

FIBROUS SUSPENSION RHEOLOGY

Pulp fiber-water systems are unique, because the fibers can interact with one another to form coherent networks (12). The strength of the network is the sum of four types of forces (13):

Colloidal - the electrostatic and electrokinetic forces that exist among small particles and are highly dependent on the distance between adjoining fibers.

Mechanical Surface Linkage - a hooking force caused by mechanical entanglement and dependent on the fiber surface fibrillation, fiber "crookedness", and fiber stiffness. It is a function of the frictional resistance to a shear force applied to disentangle two entangled fibers. (See Figure 4.)

Elastic Fiber Bending - this force is the cohesive force between fibers caused by a normal force applied at contact points. The normal forces arise when bent elastic fibers are restrained from straightening as a result of contact with other fibers. (See Figure 5.)

Surface Tension - bubbles of undissolved gas at fiber interstices produce cohesive forces due to surface tension.

At low consistencies, the most important forces holding the network together are mechanical surface linkage, and elastic fiber bending. The shear strength of the network has been measured by many researchers and can be estimated as a function of consistency using the power law (13):

$$\tau_s = a\, C_m^{\,b} \qquad (1)$$

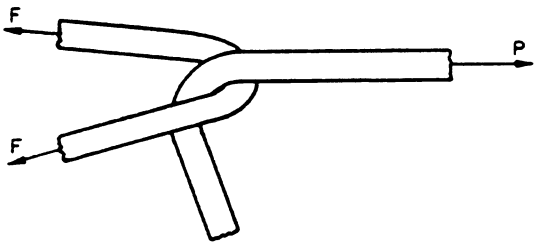

Figure 4. The mechanical surface linkage forces between fibers in a fiber network (13).

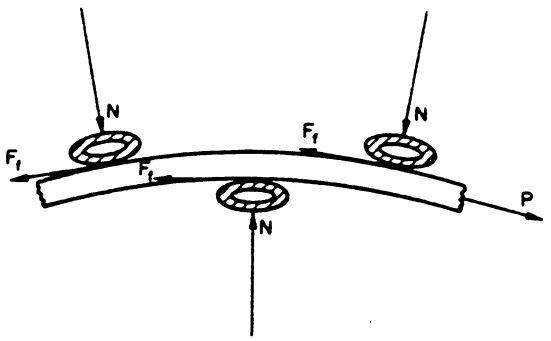

Figure 5. Elastic fiber bending forces on fibers in a fibrous network (13).

where τ_s is the disruptive shear stress (Pa),

C_m is the pulp consistency (%), and

a, b are empirically derived constants which are dependent on pulp species, and type (kraft, mechanical or sulfite). For bleached pine kraft pulp, these parameters, a and b, are 27 and 2.0, respectively (14).

As the consistency increases into the medium consistency range, a large amount of air may be present in the suspension. The fractional volume of air, the void ratio, ε, can vary considerably depending on the process used to produce the fiber concentration (such as vacuum dewatering versus pressing). For example a 19% consistency suspension can have a void ratio between 6 and 35% (13). Because of the gas phase, the suspension is no longer a continuous network. The strength of the network due to elastic fiber bending is increased due to surface tension forces around the air pockets (13). Because of the gas phase, the suspension becomes compressible, and pumping energy is expended compressing the gas phase before momentum can be transferred through the pulp network (13). Thus as the amount of gas in the pulp suspension increases, the efficiency of pumping decreases, and the wall shear stress decreases at the same time (13).

Gullichsen et al. (6), using a modified viscometer, measured the disruptive shear stress for a medium consistency pulp. They combined the medium consistency data with similar data published by Duffy et al. (14) to generate Figure 6. There was surprisingly good agreement between the two data sets considering that the data were generated using different pieces of equipment and techniques. The agreement between the data sets suggested that the same mechanism may govern the response of pulp networks to shear

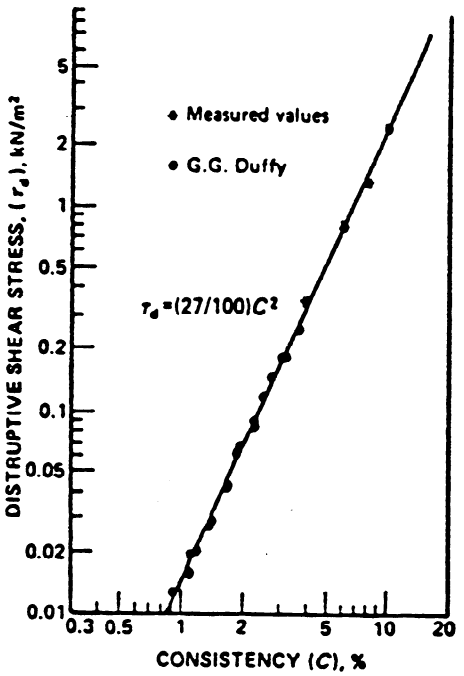

Figure 6. Disruptive shear stress as a function of rotational speed for low and medium consistency pulps (6).

forces in the 0.9 to 10% consistency range. Assuming that low and medium consistency pulp suspensions respond to shear in the same manner, Equation 1 can also be used to estimate the disruptive shear stress for medium consistency pulps. At ten percent consistency, the resulting disruptive shear stress was 2700 N m^{-2}. This value was similar to that calculated from the network's power dissipation capacity, Equation 2 (12).

$$\tau_d = (\varepsilon / \mu_{20})^{0.5} \qquad (2)$$

where τ_d is the power dissipation capacity of the pulp suspension, (s^{-1})

μ_{20} is the viscosity of water at 20 °C, (kg $m^{-1}s^{-1}$), and

ε is the power dissipation / unit volume (5×10^9 W m^{-3}) (12) for ten percent consistency pulp. From Equation 2, the disruptive shear stress was 2240 N m^{-2}.

FIBROUS SUSPENSION MASS TRANSFER

When a solid is contained by a liquid phase, the transport properties may be dramatically different from those of the liquid phase alone. In an agitated system, the mass transfer coefficient has been shown to decrease with increasing solids content (15). Mills et al. (15) used a baffled cylindrical vessel, shown in Figure 7, to suspend glass beads while air was introduced into the vessel through a ring sparger. The dissolved oxygen content was measured throughout the experiment. In this system, the measured effect of increasing the solids concentration from zero volume percent to forty volume percent was a reduction in the mass transfer coefficient to about 60% of its initial value.

In a stationary fibrous suspension, the mass transfer coefficient has been shown to increase with increasing solids content (16). Hsu (16) measured the mass transfer coefficient of oxygen into a stationary fiber bed as shown in Figure 8. Using this apparatus, he measured a four fold increase in the mass transfer coefficient when the solids content was increased from zero percent to nineteen percent consistency.

Mill's (15) and Hsu's (16) results indicate that the amount of solid phase in the system impacts on the mass transfer coefficient for a three phase system. Even though the observed effects of the solid phase were dramatically different, both indicate that the solid phase concentration could greatly impact on mass transfer measurements.

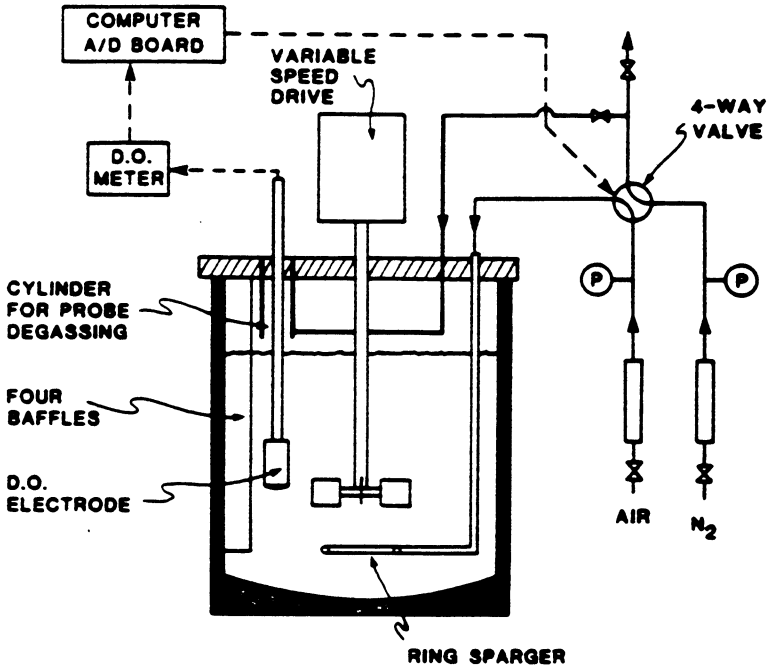

Figure 7. Gas absorption chamber for the absorption of oxygen into water containing spherical glass beads (15).

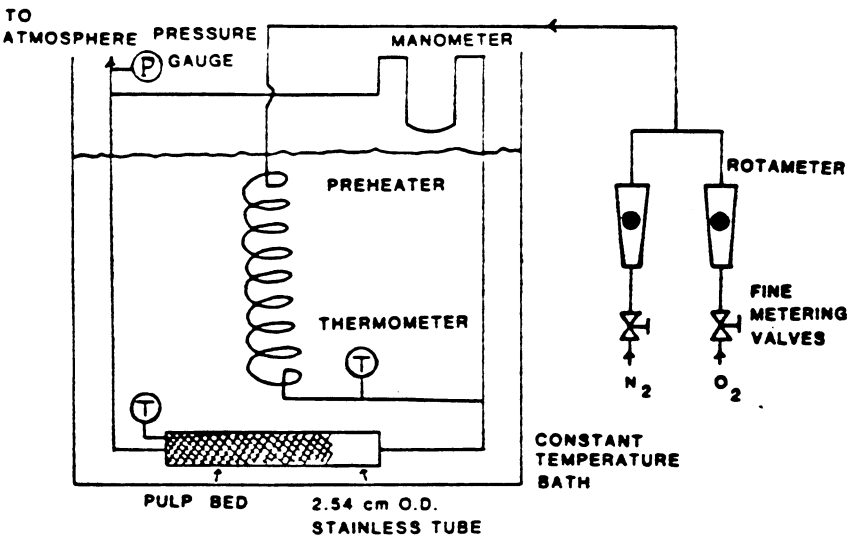

Figure 8. Apparatus used to measure the mass transfer coefficient of oxygen into a pulp suspension (16).

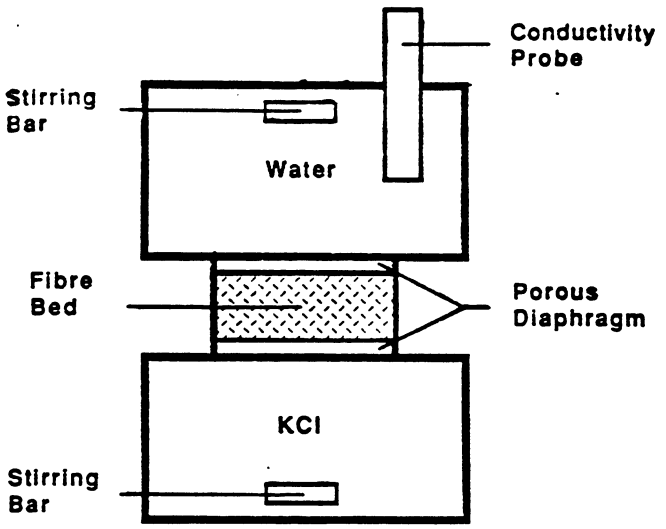

Figure 9. The double diaphragm cell used to measure the effective diffusivity of potassium chloride through pulp suspensions (18).

The presence of fibers in a suspension has also been shown to influence the diffusion rate of chlorine. Wong and Reeve (17) studied the diffusion rates in fiber beds of a non-reactive diffusing species using the double diaphragm cell apparatus shown in Figure 9. For potassium chloride, the effective diffusivity decreased linearly with increasing pulp consistency. (The effective diffusivity is the apparent diffusivity of a material that is diffusing through a porous material.) The effective diffusivity decreased by 37% as the consistency increased from 0 to 12% (which is approximately proportional to the reduction in the liquid phase available for KCl diffusion

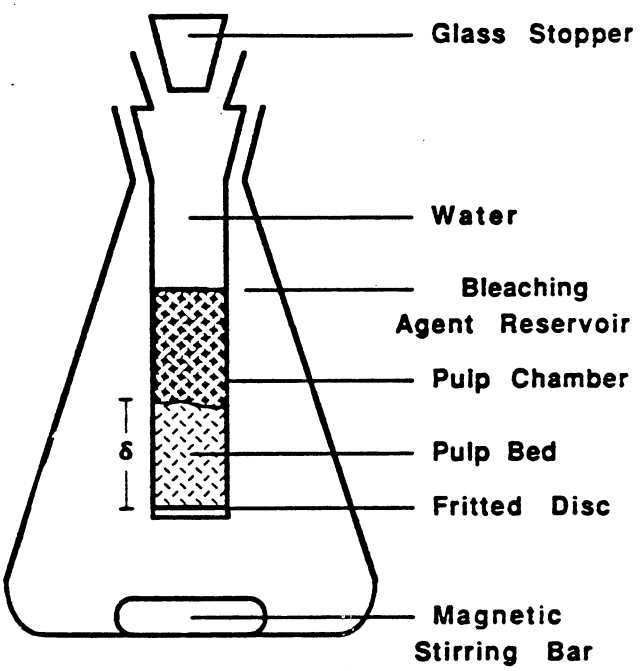

Figure 10. Diffusion apparatus used to measure the effective diffusivity of reacting chlorine through a pulp suspension (18).

assuming that the water bound by the fiber and that in the lumen is unavailable for diffusion).

The rate at which reacting species, such as chlorine and chlorine dioxide, diffuse through a stationary pulp bed was measured by Paterson and Kerekes (5); and Wong and Reeve (18). They measured the distance that reacting chlorine diffused through a pulp suspension as a function of time (in the apparatus shown in Figure 10). For simplification, Paterson and Kerekes (5) assumed 1) that the reaction between chlorine and pulp occurred only at

the diffusion front, and 2) that the reaction between chlorine and unbleached pulp was fast in comparison to the rate of diffusion. For the mathematical treatment, the resulting diffusion boundary became a well-defined reaction front. The distance that the chlorine diffused into the pulp mat was assumed to be analogous to the tarnish thickness growth resulting from a reaction between a gas and a metal surface as shown by Danckwerts (19). The tarnishing reaction is an unsteady state diffusion process with a moving boundary, and is defined by (19):

$$D_1 \frac{\partial^2 C_1}{\partial z^2} = \frac{\partial C_1}{\partial t} \qquad (3)$$

By applying a mass balance at the tarnish/metal interface, the following equation was obtained:

$$\rho\omega \frac{\partial x_1}{\partial t} = - D_1 \frac{\partial C_1}{\partial z} \qquad (4)$$

where C_1 was the concentration of gas at the metal surface, (kg m^{-3})

D_1 was the diffusion coefficient of the reacting gas, (m^2 s^{-1})

ω was the mass fraction of gaseous component in the tarnish,(dimensionless)

ρ was the bulk density of the tarnish, (kg m^{-3})

x_1 was the tarnish thickness and a function of time, (m)

t was the time, (s) and

z was the distance from the outer surface of the tarnish, (m).

The z coordinate was defined as z = 0 at the outer surface of the tarnish and z = x_1 at the metal surface.

Solving the two partial differential equations gives:

$$\frac{C_1^0}{\rho\omega} = (\pi)^{0.5}\,\alpha\exp\left(\alpha^2\right)\mathrm{erf}(\alpha) \qquad (5)$$

$$x_1 = 2\alpha\left(D_1\,t\right)^{0.5} \qquad (6)$$

where C_1^0 was the concentration of reacting gas at the outer surface of the tarnish, (kg m^{-3}) and

α was an intermediate variable and was a function of C_1^0 (dimensionless).

Paterson and Kerekes (5) used this model to predict the distance that a chlorine-lignin reaction front would travel in a pulp bed. (In their model derivation, the variable x_1 was replaced by the variable δ.) The tarnishing model predicted the diffusion front distances fairly well for low consistencies, but over estimated the diffusion distance for medium consistency pulps.

Wong and Reeve (18) repeated the work of Paterson and Kerekes using the apparatus shown in Figure 10. One difference in the two apparati was the fritted disk placed at the bottom of the pulp column in Wong and Reeve's equipment. Wong and Reeve also used the tarnishing model to treat their data. However, they modified the final equation to include the change in chlorine concentration across the fritted disk and to compensate for the consumption of chlorine by reactive species behind the diffusion front.

Figure 11 shows the difference between the predicted chlorine diffusion distance using the Kerekes (5) relationship and the experimental diffusion distance. One explanation for the difference between the theoretical

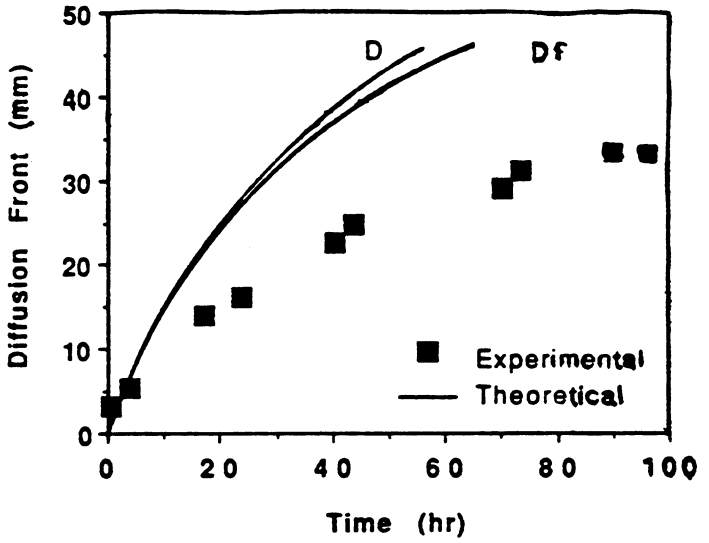

Figure 11. Prediction of the distance that a diffusion front of reacting chlorine will travel using the tarnishing model (18).

and the experimental diffusion distances is the consumption of chlorine by the pulp behind the diffusion front even though no additional bleaching takes place. When the tarnishing model is corrected for the consumption of chlorine behind the diffusion front, the theoretical curve falls on top of the measured diffusion distances as shown in Figure 12 (Wong and Reeve's relationship (18)).

In an agitated system, convective diffusion can enhance the diffusion between fiber flocs, whereas diffusion of chlorine within a pulp floc will follow the behavior of chlorine diffusing in a fiber bed. Note that the

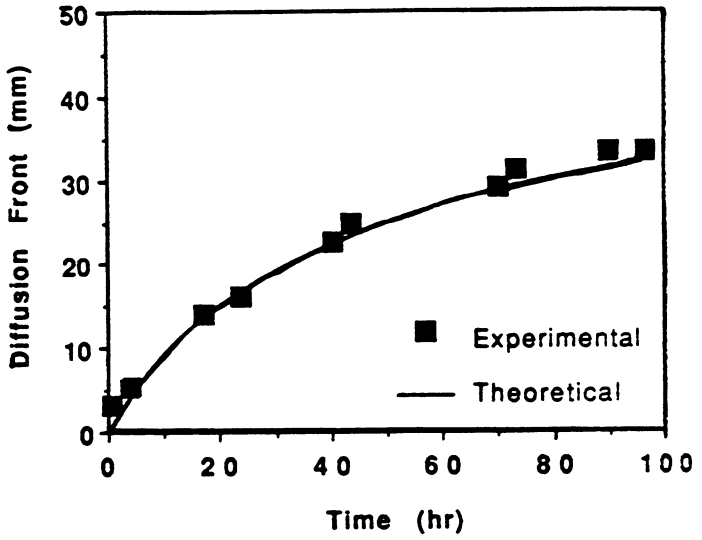

Figure 12. Prediction of the distance that a diffusion front of reacting chlorine will travel using the tarnishing model corrected for reaction behind the diffusion front (18).

fiber concentration in a given floc will be higher than that of the bulk suspension. Thus diffusion within the floc could be slower than that predicted based on the bulk consistency.

For a three-phase system and typical bleaching conditions, it is possible that a volume of gas remains in a pulp suspension after the mixing has stopped. Annau (20) measured the dissolution rate of isolated chlorine bubbles in stagnant pulp suspensions. He found that approximately one minute was required for a chlorine bubble 1.7 mm in diameter to dissolve.

Bennington et al. (21) measured the dissolution rate of 2 µl chlorine bubbles held in the interstices of unbleached kraft suspensions under stagnant conditions. Slow-speed cinematography was used to follow the

bubble dissolution. They found that the bubble initially underwent rapid dissolution followed by a slower dissolution rate. At the end of the experiment, there remained a bubble of finite volume even though theory predicted that all the chlorine should dissolve in the solution. They proposed that the final bubble was comprised of oxygen and nitrogen which had counter diffused from the liquid phase to the bubble.

CHLORINATION CHEMISTRY

Various aspects of pulp chlorination have been extensively studied, but the reaction kinetics of the system are still not completely understood. There are two predominant theories regarding the phenomena which control the reaction. The first theory proposes that the reaction is limited chemically. The ultimate conversion of lignin is determined by the initial structure of lignin, and the reaction rate of chlorine with the different lignin structural elements. In the second theory, a physical barrier prevents the chlorine atoms from reaching potential reaction sites and/or prevents the resulting chlorinated lignin from leaving the fiber wall. Several physical factors which have been suggested as potential rate-limiting factors include the accessibility of the lignin in the fiber wall, the chlorine diffusion rate in the system, the chlorinated products diffusion rates, and the bulk fluid's chlorine concentration profile.

Studies of the reaction of chlorine with lignin model compounds have identified certain reaction types which provide a basis for interpreting the complex behavior of kraft pulp residual lignin (22). These reactions, shown in Figure 13, are divided into three types: aromatic substitution, electrophillic displacement, and oxidation.

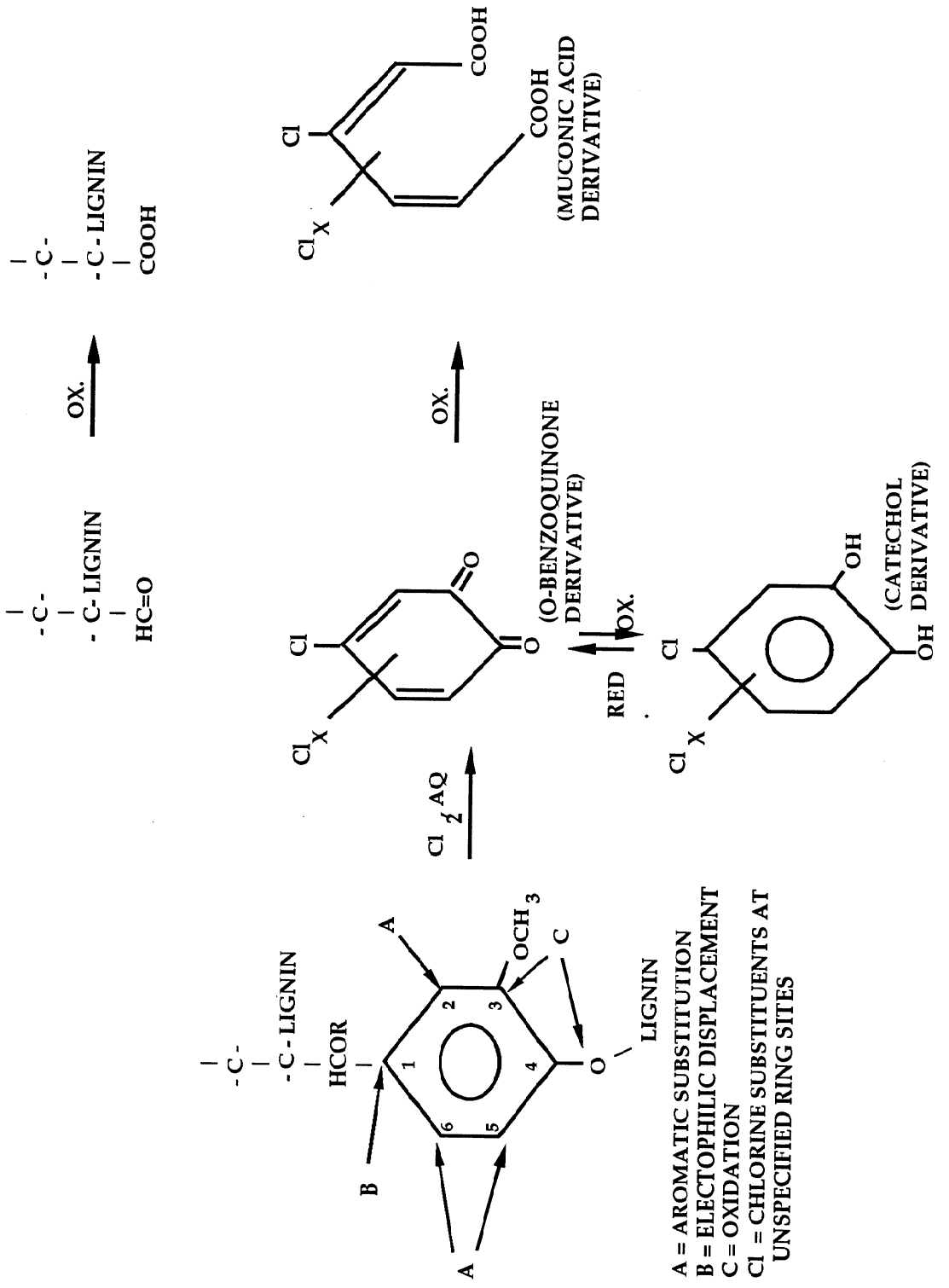

Figure 13. Reaction pathways for the reaction of chlorine and lignin model compounds (22).

Substitution of chlorine onto the aromatic ring occurs very quickly. The pattern and extent of this reaction determine the course of the subsequent reactions in the chlorination stage, as well as in the subsequent caustic extraction stage. A major factor in the resultant substitution pattern and extent of reaction is the amount of applied chlorine (23).

Other factors that affect the substitution pattern include the nature, number, and ring position of other aromatic ring substituents. For condensed guaiacyl units, there are normally three substitution sites available (23). In model compound studies, the average number of chloro-substituents usually does not exceed two chlorine atoms per phenolic nucleus due to competing oxidation reactions. The success of the oxidation reactions in model compounds may be due to the chlorine atoms greater accessibility to the model compound in a single phase system than in the solid phase reaction. In a study of residual kraft lignin, the number of chlorine atoms per C-nine unit was reported as high as 3.9, indicating that cleavage of the propyl side chain may occur, making another site available for substitution (24).

In the case of mono-substitution on a phenolic ring, chlorine exhibits a reaction site preference. The carbon at the sixth ring position is the most reactive, followed by those at the five and two positions, respectively (24). The five carbon position may be deactivated with respect to substitution if the phenolic hydroxyl is etherified.

If the alpha carbon on the propyl side chain is substituted with an alcohol group, the side chain can be electrophilically displaced as an aldehyde by a chlorine atom. This reaction, which is technically a substitution

reaction, increases the maximum number of possible substitution sites on a given C-nine unit to four (23, 24).

The most important oxidation reaction is the breakage of the interunitary ether linkage at the aromatic ring's four position. The resulting o-benzoquinoid structures are further oxidized to dicarboxylic acid fragments. Probably the most prevalent oxidation reaction is cleavage of methoxyl groups to form methanol. It has been postulated by Ni (24) that cleavage of the methoxyl group must precede oxidation of the softwood lignin macromolecule. Ni also postulated that substitution of chlorine onto the aromatic ring inhibits the demethylation reaction. Sarkanen (25) reported that demethylation of model compounds was inhibited when the positions ortho to the methoxyl group are occupied by substituents other than hydrogen. The inhibition appeared to be absent when one of the ortho substituents was a phenolic hydroxyl group. Thus if an ortho substituent was a chlorine atom, then the oxidation of the lignin molecule was inhibited.

Even though chlorine reacts selectively with lignin, carbohydrate attack does occur. The carbohydrate attack is not extensive, but can be significant, as evidenced by the accompanying decrease in pulp viscosity (22). The degradation of the carbohydrate produces chemical modifications in the cellulose chain seen as increases in the carbonyl and carboxyl content in the carbohydrate fraction of the pulp. Chlorine can also attack the glycosidic linkages of the cellulose chain which results in cleavage of the chain and the formation of aldose and aldonic acid end groups. The random glycosidic bond cleavage is responsible for the viscosity loss.

Other reactions of chlorine with the carbohydrate fraction include the oxidation of primary and secondary alcohol groups to aldehydes and keto groups (22). It is thought that free radical processes predominate in the reaction of chlorine with cellulose, since a reduction in the amount of carbohydrate degradation has been observed when a free radical scavenger is added to the system (22, 26).

Another factor that may influence subsequent reaction pathways is the diffusion rate of chlorinated lignin fragments out of the fiber. Presence of chlorolignin products near or at the reaction site may hinder further reaction by inhibiting the diffusion of chlorine to a potential reaction site (27). Grangaard (27) proposed that this may influence chlorination as he observed that chlorinated pulps extracted with mercerizing strength caustic showed the greatest lignin removal of all pulps he studied. (Soaking a pulp in caustic swells the fiber, and increases the diameter of the pores which allows the diffusion of large chlorolignin molecules out of the fiber. Mercerizing strength caustic causes the fiber to swell to its maximum size.)

In softwood kraft spent bleach liquors, characterized by Lindstrom (28, 29, 30), eighty percent of the chlorine-lignin reaction products were alkali soluble. Of the twenty percent acid labile compounds, ultrafiltration studies have indicated that only twenty percent (four percent of the total) of the chlorinated products are of molecular weight greater than 10,000. The molecular weight distributions, as determined by ultrafiltration, for both stages are shown in Figure 14. Since the product removal rate was not determined, its effect on the intrafiber chlorine diffusion rate cannot be predicted. Removal of the chlorinated lignin fragments by a caustic extraction

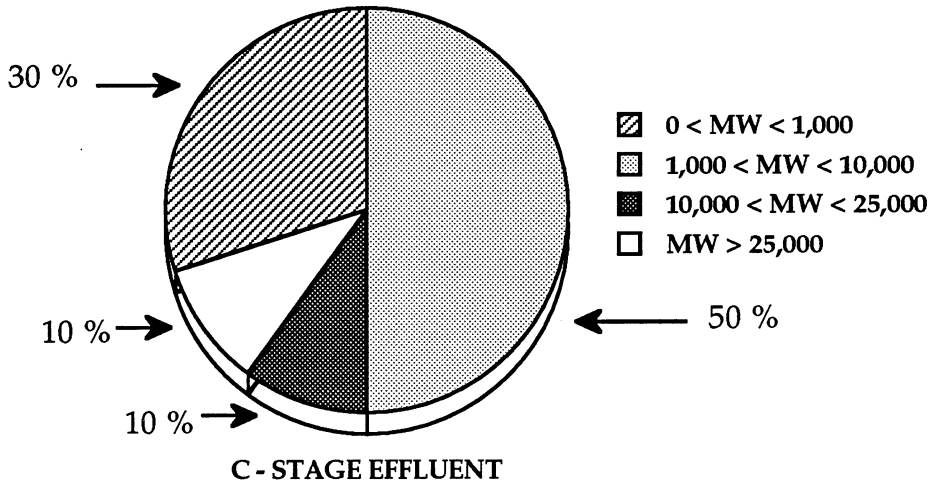

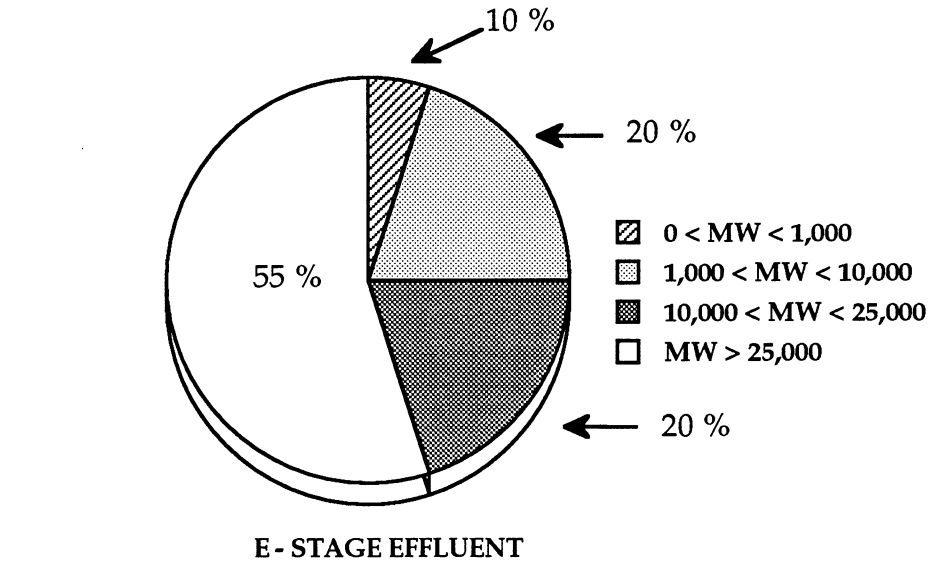

Figure 14. Molecular weight distribution of acid and alkali soluble chlorolignin fragments (28, 29, 30).

restores the initial steep chlorination rate shown in Figure 1 (1).

Goring (31) presented a model predicting the diffusion of lignin fragments from the fiber wall. To adequately model his data, he assumed a polydispersed system whereby each fragment group had its own diffusion coefficient. The estimated diffusion coefficients of the lignin fragments ranged from 1×10^{-7} to 8×10^{-20} m^2sec^{-1}. For comparison, the diffusion coefficient of chlorine in water is 1.48×10^{-9} m^2sec^{-1}, and can diffuse a distance of 3 to 5 mm in one hour in a 3% consistency suspension (5). Over long periods of time it is conceivable that the diffusion of some of these macromolecules out of the fiber may hinder chlorine diffusion into the fiber.

The amount of chlorine consumed by substitution and oxidation reactions as a function of applied chlorine is shown in Figure 15 (27). In the range of applied chlorine from 3 to 12% chlorine on pulp, the amount of chlorine consumed by substitution reactions goes through a maximum at approximately 6% chlorine on pulp. In the same range, the amount of chlorine consumed by oxidation reactions continually increases.

The effect of temperature is most significant on the oxidation reaction, as shown in Figure 16 (27). In the temperature range of 0 to 25 °C, the amount of chlorine consumed by oxidation reactions almost doubles in the first 60 minutes of the reaction. For the same pulp and temperature range, the amount of chlorine consumed by substitution reactions is essentially constant (27, 31).

During chlorination, the total lignin removed is limited by an unknown factor. The amount of lignin that cannot be removed during

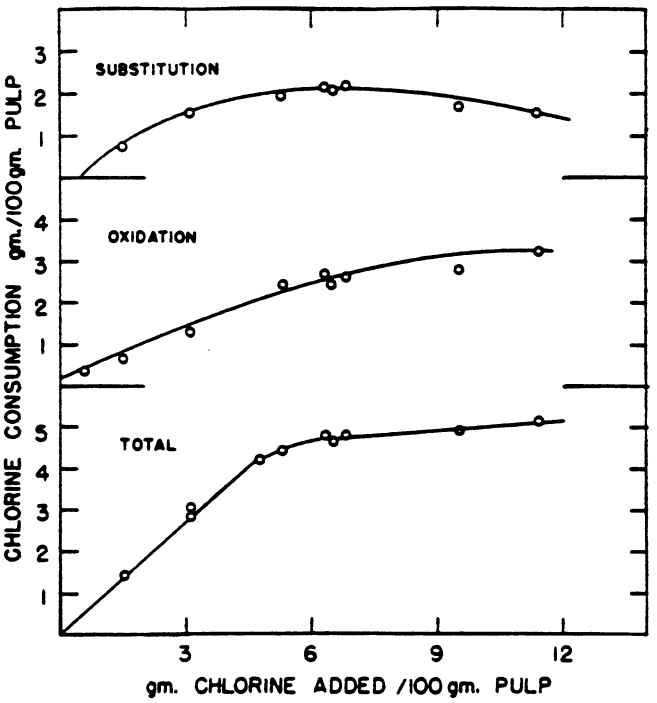

Figure 15. Total chlorine consumption, consumption by oxidation, and consumption by substitution versus amount of chlorine added to system (27).

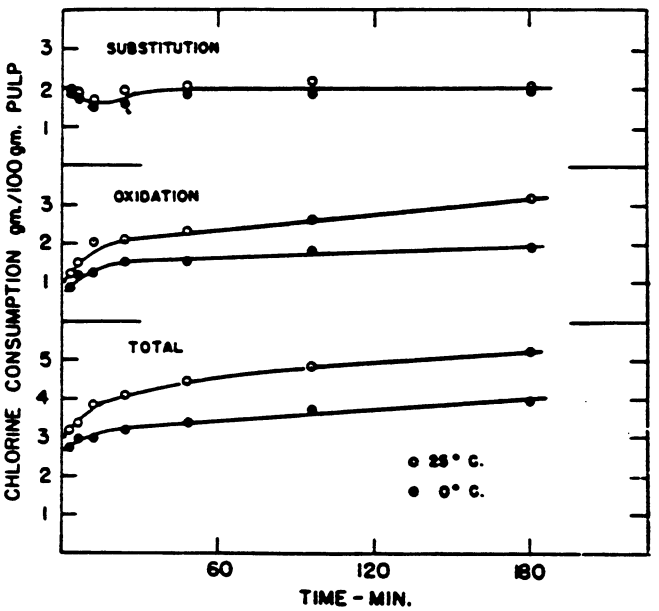

Figure 16. Effect of temperature on chlorine consumption of a balsam sulfite pulp (27).

chlorination is commonly referred to as the floor level of lignin. It has been proposed that this limit is due to complete reaction of chlorine with the accessible lignin (31, 32, 33). Kuang (34), using electron microscopy, determined that the topochemical distribution of chlorine in chlorinated kraft pulp fibers was similar to that of residual lignin. This indicated that within the resolution of their technique, all the lignin molecules were accessible to chlorine. However, there may have been some sub-microscopic domains that were inaccessible.

Pugliese (35) also measured the distribution of chlorine atoms within the fiber wall at various chlorine water exposure times. In the experiment, he exposed chlorine fibers to a quiescent chlorine solution for 0, 10, and 30 seconds. The movement of chlorine within the cell wall was stopped by cooling the fibers at the end of the desired exposure time. Using a STEM-EDS microscope technique, he determined that after ten seconds of immersion there was a statistically significant chlorine concentration gradient from the exterior of the fiber wall to the lumen. The concentration gradient became flat after 30 seconds (see Figure 17).

Kuang's (34) findings described above give some credence to the "blocking group" theory proposed by Berry et al. (1, 36, 37). They postulated that alkali labile "blocking groups" were formed during chlorination, and that these groups prevented the reaction of the remaining lignin from reacting with chlorine at appreciable rates. These authors postulated that the fast initial chlorination rate was able to be restored by either hot alkali or hot water treatment which remove the blocking groups. This theory was supported by the work by Ni (24) who proposed that the blocking group was

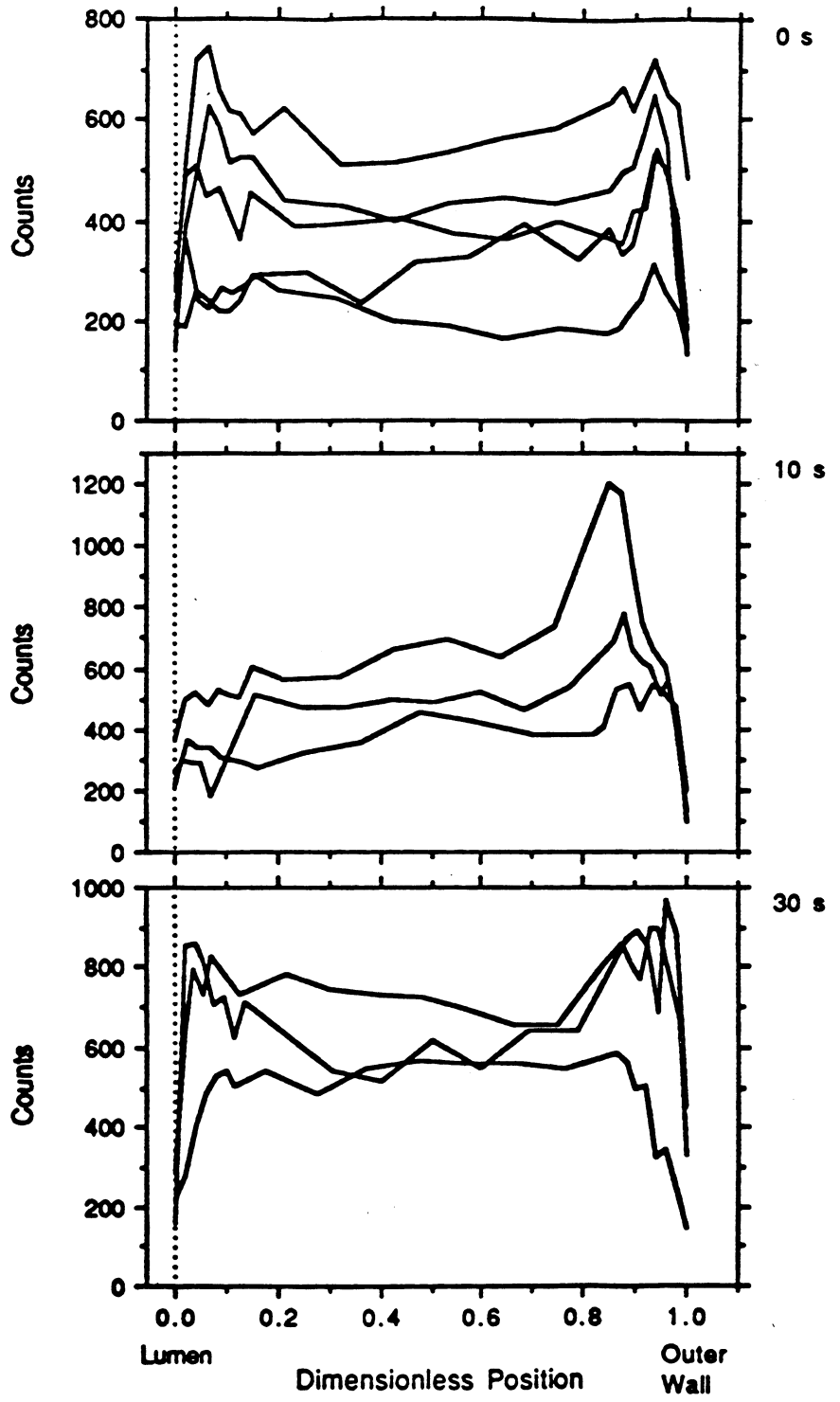

Figure 17. Chlorine concentration in a fiber wall as a function of position within the cell wall and time of exposure to a chlorine solution (35).

the tri-chlorinated guaiacyl nucleus. The blocking behavior of tri-chlorinated compounds had also been seen by Sarkanen (25). In model compound studies, Sarkanen observed that methoxyl group removal was inhibited by the presence of a chlorine atom ortho to the methoxyl group.

For syringyl nuclei, Ni (24) postulated that demethylation suppression did not occur with increasing substitution. In the syringyl reaction, the chlorine atom was able to break the phenoxy ether bond prior to demethylation (the reverse sequence of the reaction with guaiacyl nuclei). Thus the presence of the phenoxy-hydroxyl group ortho to the methoxy group did not "deactivate" the methoxy group's reactivity towards chlorine. Syringyl nuclei were able to be completely demethylated regardless of the degree of chlorine substitution.

In contrast to the blocking group theory, Pugliese (35) proposed that closure of the fibers' micropores limited the extent of chlorination. In the theory, the pores became plugged by chlorinated lignin fragments whose molar volume were larger than those of unchlorinated lignin fragments. Once the micropores became blocked, the chlorine was not able to diffuse through the micropores to other reaction sites which caused stoppage of the reaction. Chapnerkar (38) suggested that incrustations on the outside of the fiber prevented chlorination from proceeding to complete conversion of lignin.

Further support for the pore closure theory is given by the observation that after sufficient extraction time, most of the chlorinated lignin can be removed and some of the closed pores are reopened (35). Grangaard (27) swelled chlorinated pulp with an alkali solution of sufficient

strength to achieve maximum swelling. With these concentrations more lignin was removed than at normal sodium hydroxide concentrations. One explanation of this phenomenon is that at the maximum swelling point the cellulose structure is opened up enough to allow the largest chlorolignin fragments to diffuse from the fiber at an appreciable rate.

CHLORINATION KINETICS

Initially, industrial chlorination is a three-phase system in which chlorine gas is dispersed in a fiber-water slurry. In order for the chlorine to react with lignin, it must move from the gas phase into the fiber wall matrix where it can react. During the chlorination reaction, the following steps occur:

1. diffusion of chlorine molecules diffuse from the bulk gas to the gas-liquid interface;
2. transfer of chlorine from the gas phase to the liquid phase;
3. diffusion of chlorine from the gas-liquid interface to the bulk liquid;
4. diffusion of chlorine from the bulk liquid to the fiber surface;
5. chlorine diffusion through the fiber pores and fiber matrix to a reaction site;
6. reaction of chlorine with lignin to yield chlorinated-lignin products;
7. movement of the chlorinated-lignin products from the interior to the exterior of the fiber and into the bulk liquid phase.(39, 40).

These steps are shown graphically in Figure 18 (41).

If any step or series of steps are significantly slower than the other steps, then the overall rate of the reaction is controlled by the rate of the slowest step. The slowest step is called the rate determining step. The rate determining step can also be used to classify the kinetic behavior in terms of either

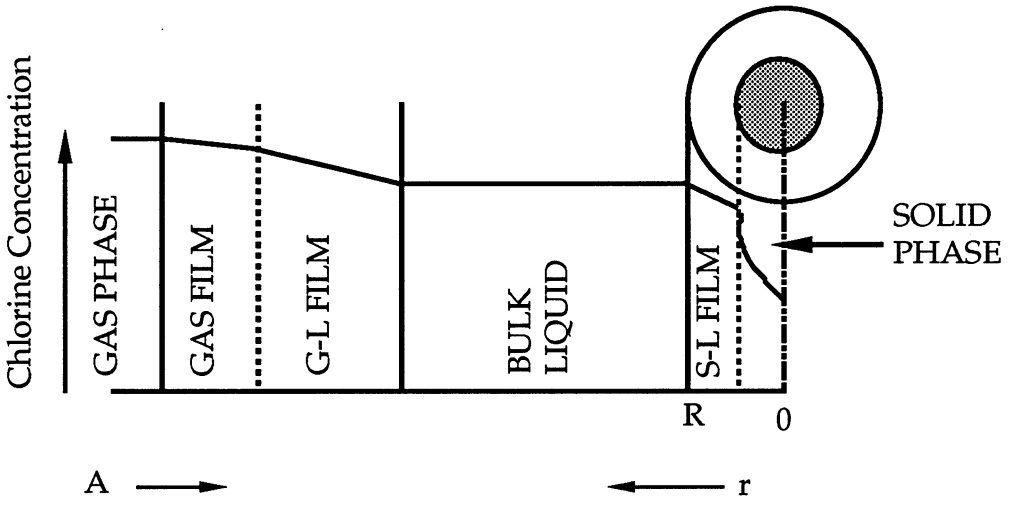

Figure 18. Profile of resistances to transfer of chlorine from the gas phase to a reaction site in the fiber wall (41).

homogeneous or heterogeneous mathematical, kinetic models. Homogeneous models are used to describe systems in which the chemical reactions control the system's behavior. This means that the chemical reaction rate is significantly slower than any physical processes. Thus, in homogeneous models, mass transfer effects are insignificant.

Heterogeneous models are used to describe systems which are not solely controlled by the reaction rate. Some of these models are flexible enough to describe systems where only mass transfer processes are important, where mass transfer and reaction rates are equally important, and where the relative importance of the two varies with the extent of reaction. Both model classes have been used to describe chlorination kinetics.

Most researchers have ignored the movement of chlorolignin fragments stating that they do not influence the initial fast phase of

chlorination. These same researchers, however, try to model the reaction over the entire reaction time frame. Only Pugliese attempted to model the effect of chlorolignin build-up in the fiber (35).

The problem with removal of the chlorolignin products is that they are not soluble in acid media. Whether the low removal efficiency is due to a pure solubility problem or a mobility problem is not known. However, one can speculate that mobility plays an important role in the removal rate.

The rate controlling step for chlorination has been widely debated through the years. There are three proposed mechanisms: external mass transfer limiting, intrafiber mass transfer limiting, and chemical reaction controlling. External mass transfer limiting refers to steps one through three above. Intrafiber mass transfer limiting refers to steps four and five, while chemical reaction refers to step six.

Overall Reaction Rate Limited by External Mass Transfer

In the pulp-water system external mass transfer processes are those processes which occur outside the fiber wall. Two examples of external mass transfer limiting processes are the transfer of a gaseous reactant to the liquid phase, and the diffusion of the reactant to the fiber surface.

In describing the dynamic bleaching process, Rapson et al. (42) abandoned the concept that the rate of diffusion of reactants into and reaction products out of the cell wall was the rate-limiting step in bleaching. Instead, they assumed that the diffusion rate of bleaching chemicals through a thick water layer surrounding the fiber limited the rate of the heterogeneous bleaching reaction. They believed that the increased rate of first chlorine

dioxide stage brightness development of dynamic versus conventional bleaching validated their hypothesis. In the dynamic bleaching process, the bleaching solution continuously moved with respect to a stationary bed of fibers. They postulated that the relative movement of the solution decreased the thickness of the fluid envelope around the fiber. It is possible, however, that the increased rate seen may have been caused by the constant chemical concentration seen by the fiber, since the bulk fluid was continually replenished with chemical. In addition, it is also possible to imagine that the renewal of bleaching solution maintained a constant gradient for diffusion of reacted products out of the fiber.

In a similar dynamic bleaching study, Ackert (43) also measured the extent of reaction using a differential flow reactor. He found that the delignification rate was slower for the high consistency pad used than for conventional low consistency chlorination. He explained that the slower rate was due to the fiber-fiber contact area being inaccessible to chlorine during the reaction. It is possible that there was undetected channelling in the reactor which resulted in lower conversions.

Experiments in gas phase chlorination at high consistencies (20 - 50%) have also shown an increase in the chlorination rate (44, 45, 46). For these experiments, fluffed high consistency pulps were placed in a chamber through which chlorine gas was passed. No mixing occurred during the experiments. The rate increase seen may have been due to the elimination of the fiber's external fluid envelope, which decreases the number of resistances by one. The pulp concentration was not critical between 20 and 50% consistency, but consistencies outside the optimum range reduced the effectiveness of chlorination. For consistencies below 20%, the chlorine gas did not penetrate

well into the wet pulp particles. Above 50% consistency there was not enough water present to promote the chlorination reaction.

The chlorine gas also served as a reservoir which replenished chlorine in the liquid phase as it was consumed. The replenishment of chlorine in the liquid phase maintained the concentration of chlorine in the pores at a constant level. In this respect gas phase bleaching was similar to dynamic bleaching as the water phase chlorine concentration was constant throughout the reaction. The reaction rate was also increased by the reduction of the liquid phase volume. Since the liquid was only in the pores, the diffusion distance that the chlorine molecule must traverse was greatly reduced. The most significant result of gas phase chlorination was that the reaction time was reduced from about one hour to one minute in pilot plant studies.

Overall Reaction Rate Limited by Internal Mass Transfer

Intrafiber mass transfer limitation of the chlorination reaction is suggested by the possibility of changes in the internal structure of the fiber wall. These structural changes could hinder or prevent the reaction between chlorine and lignin. Chapnerkar (38), for example, suggested that chlorinated lignin products formed on the fiber which prevented chlorine from penetrating the fiber wall as the reaction proceeded. Pugliese (35) suggested that changing lignin molar volumes closed micropores which prevented chlorine from diffusing into the fiber wall.

The shrinking core model, a model developed to describe coal combustion, has been used to describe chlorination (32). In the shrinking core model, the reaction occurred first at the particle's outer skin and then

progressed towards the center. As the reaction zone moved into the solid, completely converted material and/or inert solid remained (47). The shrinking core model described systems where the solid was completely converted. Karter (32) used this model to describe the chlorination kinetics in a tubular reactor. Karter compared model predictions for film diffusion controlling, intra-fiber wall diffusion controlling, and chemical reaction controlling. The intra-fiber wall diffusion model gave the best fit of the data.

In order to fit the shrinking core model to his data, Karter made two corrections. First, he corrected the lignin concentration by subtracting a floor level of lignin so that mathematically, the reaction would go to completion. Second, he corrected both the lignin concentrations and the total conversion using a coefficient to adjust the equation for the dependence of the diffusion rate on the distance that the reaction front had proceeded into the core. The coefficient was determined by a best fit of the data.

Pugliese (33) modeled chlorination using a variation of the shrinking core model called the grain model (48). In Pugliese's model, the fiber walls were described as parallel plates comprised of lignin, cellulose and hemicellulose spheres or grains. During the reaction, the chlorine diffused along the pores between the grains and reacted with the grain it encountered. The grains were converted according to the shrinking core model. However, the shrinking core model was modified so that the grains changed size based on the difference of the reactant's molar volume compared to that of the products. In the case of chlorine-lignin reaction, the chlorinated grains were larger than the unreacted grains. As a chlorinated grain grew, it could contact its neighbor which resulted in closure of the micropore between two grains and prevented any further chlorine diffusion along that pore. Because of pore closure, the

reaction could stop prior to complete conversion of lignin due to steric hindrances. Pugliese (33) used solute exclusion techniques to determine that the number of pores with diameters smaller than 52 angstroms decreased during chlorination. Measurement of the pore size distribution after extraction showed that some of these pores were reopened. One drawback of this model is that it underpredicts chlorine conversions at reaction times of less than 10 seconds.

Overall Reaction Rate Limited by Chemical Reaction

Many researchers have concluded that the chemical reaction controls chlorination. Chapnerkar (38) studied the reaction kinetics after the initial phase of the reaction was almost complete. For his homogeneous model, he used pseudo-first order kinetics to describe the system, and concluded that the kinetics were best modeled by two parallel reactions. When he assumed that the chlorine concentration remained constant during the reaction, the lignin concentration at any time, t, was determined by:

$$L_1 = A_c \exp\left(-k_1 t\right) + B_c \exp\left(-k_2 t\right) \qquad (7)$$

where L_1 = lignin content corrected for the fraction that reacts instantaneously, (kg m^{-3})

A_c, B_c = constants, (kg m^{-3})

k_1 = rate constant for the fast reaction, (s^{-1})
$= 1.12 \exp(-14{,}000/RT_K)$

k_2 = rate constant for the slow reaction, (s^{-1})

$= 3.32 \exp(-40{,}000/RT_K)$

R = universal gas constant, (KJ $mole^{-1}$)

t = time, (s) and

T_K = temperature (K).

He estimated the amount of chlorine consumed per gram of lignin to be 1.3 grams Cl_2/gram lignin or a molar ratio of 2.2 moles of chlorine per mole of lignin. This ratio was found to be independent of initial chlorine concentration.

In another study, Russell (49) used a tubular flow reactor to study the initial phase of kraft pulp meal chlorination. He used pulp meal instead of whole fibers, because the whole fibers would not flow consistently through the reactor. He justified the use of pulp meal by stating that the grinding of the fibers only reduced the pulp viscosity by 1.3%, but grinding of the fiber dramatically increased the fiber surface area. In addition to increasing the surface area, the grinding process may have caused irreversible microscopic changes in the fiber which may have influenced the chlorination reaction. The most significant morphological change due to the pulp processing may have been the collapsing of micropores upon drying the pulp for grinding that may not have reopened when the pulp was rewetted.

To simplify the mathematical treatment, Russell (49) also tried to use a pseudo first order kinetic model to describe the initial phase of the reaction. For his model, he assumed that the rate constant was the product of the chlorine concentration and the true rate constant. This assumption was proven not valid for his system as he discovered that the dependence of the rate constant on the chlorine concentration was extremely non-linear. He proposed that the variable nature of the chlorine concentration dependence resulted from a shift in the mechanism of chemical attack and/or an alteration

in the accessibility of lignin for reaction. Thus he concluded that a homogeneous model may be ill-suited for describing the chlorination rate.

At low chlorine concentrations, he postulated that there was a competition between the intrafiber chlorine diffusion and non-substitution type reactions. With the pseudo-rate constant, the reaction order varied with respect to lignin from 1.6 to 2.0 depending on the type of pulp meal and the reaction conditions.

Ackert (43) used two parallel reactions to describe chlorination kinetics. He incorporated a floor level of lignin in his model in a similar manner to that for Karter's (32) shrinking core heterogeneous model. The floor level was defined as the concentration of lignin in the fiber that could not be removed in chlorination.

Ni (24) also used parallel reactions to describe chlorination. The mechanism supporting the demethylation model was described earlier. The complex reaction scheme model incorporated the rate constants from twelve reactions occurring both in series and parallel. A correction factor was also incorporated in the model and used to adjust the initial lignin content for the amount of lignin which reacted with chlorine instantaneously. Although the model predicted the methoxyl content of the residual lignin very well, it under predicted the Cl/C-nine ratio throughout the reaction period.

PROBLEM STATEMENT

To respond to the market place, the pulp and paper industry is increasing its dependence on non-chlorine containing bleaching agents such as oxygen, ozone and hydrogen peroxide. Both oxygen and ozone are gaseous bleaching agents that have a low solubility in water. The low solubility of reactants in water has influenced the type of pulp system considered for industrial installations. For ozone which has a much higher solubility than oxygen, low , medium , and high consistency systems are being evaluated. For oxygen, only medium , and high consistency systems are viable.

As the industry moves towards medium consistency pulp processing, the mixing technology is evolving to meet the demands of the trend. The new technologies create a highly turbulent mixing zone to ensure intimate commingling of pulp and bleaching agent. Little information is available in the literature that describes the impact of this technology on the initial phase of pulp chlorination The impact can be measured by amount of chlorine available for chlorination in the liquid phase or that which has had the opportunity to react with lignin.

Questions arise about the performance of these mixers and how they affect the transfer of gas into a medium consistency pulp suspension and how their highly turbulent mixing zone affects the initial phase of medium consistency pulp chlorination.

EXPERIMENTAL PLAN

For medium consistency chlorination, the chlorine must be added to the pulp as a gas. Because of this the applied chlorine must diffuse from the gas phase, to the gas-liquid interface, cross the interface into the liquid phase, diffuse through the bulk liquid to a fiber, diffuse into the fiber wall to a potential reaction site and then react with the lignin followed by the removal of reaction products from the fiber wall. Perturbation of any one of these processes will impact on the consumption of chlorine and its reaction with lignin. If the system is perturbed so that one or more of these processes become significantly slower than the rest, then this process will control both the rate and extent of reaction.

Since a chlorine molecule initially in the gas phase must undergo each process in series, the overall resistance to mass transfer is the sum of all the individual resistances (50) as shown in Figure 19. If the concentration of lignin is large enough with respect to the chlorine concentration, the reaction can be considered to be first order with respect to chlorine, with a rate constant, k_c.The rate of reaction is given by:

$$-r_{Cl} = \frac{a_i}{V_1}\frac{dN_{Cl}}{dt} = k_{g\,Cl}\,a_i\left(p_{Cl} - p_{Cli}\right) = k_{l\,Cl}\,a_i\left(C_{Cl\,i} - C_{Cl}\right)$$

$$= k'_{l\,Cl}\,a_s\left(C_{Cl} - C_{Cl\,s}\right) = k_c\,C_{Cl\,s} \qquad (8)$$

where r_{Cl} is the reaction rate (moles $m^{-3}\,s^{-1}$),

V_l is the liquid volume (m^3),

a_i is the gas - liquid interfacial surface area (m^2),

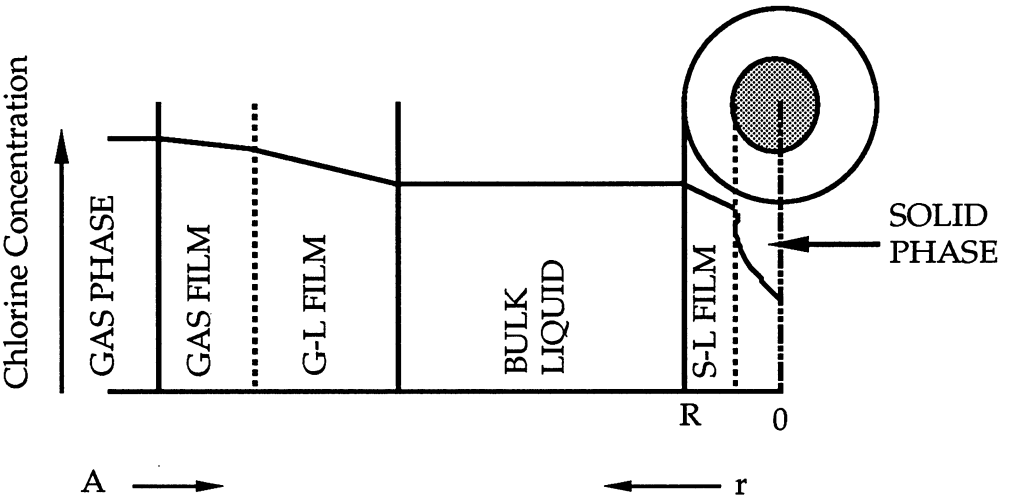

Figure 19. Resistances to mass transfer for the three phase medium consistency chlorination system (41).

N_{Cl} is the chlorine mass flux, (moles m^{-2} s^{-1})

$k_{g\,Cl}$ is the gas side mass transfer coefficient, (moles N^{-1} m^{-3} s^{-1})

p_{Cl} is the partial pressure of chlorine in the gas phase, (N m^{-2})

p_{Cli} is the partial pressure of chlorine in the gas phase at the gas-liquid interface, (N m^{-2})

$k_{l\,Cl}$ is the liquid side mass transfer coefficient, (m^2 s^{-1})

C_{Cl} is the concentration of chlorine in the bulk liquid phase, (moles m^{-3})

C_{Cli} is the liquid phase concentration of chlorine in the gas-liquid interface, (moles m^{-3}),

$k_{l\,Cl}'$ is the liquid side mass transfer coefficient for mass transfer to the solid phase, (m^2 s^{-1}),

a_S is the liquid - solid interfacial surface area ((m^2),

C_{Cls} is the liquid phase concentration of chlorine in the solid-liquid interface, (moles m^{-3}) and

k_c is the reaction rate constant, (s^{-1}).

The concentration of chlorine at the gas - liquid interface in the liquid phase can be related to the partial pressure of chlorine in the gas phase by the following equation (51):

$$p_{Cli} = H C_{Cli} \qquad (9)$$

where H is the Henry's law constant for chlorine, (N m $mole^{-1}$).

Substituting and recombining gives:

$$-r_{Cl} = \frac{1}{\frac{1}{H k_{g\,Cl} a_i} + \frac{1}{k_{l\,Cl} a_i} + \frac{1}{k'_{l\,Cl} a_s} + \frac{1}{k_c}} C_{Cl} \qquad (10)$$

Thus if any one resistance is significantly larger than the others it will control the overall rate of reaction. For the chlorination system used, a pure chlorine gas was used which minimized the gas phase resistance to mass transfer. The $H\,k_{g\,Cl}\,a_i$ term was assumed to be infinite (the partial pressure of chlorie gas >> partial pressure of other gaseous components).

To determine the rate-limiting step for the initial phase of chlorination, the medium consistency chlorination system was perturbed by varying the liquid-side resistance to mass transfer. Three cases were investigated. In the first case, the mass transfer coefficient was determined when there was no liquid-side reaction other than the hydrolysis of chlorine in water. In this situation the k_c term of Equation 10 was eliminated. The k_{lCl}' term was also eliminated, because there was no mass transfer to the solid phase. In this instance, the lower limit for the mass transfer coefficient was determined.

In the second case, a fast, liquid phase reaction was used to minimize the liquid phase resistance to mass transfer. In this case, the bulk chlorine concentration was near zero (due to consumption by the reaction), and the concentration gradient across the gas-liquid boundary did not change with time. The second case sets the upper limit for the amount of chlorine that can be absorbed by the system. For this case, the chlorine was consumed by sodium hydroxide to form sodium hypochlorite which was easily measured.

In the final case, the absorbed chlorine was reacted with lignin in the solid phase. If the reaction of chlorine with lignin was fast when compared to the gas-liquid mass transfer resistance, then the observed mass transfer rate would be the same as that for the second case. If the reaction rate was slow when compared to the mass transfer rate, then the observed mass transfer rate would be approximately the same as the first case. If the observed mass transfer rate fell between the two extremes, then the system's response to perturbation would be used to help elucidate the rate-limiting step.

These perturbations included:

1) Increasing the system temperature. A higher temperature would impact on the reaction rate by decreasing the intrinsic reaction rate resistance portion of Equation 10.

2) Increasing the mixing rate of the system, which would increase the interfacial area between the gas and liquid phases. As a_i increases, the resistances that depend on it decrease.

3) Increasing the amount of applied chlorine increases the maximum bulk chlorine concentration which could increase the reaction rate.

4) Increasing the pulp consistency would decrease the diffusion distance from the gas liquid interface to the fiber surface (the consistency effect was not measured in this work).

EXPERIMENTAL DESIGN

Four sets of experiments were run during this work to characterize the reactor and measure the chlorine mass transfer coefficient for the three cases discussed above.

The first set was designed to characterize the reactor's residence time distribution and its mean space time. The residence time distribution is a measure of the dispersion of residence times for all the particles in the reactor. The mean space time is the average residence time of all the particles (39).

A standard 2^3 full factorial design was used to estimate the reactor's mean space time and residence time distribution (39). The design was run three times so that the experimental error could be estimated. For this experiment the independent variables investigated were the pulp flow rate, gas flow rate, and mixer rotor speed.

The second set was designed to measure the mass transfer coefficient for the absorption of chlorine into an inert pulp suspension. The third set was designed to measure the mass transfer coefficient for the absorption of chlorine into an inert pulp suspension with a fast liquid phase

reaction. The fourth set was designed to measure the mass transfer coefficient for the absorption of chlorine into a reactive pulp suspension.

The same experimental design was used for the last three sets of experiments. For the mass transfer experiments, a Box-Behnken three factor incomplete factorial experimental design was used (52). In this design, two of the three independent variables were varied while the third was held constant at its midpoint. This was done for the three pair combinations. A set of three experiments was also run at the experimental midpoint in order to estimate the experimental error. The whole design was repeated so that a better estimate of the experimental error could be made. Since the independent variables were varied over three levels, the response surface's curvature due to quadratic effects were estimated. The independent variables investigated were the mixer's rotor speed (shear rate), the chlorine charge (gas flow rate) and the system temperature.

DATA ANALYSIS

Calculation of the Mass Transfer Coefficient

For the data analysis, the mixer was assumed to behave like a continuous stirred tank reactor (CSTR). The rate at which chlorine was absorbed by the pulp suspension could be described as follows (50):

$$N_{Cl} = k_l \left(C_{Cli} - C_{ClB} \right) \qquad (11)$$

where N_{Cl} is the flux of chlorine into the liquid phase, (moles m^{-2} s^{-1})

k_l is the liquid side mass transfer coefficient, (m s^{-1})

C_{Cli} is the concentration of chlorine at the interface and is a function of the solution temperature, (moles m^{-3})

C_{ClB} is the bulk phase chlorine concentration, (moles m^{-3}) and $[C_{Cli} - C_{ClB}]$ is the concentration difference between the interface and the bulk liquid.

The molar flow rate of chlorine in the liquid phase can also be calculated from a material balance around the system:

$$\text{Input} + \text{Generation} = \text{Output} + \text{Accumulation} \qquad (12)$$

For the CSTR system studied with no reaction, the accumulation and generation terms of Equation 12 are zero. The material balance becomes:

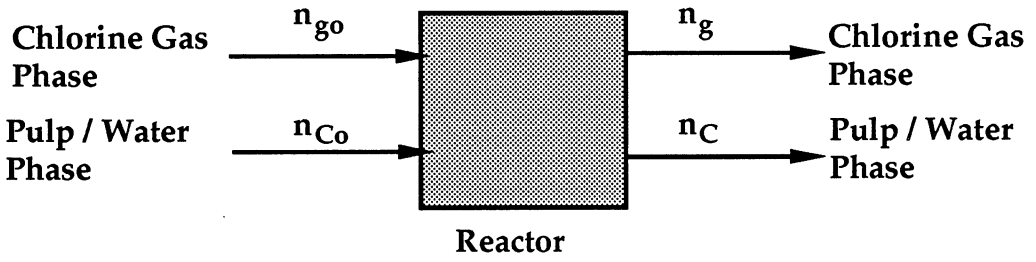

where n_{go} is the inlet flow rate of chlorine in the gas phase, (moles s^{-1})

n_g is the outlet flow rate of chlorine in the gas phase, (moles s^{-1})

n_{co} is the chlorine inlet flow rate in the liquid phase, (moles s^{-1})

n_c is the chlorine outlet flow rate in the liquid phase, (moles s^{-1}).

$$n_{co} + n_{go} = n_c + n_g \qquad (13)$$

For the gas phase, the gas flow rate is equal to (ideal gas law):

$$n = \frac{P\,V_g}{R\,T_K} \qquad (14)$$

where P is equal to the system pressure, (atm)

V_g is the gas volume, (cm^3)

R is the ideal gas constant, (cm^3 atm $moles^{-1}$ K^{-1})

T_K is the system temperature, (K).

The inlet liquid phase chlorine molar flow rate is equal to:

$$n_{co} = v_o C_o \tag{15}$$

where v_o is the inlet volumetric flow rate, (cm^3 s^{-1}) and

C_o is the liquid phase chlorine concentration, (moles cm^{-3}).

Substitution of Equations 14 and 15 into Equation 13 and replacing n_C with v_oC gives:

$$v_oC_o + V_{go}\frac{P}{RT_K} = v_oC + V_g\frac{P}{RT_K} \tag{16}$$

Upon rearrangement it becomes:

$$\frac{P}{RT_K}\left(V_{go} - V_g\right) = v_o\left(C - C_o\right) \tag{17}$$

The molar flux for the liquid phase, N_{Cl}, is equal to the molar flow rate divided by the area for mass transfer, A:

$$-N_{Cl} = \frac{1}{A}v_o\left(C - C_o\right) = \frac{1}{A}\left(V_{go} - V_g\right)\frac{P}{RT_K} \tag{18}$$

The molar flux is also equal to:

$$N_{Cl} = k_l\left(C_{Cli} - C\right) \tag{19}$$

where C_{Cli} is the interfacial chlorine concentration, (moles cm^{-3}). Substituting for N_{Cl}:

$$k_l\left(C_{Cli} - C\right) = \frac{1}{A} v_o \left(C - C_o\right) \tag{20}$$

$$k_l A = v_o \frac{C - C_o}{C_{Cli} - C} \tag{21}$$

Let the space time of the reactor, τ, be equal to the reactor volume divided by the volumetric flow rate, V/v_o. Substitution for v_o gives:

$$k_l A = \frac{V}{\tau}\left(\frac{C - C_o}{C_{Cli} - C}\right) \tag{22}$$

Let the interfacial area, a, be the area for mass transfer divided by the reactor volume (A/V). The mass transfer coefficient for the system can be calculated as follows:

$$k_l a = \frac{1}{\tau}\left(\frac{C - C_o}{C_{Cli} - C}\right) \tag{23}$$

For this system, the initial concentration of chlorine in the liquid phase is zero ($C_o = 0$). Thus, the Equation 23 simplifies to:

$$k_l a = \frac{1}{\tau}\left(\frac{C}{C_{Cli} - C}\right) \tag{24}$$

For this work the value of C_{Cli} (the interfacial chlorine concentration) was assumed to be the equilibrium chlorine concentration for the liquid temperature.

Calculation of the Chlorine-Lignin Reaction Rate Constant

The chlorine lignin reaction can be described by Equation 25.

$$Cl_2 + \text{Lignin} \rightarrow \text{Products} \qquad (25)$$

Since the mixer was described as a continuous stirred tank reactor, the reaction rate was the same at every point in the reactor (39). A material balance on the lignin over the reactor volume at steady state is:

$$n_1^o - \left[n_1 + r_1 V_r \right] = 0 \qquad (26)$$

where n_l^o is the molar flow rate of lignin at the reactor inlet, (mole s^{-1})

n_l is the molar flow rate of lignin at the outlet, (moles s^{-1})

r_l is the rate of reaction for the chlorine-lignin reaction in Equation 25, (moles m^{-3} s^{-1})

V_r is the reactor volume (m^3),

$n_l + r_l V_r$ is the total lignin output per unit time.

Thus

$$r_1 = \frac{n_1^o - n_1}{V_r} \qquad (27)$$

From Equation 25, the reaction rate is also equal to:

$$r_1 = k_{c2} C_{ClB} C_L \qquad (28)$$

where k_{c2} is the reaction rate constant, (m^3 $moles^{-1}$ s^{-1})

C_{ClB} is the bulk phase chlorine concentration, (moles m^{-3}), and

C_L is the concentration of lignin, (moles m^{-3}).

Substitution of Equation 21 into Equation 20 gives:

$$k_{c2} C_{ClB} C_L = \frac{n_1^o - n_1}{V_r} \qquad (29)$$

Solving for k_c gives:

$$k_{c2} = \frac{n_1^o - n_1}{C_{ClB} C_L V_r} \qquad (30)$$

Calculation of the Residence Time Distribution and Mean Space Time

A reactor's residence time distribution (RTD) is an estimate of the distribution of retention times in the reactor for each individual flow element (39). A reactor's RTD can be estimated using response stimulus techniques. In these techniques, a perturbation in a flow parameter at the reactor inlet is created and then this variable is measured at the reactor outlet as a function of time. The parameter value versus time profile can be used to mathematically characterize the reactor. For these experiments, the concentration of KCl in the pulp suspension was the inlet parameter which was perturbed.

For this work, the reactor was assumed to behave like a continuous stirred tank reactor (CSTR). For a CSTR, a step change in concentration of an inert material or tracer made at the reactor inlet will result in an outlet concentration versus time profile or F-curve (39):

$$\frac{C}{C_0} = 1 - \exp\left(-\frac{t_s}{\tau}\right) \qquad (31)$$

where C is the tracer concentration at time, t_s, (moles m^{-3}),

C_0 is the tracer concentration of the step input zone, (moles m^{-3}),

t_s is the time elapsed from the introduction of the step input, (s),

τ is the mean space time of the reactor (s).

Because of the reactor's physical set-up, a plug flow zone preceded the stirred reactor portion during the RTD experiments. For this system, Equation 31 was modified to include the plug flow portion of the system as follows:

$$\frac{C}{C_0} = 1 - \exp\left(-\frac{T_{OVERALL} - T_{PF}}{\tau}\right) \qquad (32)$$

where $T_{OVERALL}$ is the time elapsed from the start of an experiment.

τ is the mean space time of the reactor, (s) and

T_{PF} is the time required for the step change in tracer concentration to reach the reactor, (s).

τ and T_{PF} can be estimated by regression of the natural log of 1-normalized outlet concentration versus time. The regression equation is:

$$\ln\left(1 - \frac{C}{C_0}\right) = -a\,T_{OVERALL} + b \qquad (26)$$

where $a = 1/\tau$ and $b = T_{PF} / \tau$. In the limiting case, where the reactor contains only a CSTR portion, b equals zero.

Representative F-curves for the flow-through reactor's residence time distribution experiments is shown in Figure 20. Figure 21 is the corresponding plot of $\ln(1- C/C_0)$ versus time. Figure 21 is used for estimation of the plug flow time and the mean space time.

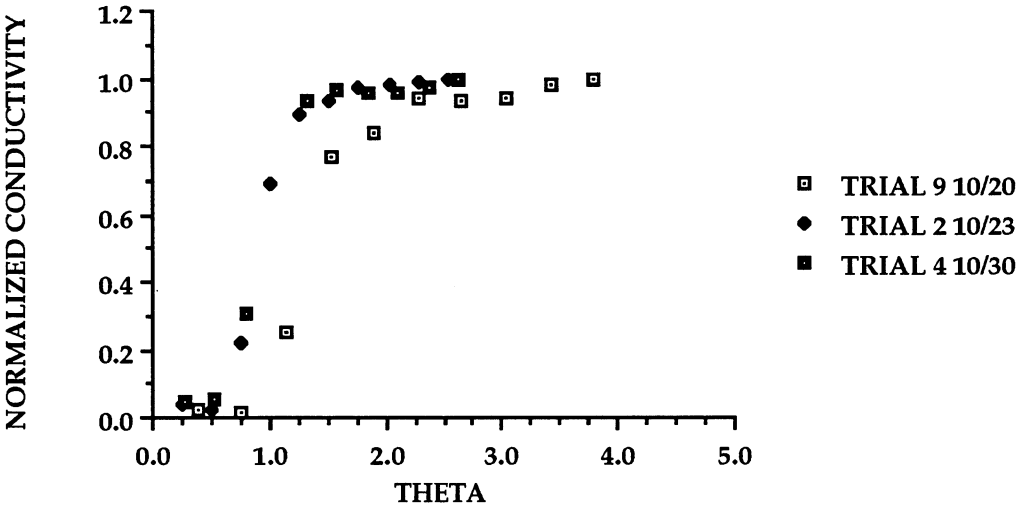

Figure 20. Representative F-curve with a step input change in inlet concentration. Low level of RPM - Low level of gas - High level of piston. (Theta = time elapsed/total run time)

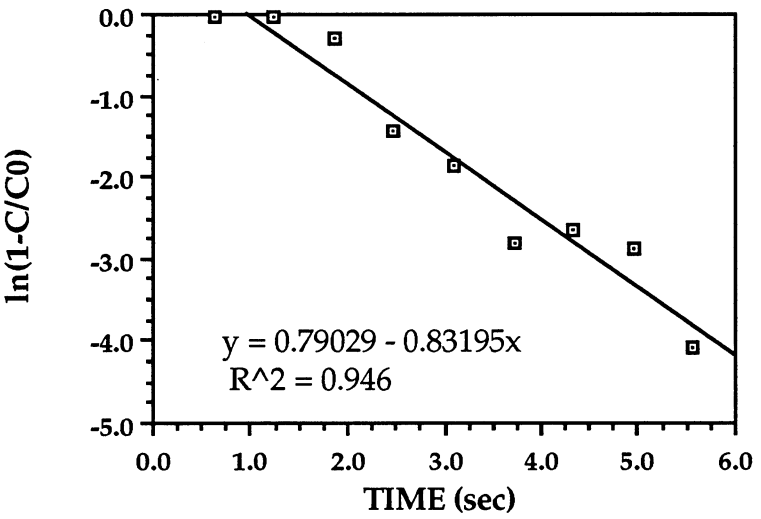

Figure 21. Plot of the natural log of 1 - the normalized outlet KCL concentration as a function of time.

MATERIALS AND METHODS

The approach to this thesis was twofold: 1) develop the equipment necessary to chlorinate medium consistency pulp, and 2) to measure the effects of mixer variables on the chlorination reaction so that the rate-limiting step could be determined. This section will describe the equipment and experimental methods used.

Two pieces of equipment were considered: a batch system and a continuous system. The batch system was built and used for chlorinations by other researchers (3). The continuous system was built for this work, because the reaction zone was well-defined versus the batch system used by Reeve and Earl (3). In the batch system, the volume of the reactor changed to reflect changing gas volumes. In addition, the flow through system also better simulated the actual mixing of commercial medium consistency mixers. The flow through reactor used was originally designed and built as part of a Master's thesis (53).

DESCRIPTION OF FLOW THROUGH MIXER

Two constraints were placed on the equipment design: 1) the power density in the mixing zone equaled 2.5×10^7 W m^{-3} (this energy density was within the range of commercial equipment for the processing of medium consistency pulp suspensions (12)), and 2) continuous flow of pulp through the mixing zone must be maintained. The free volume of the mixer was determined by the desired energy density, and the drive motor size. The free volume was set to 2.95×10^{-4} m^3 based on the above criteria. The design calculations for the mixer are given in Appendix I.

A schematic of the mixer is shown in Figure 22. The ensuing sections describe the major components of the apparatus: the mixing chamber and pulp reservoir, the hydraulic unit, the gas delivery system, the automatic pulp sampler, and the peripheral instrumentation.

The mixing chamber, shown in Figure 22, consisted of three parts: a lexan cylinder (0.114 m inner diameter by 0.051 m in height), a PVC base plate (9.5×10^{-3} m thickness), and the top which was part of the pulp reservoir. The chamber wall had three 0.0127 m by 0.0127 m by 0.051 m baffles located 120 degrees apart to give additional mixing. A thermocouple port and a gas injection port were also located around the perimeter of the mixer.

The pulp exited the chamber through a 0.0254 m by 0.102 m long circular channel located between a baffle and the gas inlet port. The pulp flow was regulated by a gate at the end of the outlet tube. During experiments, the gate was either fully open or closed. An o-ring seal was used to prevent leakage of the suspension from around the gate. In the open position, the gate did not impede the flow of pulp from the reactor.

The rotor head in the mixing chamber was a 0.051 m square Kynar block, 0.0444 m high, and had a 0.0127 m by 0.0127 m baffle on each side. The rotor head was constructed out of a single piece of kynar with a 316 SS shaft. Exposure of the shaft to the corrosive chlorination conditions was minimized by a silicone rubber collar inserted between the rotor head and the mixer floor. No evidence of shaft corrosion was seen during the experiments.

The rotor shaft was driven by a 10 hp motor (480 volts-3 phase) whose speed was controlled by a Dynamic^{TM} direct drive unit. The maximum

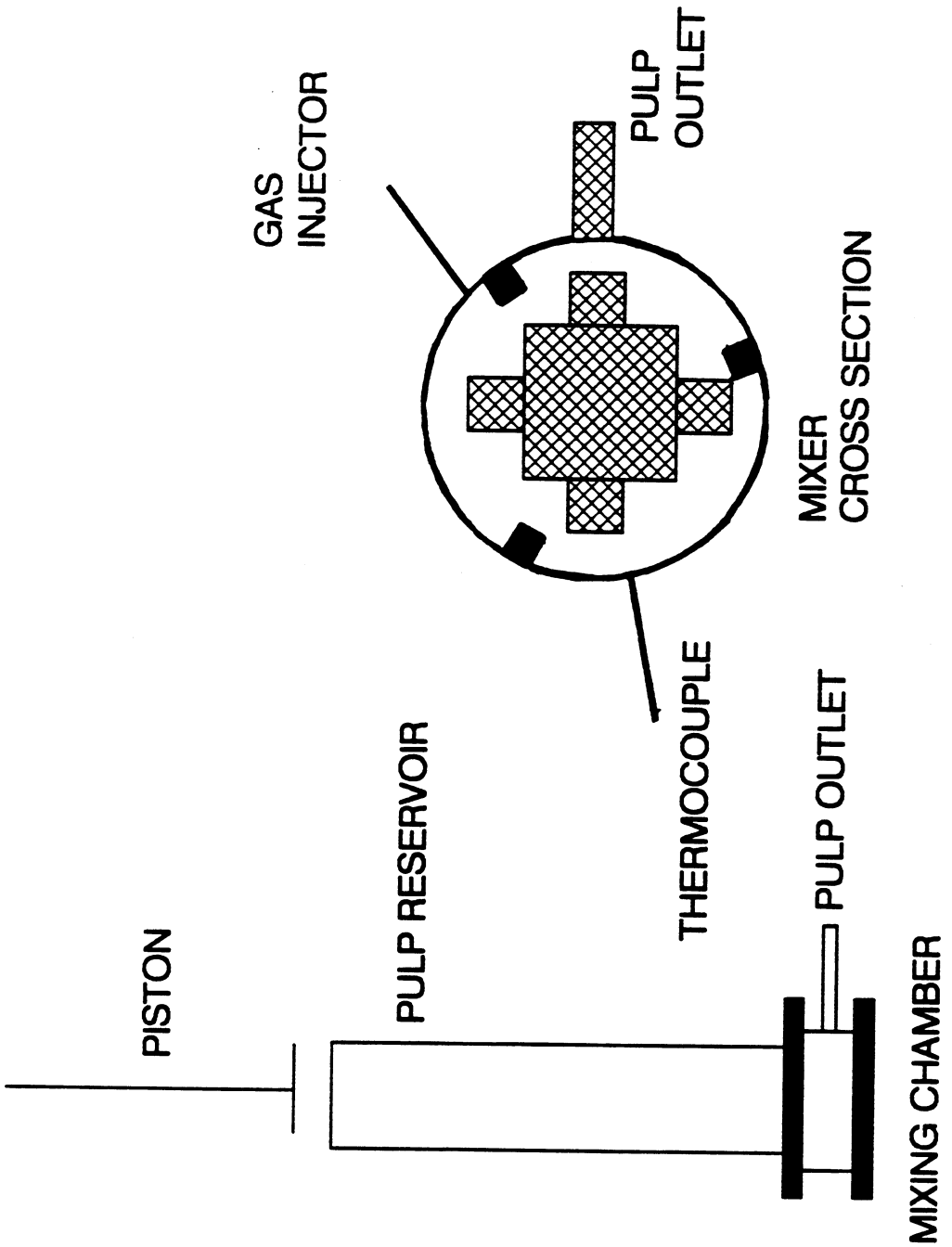

Figure 22. Medium consistency, high shear, flow through mixer schematic.

rated speed of the motor was 1750 rpm. A belt and pulley system was used to increase the rotational speed of the rotor shaft. Because the motor speed was lower than that required for pulp fluidization, the sheave ratio of the drive shaft to the rotor shaft was 1 to 2 so that the maximum rotor shaft speed was 3500 rpm. The rotor speed recorded during the experiments was based on a doubling of the direct drive unit's rotational speed.

An Omega J-type thermocouple was used to record the reaction temperature. It was inserted into the reactor through a swagelock fitting. It was adjusted so that the tip of the thermocouple protruded into the chamber 6.35×10^{-3} m. The thermocouple was calibrated against a thermometer which had been calibrated against an NBS standard thermometer. The calibration curve is shown in Appendix II. During the experiments, the temperature signal was captured by the TransEra data acquisition system described later.

The pulp reservoir above the rotor held the unreacted pulp during an experiment. The reservoir was constructed from a section of clear PVC pipe (0.0762 m diameter by 0.91 m long). Translucent pipe was used so that the level of pulp in the reservoir could be observed. Both ends were flanged for attachment to the flow through chamber and the supporting structure. The bottom flange served as the top for the mixing chamber.

The pulp in the reservoir was moved through the mixing chamber by a hydraulically driven piston. The piston velocity was controlled by a Racine hydraulic pump and needle valve, and ranged from 0.30 m s^{-1} to 1.83 m s^{-1}. The piston stroke velocity was calibrated by measuring the time required for the piston to travel 0.46 m using a stopwatch. The results of the calibration, and its reproducibility are summarized in Appendix II.

A teflon piston cup was attached to the end of the hydraulic ram to push the pulp into the mixer chamber. The ends of the cup were flared so that the the back pressure generated by the pulp's resistance to flow expanded the cup's bottom. The cup's expansion created a seal between the cup and the pipe wall ensuring that the reservoir wall was wiped clean of pulp. The piston cup was coated with silicone vacuum grease to prevent deformation of the teflon piston cup during its insertion into the top of the reservoir, and to help create a seal between the cup and the reservoir wall.

The piston cylinder, the chamber, and the rotor shaft bearings were mounted on an I-beam to ensure proper alignment. The piston and the pulp reservoir were aligned before each trial so that the piston cup would not get damaged upon entry into the reservoir.

Gas Delivery System

Chlorine and nitrogen gas were available for use in the system. The gas cylinders were connected to each other by a manifold. The nitrogen gas cylinder and regulator were isolated from the chlorine cylinder by closing a ball valve at its regulator outlet. Closure of this valve was necessary to prevent corrosion of the nitrogen regulator by chlorine gas. Nitrogen gas was used as the gas source for both the preliminary experiments and to purge the gas lines after each chlorination run.

For the residence time distribution study experiments, the gas flow was measured and controlled with a Teledyne-Hastings mass flowmeter (model number CSH-50KGR). The flowmeter automatically compensated for gas temperature and pressure variations. It was also able to adjust the gas flow to

the desired rate in less than ten seconds. The mass flowmeter was calibrated against an NBS standard wet test meter using nitrogen and argon. Two gas species were used to determine the effect of molecular weight on the mass flowmeter's output. Over the range tested, the mass flowmeter gave a linear output. There was a slight difference in the calculated flowrates based on molecular weights. The calibration curves are summarized in Appendix II.

After some preliminary chlorination experiments, the mass flowmeter became so corroded that it was replaced by a factory-calibrated rotameter which was designed for wet gaseous chlorine service.

Downstream of the flowmeter was a junction where the gas could flow to the reactor or to the chlorine scrubber. The gas flow direction was controlled by two remotely operated solenoid valves. There was a check valve and a barometric loop to prevent liquid from the reactor from backing up into the gas line. All the gas piping was CPVC pipe, 6.35 mm in diameter, except for the gas manifold which was 316 stainless steel, 6.35 mm in diameter.

A sodium thiosulfate scrubber system was used to quench excess chlorine gas during the mixer start-up and shutdown. This system was composed of a scrubbing column, a scrubbing solution reservoir, and a recirculating pump. The chlorine gas was diverted to the scrubber prior to starting a run so that the target gas flow was reached before an experiment was started. The chlorine gas was again diverted to the scrubber at the end of a run while the gas line was purged with nitrogen. The final purging was necessary to minimize corrosion of the stainless steel wetted parts in the flowmeter and the solenoid valves.

Automatic Sampler

During the residence time distribution studies, a sampling device was used to collect pulp samples at discrete time intervals from the reactor outlet. The sampling device was composed of a rotating table with ten sample holders evenly spaced around the table's perimeter. The sample holders were sections of 5.08×10^{-2} m diameter by 0.127 m long schedule 80 PVC nipples. They were cut so that the pulp entered the holder and remained there until the end of the experiment. The rotational speed of the sampling device was controlled by a variable speed, friction drive unit. The rotational speed of the sampling device controlled the time interval between samples. Prior to each experiment, the time for three table revolutions was measured and recorded.

Flow Through Mixer Instrumentation

The mixing chamber temperature was measured by an Omega J-type thermocouple. The temperature signal from the thermocouple was sent to a TransEra MDAS 7000 data acquisition system. The temperature data acquired by the TransEra were subsequently downloaded to a TANDY portable computer at the end of the experiment for further analysis. The data acquisition program is listed in Appendix III.

PRODUCTION AND CHARACTERIZATION OF PULP

Two pulp sources were used in the experimental program. The first pulp used was a fully bleached eucalyptus drylap pulp for the chlorine absorption experiments. All the eucalyptus drylap pulp used in the study was

slushed at the same time in a high consistency pulper at neutral pH. After slushing, the pulp was dewatered in a centrifuge and then stored at 5 °C.

The second pulp was a never-dried mixed hardwood pulp donated by a Member Company. It was used for the residence time distribution study and the experiments in which some of the chlorine absorbed was consumed by the reaction with lignin. The wood species in the pulp mixture are summarized in Table 1.

Table 1. Pulp Characterization for Mixed Hardwood Brownstock.

SPECIES	FRACTION (%)
Maple	55 - 65
Beech	25 - 35
Birch	5 - 10
Oak	< 5
Other	<10

RESIDENCE TIME DISTRIBUTION EXPERIMENTAL METHOD

The following experimental procedure was used for the residence time distribution study. (Refer to the reactor drawing in Figure 22.)

1) With the pulp reservoir removed from the reactor, the mixing chamber was filled with unbleached pulp that was free of the tracer material.

2) The pulp reservoir was reattached to the mixer.

3) An additional amount of unbleached pulp was then added to raise the pulp level in the reservoir to 0.076 m above the top of the mixing chamber. The top was levelled off to ensure a sharp transition between the tracer free pulp and the pulp containing the tracer material.

4) Next, pulp that was adjusted to the desired consistency with a tracer solution was loaded into the pulp reservoir on top of the tracer free pulp. Care was taken not to disturb the interface between the two pulp layers.

5) The gas flow was started and diverted to the scrubber system.

6) The automatic sampler was started.

7) The piston was started when the gas flowrate was at the target rate.

8) As soon as the piston cup contacted the pulp column, the mixer's rotor was started, the outlet was opened, and the gas was sent from the scrubber to the mixing chamber.

9) The pulp samples collected at the mixer outlet were tested for tracer concentration. Because of the complex nature of an experimental run, two people were necessary to operate the equipment.

The gas used for this study was nitrogen, because it was an inert gas and had a low solubility in water (54). The inert tracer material was potassium chloride. The conductivity of the pulp solution was the parameter

measured at the reactor outlet. Calibration of the Omega conductivity probe in several consistency pulp suspensions is outlined in Appendix IV. From these experiments, it was found that the ion exchange capacity of the pulp did not interfere with the conductivity measurement at pulp consistencies up to ten percent. The conductivity measured for the KCl solutions did not significantly deviate from the conductivities reported in the Literature after correction for the conductivity cell constant (54). The conductivity versus KCl concentration exhibited some curvature at high KCl concentrations as shown in Figure 23. At low KCl concentrations, however, the curvature was slight; and the conductivity was assumed to be a linear function of the KCl concentration for KCl concentrations below five weight percent which was the operating range used for these experiments.

CHLORINE ABSORPTION EXPERIMENTAL METHOD

The experimental procedure used for the chlorine absorption experiments was similar to that used for the residence time distribution study discussed above. The differences in the procedure are discussed below.

First, chlorine gas was used instead of nitrogen. At the end of each run, the gas lines were purged with nitrogen to clear the system of chlorine. The purging was necessary to minimize the corrosive nature of wet chlorine gas.

The second difference was in the sample collection. For the two experiments where the chlorine was absorbed by the bleached pulp suspension, pulp samples were immediately quenched at the reactor's outlet by an acidified potassium iodide solution. The solution was then titrated with

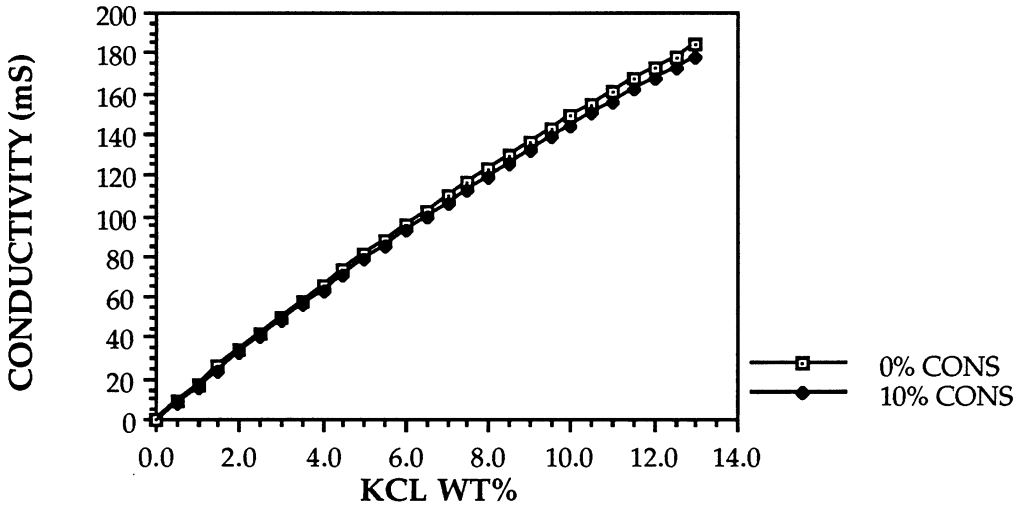

Figure 23. Conductivity of potassium chloride in pulp suspensions.

a 0.1 N sodium thiosulfate solution to determine the chlorine concentration in the liquid phase.

For the experiment where the chlorine reacted with the solid phase, two pulp samples were obtained. The first pulp sample was quenched with an acidified potassium iodide solution. The liquid phase was titrated for residual chlorine, after which the pulp was washed with water. The second sample was put in a gas-tight plastic bag and placed in a water bath set at the desired temperature for 10 minutes. At the end of 10 minutes, the residual chlorine was measured, and the pulp was washed. Both samples were then extracted with sodium hydroxide for one hour at 70 °C. After washing, the extracted pulp samples were tested for residual lignin content (CE kappa number) using TAPPI test method T236 (55).

The amount of chlorine absorbed by the liquid phase in the first two experiments was calculated from the measured concentration in the liquid phase. The amount of chlorine absorbed for the third experiment was the sum of the chlorine concentration measured in the first sample plus the amount of chlorine that reacted with the lignin while the pulp was in the mixing chamber. The amount of chlorine consumed by the lignin can be estimated using the stoichiometric coefficient of the chlorine-lignin reaction.

ESTIMATION OF THE STOICHIOMETRIC COEFFICIENT OF THE CHLORINE-LIGNIN REACTION

The reaction of chlorine with lignin can be described by Equation 27:

$$a\ Cl_2 + \text{lignin} \rightarrow \text{Products} \qquad (34)$$

The coefficient, "a", in Equation 27 is the stoichiometric coefficient for chlorine in the chlorine-lignin reaction. Once this value is calculated, the amount of chlorine consumed in the reaction can be calculated based on the measured lignin consumption. To estimate the stoichiometric coefficient, a series of batch low consistency chlorinations were performed.

The experimental conditions for these experiments are summarized in Table 2. These experiments were done at 3.0% consistency in bottles placed in a 35 ^{o}C water bath for 10 minutes. The amount of applied chlorine ranged from 0.24 to 2.70% chlorine on pulp. At the end of the

Table 2. Low Consistency Batch Chlorination Conditions for "a" Determinations.

Conditions	Chlorination	Extraction
Consistency (%)	3.0	10.0
Chemical Charge, (%)	0.24	*
	0.61	
	0.98	
	1.35	
	2.70	
Temperature (°C)	35.0	75.0
Time (min)	10.0	60.0

* The amount of NaOH charged in the extraction stage was 0.55 times the chlorine charge or the amount of NaOH required to raise the initial pH of the pulp suspension to 11.0.

Pulp Initial Kappa Number 12.25

chlorination reaction, the samples were tested for residual chlorine and washed. In these experiments all the applied chlorine was consumed.

The washed samples were extracted with sodium hydroxide for one hour at 75 °C. The extracted samples were then tested for residual lignin by measuring the kappa number of the pulp according to TAPPI test method T236 (55).

Since all the chlorine was consumed, the charge was not corrected for residual chlorine. The mass of lignin removed in the batch chlorination was the difference in Kappa number times the Klason lignin conversion factor (0.15%/ kappa number) times the sample size (20 OD grams) as shown in Equation 35:

$$lignin_{removed} = (12.25\text{-}K_{CE}) * 0.0015 * 20 \text{ g pulp} \qquad (35)$$

Assuming that the residual hardwood kraft lignin molecule can be described by a series of syringyl and guaiacyl monomers linked together in a 1 to 1 ratio (24), the average molecular weight of the monomer was 211. (Based on the estimates of Kempf et al. (23) and Dence et al. (56), the molecular weight of kraft-milled wood lignin was 196 for guaiacyl nuclei and 226 for syringyl nuclei.) For the data in Table 3 and Figure 24, the number of moles of lignin removed for the 2.70% applied chlorine case above is:

$$(12.25\text{-}4.78) \times 0.0015 \times 20 / 211 = 0.00106 \text{ moles of lignin} \qquad (36)$$

which reacted with 0.0077 moles of chlorine. The coefficient, "a" in Equation 27, is 7.25. Calculation of the stoichiometric coefficient for each of the five conditions gives 1.67, 2.66, 2.68, 3.93, and 7.25 for chlorine dosages of 0.24, 0.61, 0.98, 1.35, and 2.70% on pulp, respectively.

The ratio should be constant if both reactants are present in sufficient amounts. For low chlorine dosages, the chlorine is totally consumed corresponding to a low coefficient. At higher dosages of chlorine the lignin is removed according to the coefficient. However, there is a limit to the amount of lignin that can be removed. Once that limit is reached, any additional chlorine present will react with the chlorolignin products to form more highly substituted chlorolignin fragments without reducing the amount of residual lignin. The excess chlorine can also react with the carbohydrate fraction of the pulp. For this particular pulp, the limit or "floor" lignin level was approximately a 5.0 kappa number.

Thus, for chlorine charges above 0.24% on pulp, there is enough

Table 3. Extracted Kappa Number Results for the Low Consistency Chlorinations.

Chlorine Charge	Kappa 1	Kappa 2	Kappa 3	Ave Kappa
0.24	9.17	9.31	9.28	9.25
0.24	9.25	9.60	9.51	9.45
0.61	7.53	7.26	7.20	7.33
0.61	7.95	8.13	7.89	7.99
0.98	4.32	4.50	4.25	4.36
0.98	5.54	5.28	5.48	5.43
1.35	7.32	5.01	4.83	5.72
1.35	4.94	5.03	4.95	4.97
2.70	5.70	4.74	5.88	5.44
2.70	4.32	3.90	4.17	4.13

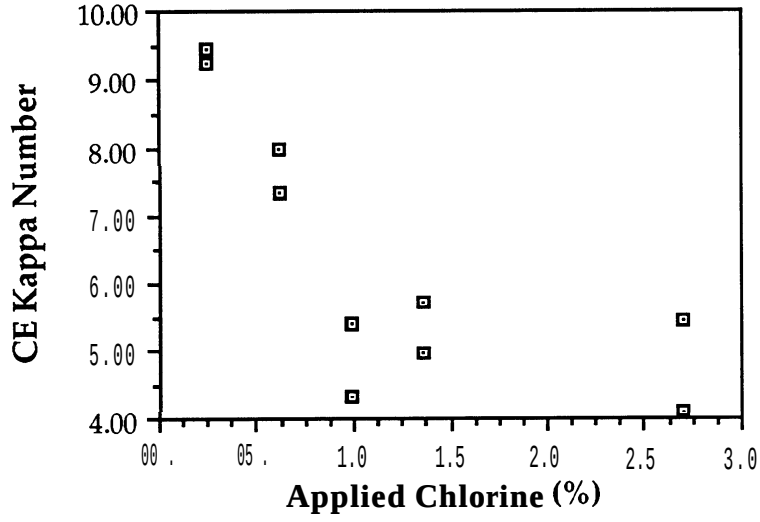

Figure 24. Chlorinated-extracted kappa number of a hardwood pulp as a function of applied chlorine (low consistency).

chlorine available to react with the lignin in a stoichiometric manner unless an excess amount of chlorine required to reach the floor level of chlorine is applied. For this pulp, the stoichiometric ratio of 2.67 was used (the average of 0.61 and 0.98% chlorine on pulp bleaches). Chapnerkar (38) calculated 2.22 as the molar ratio. Ni (24) calculated the stoichiometric coefficient for guaiacyl lignin as 3.7. He postulated that the ratio for syringyl lignin would be about 2. Assuming that the guaiacyl to syringyl ratio in hardwood lignin is 1 to 1, the stoichiometric coefficient for his work would be approximately 3. The value calculated for the commercial hardwood used in this work is within the range expected from the literature. This value is used in subsequent calculations to determine the amount of chlorine consumed by lignin in the solid phase reaction.

RESULTS AND DISCUSSION

RESIDENCE TIME DISTRIBUTION

The residence time distribution study was designed to measure the dependence of the reactor's mean space time and the plug flow time on three mixer variables. A full factorial experimental design was used and replicated twice so that the experimental error could be estimated directly from the data. The mixer variables of interest were the pulp flow rate, the mixer's rotor speed, and the gas flow rate. The set points for these independent variables are summarized in Table 4. As described in the previous section, the gas used was nitrogen. In these experiments, the time required for a step change in liquid phase conductivity was measured at the reactor outlet. A representative concentration versus time F-curve is shown in Figure 25. The conductivities were normalized by dividing the sample conductivities by the maximum conductivity measured for a given experiment. The F-curves for all the RTD experiments are summarized in Appendix V. The mean space time and plug flow time were calculated using a linear least squares regression technique (57).

Flow Through Mixer Mean Space Time

The calculated mean space time for each experiment is shown in Table 5. One of the mean space time values was determined to be an outlier. A mean space time value was determined to be an outlier, if its value did not fall within its expected range. The expected range was calculated as the treatment average plus or minus two times the standard deviation of the experiment (95% confidence interval). The experimental standard deviation

Table 4. Residence Time Distribution Experiment Independent Variable Levels.

Level	Gas Flow (sccs N_2)*	Rotor Speed (rpm)	Pulp Flow rate (cc/sec)
Low	0	1500	290
High	70	2500	701

*sccs - standard cubic centimeters per second at 20°C and 1 atm.
Pulp consistency - 8%.
Temperature - 20 °C

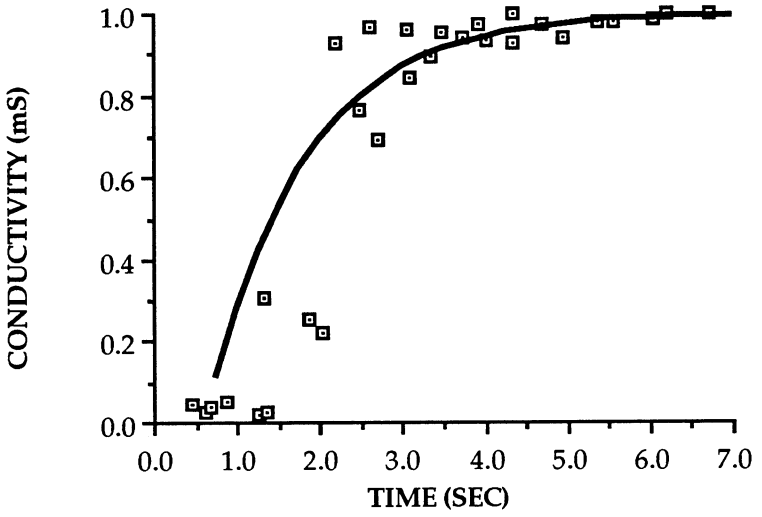

Figure 25. Representative F-curve for the residence time distribution study. Normalized conductivity of potassium chloride in a pulp suspension at the exit of the flow through reactor as a function of time.

Table 5. Calculated Values for the Mean Space Time of the flow-through Reactor

Treatment Number	Rotor Speed (rpm)	Pulp Flow Rate (cc/sec)	Gas Flow Rate (sccs)	Mean Space Time Block 1 (sec)	Block 2 (sec)	Block 3 (sec)	Average (sec)
1	1500	290	0	0.84	0.68	0.64	0.72
2	1500	701	0	0.41	0.19	0.36	0.32
3	1500	290	70	0.64	0.47	0.30	0.47
4	1500	701	70	0.37	0.35	0.34	0.35
5	2500	290	0	0.41	0.45	0.70	0.52
6	2500	710	0	0.41	0.12	0.46	0.33
7	2500	290	70	0.96	0.43	3.08*	0.70
8	2500	701	70	0.38	0.31	0.33	0.34

* Outlier as defined by analysis of Table 6. Value replaced by 0.695.

was estimated by an analysis of variance in which each set of experimental conditions was considered to be a different treatment.

The analysis of variance for the mean space time is summarized in Table 6. The error mean square is an estimate of the mean space time variance and is also included in Table 6. For these experiments, the mean space time's standard deviation was estimated to be 0.510. Using this value for the mean space time's standard deviation, only one value of the calculated mean space time met the criteria for an outlier. The outlier value was replaced by the average mean space time for the other two experiments with the same experimental conditions in subsequent data analysis.

Table 6. Outlier Analysis of Variance for the Mean Space Time

Source	Degrees of Freedom	Sum of Squares	Mean Square
Treatment	7	3.305	0.472
Error	16	4.16	0.26
Total	23	7.465	

Sample Variance $s^2 = 0.26$ Outlier $= \bar{x} \pm 2s$

Sample Standard Deviation $s = 0.51$ $= \bar{x} \pm 1.02$

The analysis of variance of the dependence of the mean space time on the gas flow rate, the rotor speed, and the pulp flow rate is shown in Table 7. The levels of the independent variables used are summarized in Table 5. The variable with the greatest impact on the mean space time was the pulp flow rate as shown in the regression equation at the bottom of Table 7.

For a noncompressible, Newtonian fluid, if the fluid's volumetric flow rate is increased by a factor of 2.4, then the average residence time in the reactor would be reduced by a factor of 2.4. In this case, when the volumetric flow rate of the pulp was increased by a factor of 2.4, the average residence time was only decreased by a factor of 1.8 which suggests that the pulp suspension was either compressible or that the flow volume changed.

There are two possible explanations for this observation. The first explanation is the compressible nature of medium consistency pulps. Kerekes et al. (13) state that there can be a substantial volume of air present in a medium consistency suspension. The void volume, ε, must be considered

Table 7. Analysis of Variance for the Reactor's Mean Space Time

Source	Degrees of Freedom	Sum of Squares	Mean Square	F-Ratio
Main Effects				
Rotor Speed	1	0.000204	0.000204	0.09
Pulp Flow rate	1	0.424	0.424	18.48*
Gas Flow rate	1	0.000337	0.000337	0.15
2 Factor Interactions				
Rotor - Pulp	1	0.000375	0.000375	0.015
Rotor - Gas	1	0.061	0.061	2.66
Pulp - Gas	1	0.005	0.005	0.22
3 Factor Interaction	1	0.076	0.076	3.30
Error	16	0.367	0.023	
Total	23	0.936		

*Significant Effects $F_{crit,0.095,1,16} = 4.49$

Regression Equation

$$\tau = 0.6008 - 0.265\ P_c$$

$P_c = (P - 290)/410$

τ - Mean Space Time

P - Pulp Flow Rate

P_c - Coded Pulp Flow Rate

Source	Degrees of Freedom	Sum of Squares	Mean Square	F-ratio
Regression	1	0.421	0.421	18.241
Residual	22	0.508	0.0231	
Total	23	0.929		

95% Confidence Interval for the P_c Coefficient = $- 0.265 \pm 0.124$

$R^2 = 0.453$

and can vary considerably for a given consistency. Because of the air in the suspension, the suspension becomes compressible, and energy must be expended compressing the pulp suspension so that it will flow through the pipe (13, 14).

In these experiments, the pulp column was observed to compress due to the pressure applied by the piston. The column compressed until it started to flow. When charging the column with pulp before an experimental run, care was taken to minimize the air content.

The second possible explanation for the smaller than expected change in mean space time is an increase in the reactor volume at the higher flow rate. The mean space time for the low level of pulp flow rate was expected to be 1.3 seconds, but the average value was 0.60 seconds. The calculated mean space time was only 46% of the expected value implying that 54% of the reactor volume was not available for pulp flow and should be considered to be dead volume. At the high level of pulp flow rate, the expected value of the mean space time was 0.53 sec, while the average calculated value was 0.34 seconds. The corresponding dead volume for the high pulp flow rate was 37% of the reactor volume. At the higher flow rate, there was about 30% more of the reactor volume available for flow than at the lower pulp flow rate.

With a smaller amount of dead volume at the higher pulp flow rate, the mean space time would be higher than expected based on the dead volume at the lower pulp flow rate. A 30% decrease in dead volume would increase the mean space time by 30%, and could account for the 25% higher

than expected mean space time at the higher pulp flow rate. During the experiments, pulp was observed to build up around the exterior baffles.

Flow Through Mixer Plug Flow Time

The data analysis of the plug flow time was performed in the same manner as that for the mean space time. The data for the plug flow time are summarized in Table 8. Outlier analysis was also done on the data as shown in Table 9. The outlier analysis indicated that one value of the plug flow time was outside the range of expected values for the data. This value is indicated by an asterisk in Table 8. The outlier was replaced by the treatment average for subsequent data analysis.

The analysis of variance of the plug flow time as a function of the gas flow rate, the pulp flow rate, and the rotor speed is summarized in Table 10.

For the low level of pulp flow rate, the measured value was 1.43 seconds which was 30% higher than that calculated, while that for the high level was 0.48 seconds which 13% higher than expected. The measured plug flow time values are longer than those expected because of the compressibility of the pulp suspension.

Regression analysis of the plug flow time produces the following equation:

$$T_{PF} = 1.279 - 0.8008\ P \qquad (37)$$

where P_c is the coded pulp flow rate described at the bottom of Table 10.

Table 8. Calculated Values for the Plug Flow Time of the Flow Through Mixer.

Treatment Number	Rotor Speed (rpm)	Pulp Flow Rate (cc/sec)	Gas Flow Rate (sccs)	Plug Flow Time Block 1 (sec)	Block 2 (sec)	Block 3 (sec)	Average (sec)
1	1500	290.7	0	1.11	1.21	1.45	1.26
2	1500	701.8	0	0.42	0.59	0.68	0.56
3	1500	290.7	70	1.40	1.19	3.11*	1.90
4	1500	701.8	70	0.42	0.07	0.45	0.31
5	2500	290.7	0	1.56	1.80	1.67	1.68
6	2500	710.8	0	0.53	0.78	0.86	0.72
7	2500	290.7	70	0.75	1.50	0.41	0.88
8	2500	701.8	70	0.09	0.49	0.36	0.31

* Outlier as defined by analysis of Table 9. Value replaced by 1.30.

Table 9. Outlier Analysis of Variance for the Plug Flow Time.

Source	Degrees of Freedom	Sum of Squares	Mean Square
Treatment	7	7.62	0.472
Error	16	3.196	0.1997
Total	23	10.816	

Sample Variance $s^2 = 0.1997$

Sample Standard Deviation $s = 0.447$

Outlier $= \bar{x} \pm 2s$

$= \bar{x} \pm 0.894$

Table 10. Analysis of Variance of The Reactor's Plug Flow Time

Source	Degrees of Freedom	Sum of Squares	Mean Square	F-Ratio
Main Effects				
Rotor Speed - R	1	0.070	0.070	0.35
Pulp Flow rate - P	1	5.43	5.43	27.2*
Gas Flow rate - G	1	0.244	0.244	1.22
2 Factor Interactions				
Rotor - Pulp	1	0.213	0.213	1.06
Rotor - Gas	1	0.952	0.952	4.76*
Pulp - Gas	1	0.099	0.099	0.494
3 Factor Interaction	1	0.608	0.608	3.04
Error	16	3.197	0.20	
Total	23	10.816		

*Significant Effects $F_{crit,0.95,1,16} = 4.49$

Regression Equation

$$T_{PF} = 1.279 - 0.800\ P_c$$

$P_c = (P - 290)/410$

T_{PF} - Plug Flow Time

P - Pulp Flow rate

P_c - Coded Pulp Flow Rate

Source	Degrees of Freedom	Sum of Squares	Mean Square	F-ratio
Regression	2	4.593	2.297	30.939
Residual	21	1.5589	0.0742	
Total	23	6.1525		

95% Confidence Interval for P_c Coefficient = 0.8008 ± 0.264

$R^2 = 0.746$

The presence of the intercept in Equation 37 suggests that there was a lag time between the piston's contact with the pulp column and the initiation of pulp movement. (The pulp column compressed as the downward flow was transferred through the pulp column.)

The dependence of the plug flow time on the gas flow rate may be due to the dependence of the frictional resistance to flow on the gas content of medium consistency pulp. Duffy et al. (14) measured the dependence of the wall shear stress on the volume percentage of air in 19% consistency pulp. Increasing the air content from 6.6 volume percent to 20.6 volume percent at 100 kPa decreases the wall shear stress by about 50%.

CHLORINE EXPERIMENTS

The purpose of this portion of the experimental program was to determine how the mass transfer of chlorine gas affected the initial phase of medium consistency pulp chlorination. In this system, the medium consistency pulp suspension and chlorine gas were mixed for a short time in a turbulent mixing zone.

In the first series of experiments, the absorption of chlorine into an eight percent-bleached pulp suspension was investigated. In the second series, the concentration of chlorine absorbed by an 8% consistency pulp suspension with sodium hydroxide (NaOH) solution was measured. In the third set of experiments, the absorption of chlorine into an unbleached pulp suspension was measured. In all cases, the absorption rate was expected to be influenced by the temperature of the pulp, the amount of gas applied, and the amount of turbulence induced by the rotor. The experimental conditions

used for the three sets of experiments were the same and are summarized in Table 11.

Chlorine Absorption in the Absence of Chemical Reaction

Prediction of the Amount of Chlorine Absorbed in the Absence of Chemical Reaction

In this set of experiments, chlorine was absorbed into a bleached pulp suspension using the flow through reactor. The resulting absorption of chlorine for each experiment is shown in Table 12. In order to estimate the experimental error, the whole Box-Behnken experimental design was run twice. In Table 12, the block variable represents the two replicates. The reactor temperature for each experiment varied from the target, because the pulp mass lost heat to the atmosphere and gained heat from the frictional energy dissipated in the reactor.

For the three levels of chlorine dosage, the maximum possible chlorine concentrations were 0.213, 1.28 and 2.34 g/l for chlorine charges of 0.24, 1.47, and 2.70% on pulp respectively. Table 12 shows that, on average, 45% of the chlorine available for absorption was captured in the liquid phase.

The data were analyzed in two ways. First a regression equation predicting the amount of absorbed chlorine was generated. Secondly, the measured value for the chlorine absorption was used to calculate the mass transfer coefficient for the system.

The regression equation calculated for the amount of absorbed chlorine is:

Table 11. Chlorine Absorption Experiments - Experimental Conditions.

Variable	Low	Middle	High
Temperature (°C)*	20.0	35.0	50.0
Rotor Speed (RPM)	200.0	1500.0	2800.0
Applied Chlorine (%)	0.24	1.47	2.70
(g/l)**	0.21	1.28	2.34

Pulp Consistency 8%

Pulp Source
Unbleached - Mixed Hardwood
Pulp initial Kappa Number - 12.25
Bleached - Commercial Eucalyptus
Mixer Mean Space Time - 0.60 seconds
Reactor Volume Available for Flow - 1.371×10^{-4} m^3

* Initial Pulp Temperature.

** Liquid phase concentration that would result if all the chlorine were absorbed.

Table 12. Absorption of Chlorine into an Inert Pulp Suspension in the Absence of Chemical Reaction.

Applied Chlorine (%)	RPM	Actual Temp. (°C)	Block	Equil. Solubility (g/l)(58)	Absorbed Chlorine (g/l)	Predicted Chlorine (g/l)
2.70	2800	39.0	1	4.87	1.25	1.164
2.70	1500	48.0	1	4.21	0.62	0.837
2.70	1500	23.0	1	6.84	0.83	0.837
2.70	200	35.0	1	5.28	0.52	0.564
1.47	2800	53.0	1	3.93	0.86	0.869
1.47	2800	23.0	1	6.84	0.91	0.869
1.47	1500	38.0	1	4.97	0.70	0.677
1.47	1500	38.0	1	4.97	0.69	0.677
1.47	1500	37.0	1	5.08	0.58	0.677
1.47	200	53.0	1	3.93	0.47	0.510
1.47	200	26.0	1	6.40	0.58	0.510
0.24	2800	37.0	1	5.08	0.17	0.269
0.24	1500	53.0	1	3.93	0.10	0.126
0.24	1500	24.0	1	6.69	0.17	0.126
0.24	200	37.0	1	5.08	0.16	0.091
2.70	2800	38.0	2	4.97	0.92	1.00
2.70	1500	48.0	2	4.21	0.69	0.699
2.70	1500	25.0	2	6.54	0.97	0.699
2.70	200	35.0	2	5.28	0.48	0.558
1.47	2800	51.0	2	4.02	0.72	0.728
1.47	2800	21.0	2	7.14	0.66	0.728
1.47	1500	37.0	2	5.08	0.66	0.554
1.47	1500	35.0	2	5.28	0.55	0.554
1.47	1500	35.0	2	5.28	0.57	0.554
1.47	200	45.0	2	4.42	0.34	0.403
1.47	200	23.0	2	6.83	0.43	0.403
0.24	2800	38.0	2	4.97	0.17	0.194
0.24	1500	50.0	2	4.07	0.07	0.076
0.24	1500	24.0	2	6.69	0.01	0.076
0.24	200	35.0	2	5.28	0.04	0.049

$$\sqrt{C_{Cl}} = 0.90 + 0.28\,K - 0.188\,K^2 + 0.109\,R + 0.0548\,K\,R - 0.0788\,B \quad (38)$$

where C_{Cl} is the concentration of chlorine in the aqueous phase, (g l^{-1}),

K is the coded chlorine charge,

R is the coded rotor speed, and

B is the experimental block number.

For all the regression calculations, the variables were transformed so that their values were either 1, 0, or -1. The conversion factors are shown in the Footnote of Table 13. The analysis of variance for the regression equation is shown in Table 13.

The chlorine concentration values calculated from Equation 38 are listed in Table 12. Figure 26 is a plot of the predicted versus the actual amount of absorbed chlorine. The line in Figure 26 is the line generated when the predicted value equals the actual values. From this plot there is no evidence of lack of fit for the regression equation. The F-ratio for lack of fit is not significant as shown at the bottom of the Table.

It is surprising that the temperature did not affect the amount of chlorine that was absorbed. One would expect that the change in chlorine solubility over the temperature range would impact the resulting chlorine concentration. (The solubility of chlorine drops from 6.54 g l^{-1} at 25 ^{o}C to 4.07 g l^{-1} at 50 ^{o}C (58).)

The significance of the block variable reflects a systematic day to day variation in the amount of chlorine absorbed. It could possibly reflect deterioration of the gas injection equipment with time due to the corrosive

Table 13. Analysis of Variance Table for the Equation Predicting the Amount of Chlorine Absorbed by an Inert Pulp Suspension in the Absence of Chemical Reaction.

Regression Equation

$$\sqrt{C_{Cl}} = 0.90 + 0.28\,K - 0.188\,K^2 + 0.109\,R + 0.0548\,K\,R - 0.0788\,B$$

Source	Degrees of Freedom	Sum of Squares	Mean Square	F-ratio
Regression	5	1.7836	0.3567	75.654*
Residual				
Lack of Fit	12	0.0670	0.00558	1.449**
Pure Error	12	0.0462	0.00385	
	24	0.1132	0.00472	
Total	29	1.8968		

$$* \text{ F-ratio} = \frac{MS_{REG}}{MS_{RES}} \qquad ** \text{ F-ratio} = \frac{MS_{LOF}}{MS_{PE}}$$

Coded Applied Chlorine K = (Applied Chlorine - 1.47)/1.23
Coded Rotor Speed R = (Rotor Speed - 1500)/1300
Experimental Block (Replicate) B = 1 or 2

95% Confidence Interval for the K Coefficient = 0.280 ± 0.0344
95% Confidence Interval for the K^2 Coefficient = -0.188 ± 0.050
95% Confidence Interval for the R Coefficient = 0.109 ± 0.0344
95% Confidence Interval for the K R Coefficient = 0.0548 ± 0.0486
95% Confidence Interval for the B Coefficient = -0.0788 ± 0.050

$R^2 = 0.940$

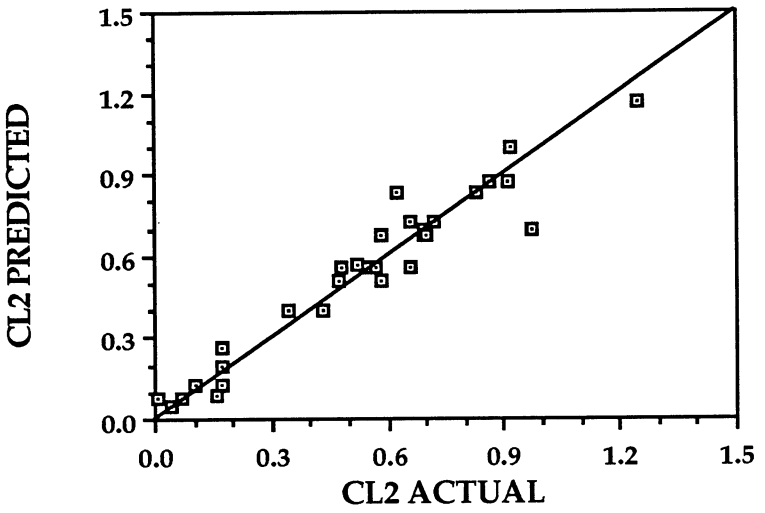

Figure 26. Predicted versus actual chlorine absorbed by an inert pulp suspension.

nature of wet chlorine gas, since there was a significant time lapse between the two replicates. The experimental design was such that the significance of the block effect did not affect the estimation of the effects of the other variables.

Figure 27 is a plot of the predicted amount of absorbed chlorine versus the applied chlorine for the first experimental block. In this figure, the effect of increasing the amount of applied chlorine can be readily seen.

At all levels of rotor speed, the amount of absorbed chlorine goes through a maximum as the amount of applied chlorine increases. This is probably due to the dependence of mass flux on the gas-liquid interfacial surface area. The surface area of the bubbles is determined by the amount of

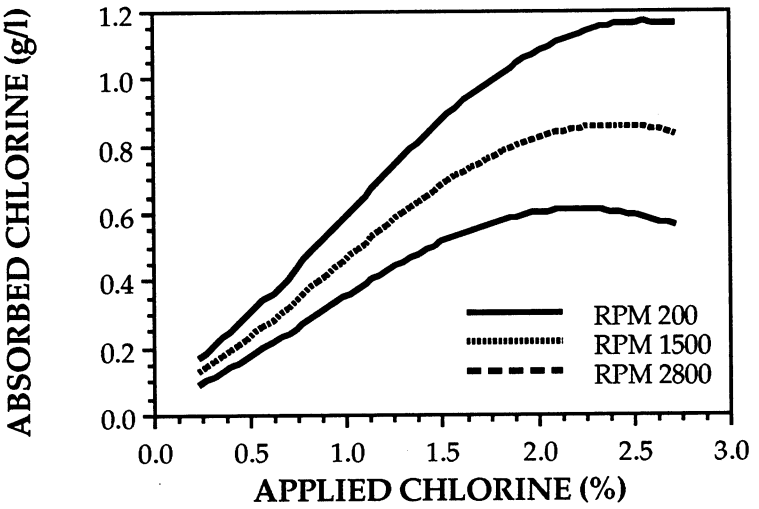

Figure 27. Predicted absorption of chlorine as a function of applied chlorine for an inert medium consistency pulp suspension.

gas applied and the shear rate in the mixer. According to this hypothesis, for a given shear rate at high chlorine charge, further increasing the chlorine gas charge results in bubble coalescence leading to an increase in the size and a decrease in the number of bubbles.

As the shear rate increases at a given chlorine charge, turbulent eddies disrupt the surface of and break up the bubbles resulting in the formation of smaller bubbles and more surface area available for mass flux. In addition, as the shear rate increases, the number of turbulent eddies increases which increases the convective diffusion of chlorine molecules away from the liquid boundary layer surrounding gas bubbles into the bulk fluid.

Prediction of the Mass Transfer Coefficient in the Absence of Chemical Reaction

Using the equation for mass transfer coefficient calculation developed in the data analysis section and shown below, the calculated values for k_la have been summarized in Table 14.

$$k_la = \frac{1}{\tau}\frac{C}{C_{Cli} - C} \tag{39}$$

The value for the space time, τ, used was 0.6.

Regression analysis of the mass transfer coefficient data indicates that the mass transfer coefficient is dependent on the amount of chlorine applied, the rate of shear in the reactor, and the pulp suspension temperature. The resulting equation is:

$$\sqrt{k_la} = 0.562 + 0.174\,K - 0.122\,K^2 + 0.0746\,R + 0.0488\,K\,R + 0.0431\,T + 0.0344\,R\,T - 0.0596\,B \tag{40}$$

where T is the coded pulp temperature in the reactor, and the other variables are the same as in the previous section. The analysis of variance for the equation is shown in Table 15 which also includes the 95% confidence interval for the coefficients in the equation.

The values predicted by Equation 40 are listed in Table 14. Figure 28 is a plot of the predicted mass transfer coefficient versus the measured value. The line in Figure 28 is the line generated when the predicted value equals the observed value. From this plot, there is no evidence of any lack of .

Table 14. Mass Transfer Coefficient for the Absorption of Chlorine into an Inert Pulp Suspension in the Absence of Chemical Reaction.

Applied Chlorine (%)	RPM	Temp. (°C)	Block	k_la	Predicted k_la
2.70	2800	39.0	1	0.494	0.488
2.70	1500	48.0	1	0.266	0.350
2.70	1500	23.0	1	0.216	0.186
2.70	200	35.0	1	0.173	0.186
1.47	2800	53.0	1	0.412	0.449
1.47	2800	23.0	1	0.238	0.265
1.47	1500	38.0	1	0.253	0.261
1.47	1500	38.0	1	0.249	0.261
1.47	1500	37.0	1	0.202	0.215
1.47	200	53.0	1	0.212	0.192
1.47	200	26.0	1	0.158	0.178
0.24	2800	37.0	1	0.0567	0.0588
0.24	1500	53.0	1	0.0430	0.0666
0.24	1500	24.0	1	0.0429	0.0306
0.24	200	37.0	1	0.0533	0.0330
2.70	2800	38.0	2	0.341	0.481
2.70	1500	48.0	2	0.298	0.283
2.70	1500	25.0	2	0.268	0.217
2.70	200	35.0	2	0.159	0.138
1.47	2800	51.0	2	0.329	0.360
1.47	2800	21.0	2	0.162	0.198
1.47	1500	37.0	2	0.232	0.201
1.47	1500	35.0	2	0.183	0.196
1.47	1500	35.0	2	0.190	0.196
1.47	200	45.0	2	0.133	0.140
1.47	200	23.0	2	0.108	0.130
0.24	2800	38.0	2	0.058	0.0354
0.24	1500	50.0	2	0.0289	0.0361
0.24	1500	24.0	2	0.0249	0.0133
0.24	200	35.0	2	0.0127	0.0146

Table 15. Analysis of Variance Table for the Equation Predicting the Mass Transfer Equation for Chlorine Absorbed by an Inert Pulp Suspension in the Absence of Chemical Reaction.

Regression Equation

$$\sqrt{k_l a} = 0.562 + 0.174\,K - 0.122\,K^2 + 0.0746\,R + 0.0488\,K\,R + 0.0431\,T + 0.0344\,R\,T - 0.0596\,B$$

Source	Degrees of Freedom	Sum of Squares	Mean Square	F-ratio
Regression	7	0.7799	0.1114	60.19*
Residual				
Lack of Fit	18	0.03652	0.00203	1.93**
Pure Error	4	0.00420	0.00203	
	22	0.0370	0.00161	
Total	29	07288		

$$* \text{ F-ratio} = \frac{MS_{REG}}{MS_{RES}} \qquad ** \text{ F-ratio} = \frac{MS_{LOF}}{MS_{PE}}$$

Coded Applied Chlorine	K = (Applied Chlorine - 1.47)/1.23
Coded Rotor Speed	R = (Rotor Speed - 1500)/1300
Coded Temperature	T = (Temperature - 35) / 15
Experimental Block	B = 1 or 2

95% Confidence Interval for the K Coefficient = 0.174 ± 0.021
95% Confidence Interval for the K^2 Coefficient = -0.122 ± 0.032
95% Confidence Interval for the R Coefficient = 0.0756 ± 0.021
95% Confidence Interval for the T Coefficient = 0.0431 ± 0.0242
95% Confidence Interval for the K R Coefficient = 0.0488 ± 0.031
95% Confidence Interval for the R T Coefficient = 0.0344 ± 0.030
95% Confidence Interval for the B Coefficient = -0.0596 ± 0.032

$R^2 = 0.95$

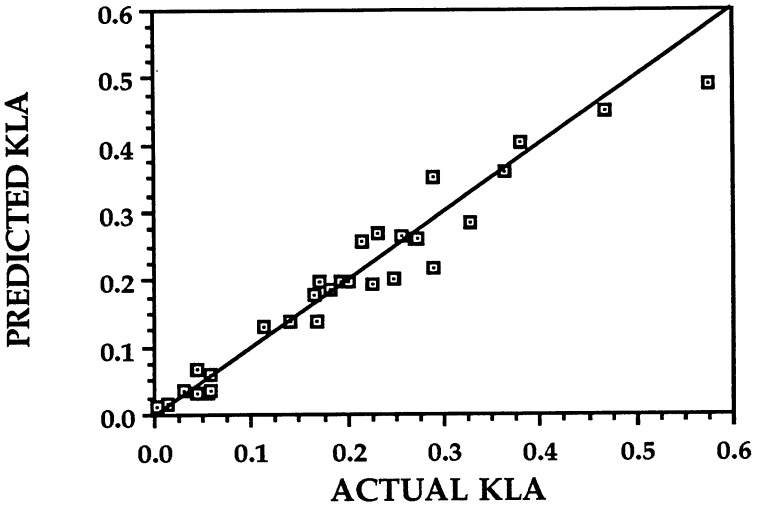

Figure 28. Predicted versus actual mass transfer coefficient for chlorine absorbed by an inert pulp suspension.

fit for the regression, nor is any expected based on the F-ratio for lack of fit shown in the table

As expected, the same terms that were significant in predicting the amount of chlorine absorbed by the suspension were important in predicting the mass transfer coefficient. In addition, the temperature of the suspension was also significant. It was expected that the temperature will increase the mass transfer coefficient as the mass transfer coefficient from bubbles in an agitated solution has been shown to be (59):

$$\frac{k\,L}{D} = 0.13\left(\frac{L^4\left(\frac{P}{V}\right)}{\rho\,\nu^3}\right)^{0.25}\left(\frac{\nu}{D}\right)^{0.33} \qquad (41)$$

where k is the mass transfer coefficient, ($m^2\ s^{-1}$)

L is the stirrer length, (m)

D is the diffusion coefficient of the material being transferred, ($m^2\ s^{-1}$)

P/V is the power per unit volume, (Wm^{-3})

ρ is the fluid density, ($kg\ m^{-3}$)

ν is the kinematic viscosity, (μ / ρ), ($m^2\ s^{-1}$) and

μ is the viscosity, ($kg\ m\ s^{-1}$).

The effect of temperature on the mass transfer coefficient may be predicted using this equation, as follows:

$$\frac{\frac{k_{35} L}{D_{35}}}{\frac{k_{25} L}{D_{25}}} = \frac{0.13 \left(\frac{L^4 \left(\frac{P}{V} \right)}{\rho_{35} \nu_{35}^3} \right)^{0.25} \left(\frac{\nu_{35}}{D_{35}} \right)^{0.33}}{0.13 \left(\frac{L^4 \left(\frac{P}{V} \right)}{\rho_{25} \nu_{25}^3} \right)^{0.25} \left(\frac{\nu_{25}}{D_{25}} \right)^{0.33}} \qquad (42)$$

$$\frac{k_{35}}{k_{25}} = \frac{D_{35}}{D_{25}} \left(\frac{\rho_{25} \left(\frac{\mu_{25}}{\rho_{25}} \right)^3}{\rho_{35} \left(\frac{\mu_{35}}{\rho_{35}} \right)^3} \right)^{0.25} \left(\frac{D_{25} \left(\frac{\mu_{35}}{\rho_{35}} \right)}{D_{35} \left(\frac{\mu_{25}}{\rho_{25}} \right)} \right)^{0.33} \qquad (43)$$

$$\frac{k_{35}}{k_{25}} = \frac{D_{35}}{D_{25}} \left(\left(\frac{\rho_{35}}{\rho_{25}} \right)^2 \left(\frac{\mu_{25}}{\mu_{35}} \right)^3 \right)^{0.25} \left(\frac{D_{25} \rho_{25} \mu_{35}}{D_{35} \rho_{35} \mu_{25}} \right)^{0.33} \qquad (44)$$

Using the diffusion coefficient, viscosity, and density summarized in Table 16, the ratio of the mass transfer coefficient at 35 °C to

Table 16. Transport Properties used for Equation 44.

Transport Property	25°C	35°C	Ref.
Diffusivity of Chlorine (8 % consistency $cm^2 s^{-1}$)	1.04×10^{-5}	1.49×10^{-5}	(18)
Viscosity of Water ($kg\ m^{-1} s^{-1}$)	8.94×10^{-4}	7.228×10^{-5}	(58)
Density of Water ($kg\ m^{-3}$)	996.96	993.65	(58)

that at 25 °C is 1.32. The ratio of the mass transfer coefficient measured at 35 °C to that at 25 °C in this experiment is 1.17 which is within the range expected from theory.

Figure 29 shows the dependence of the mass transfer coefficient on the amount of applied chlorine and the rotor speed at 35 °C. The shape and relative positions of these curves are similar to those in Figure 27 for the corresponding amount of absorbed chlorine for the reasons noted above in the discussion of Figure 27. The driving force for the transfer of chlorine into the pulp suspension is provided by the difference between the concentration of chlorine in the bulk liquid phase and that at the gas - liquid interface. In the absence of chemical reaction, this driving force will necessarily decrease as the extent of mass transfer increases, and the overall mass transfer rate will be a minimum for given values of other significant variables.

A second point of reference is provided by observation of the rate of mass transfer in the presence of a liquid - phase chemical reaction. The

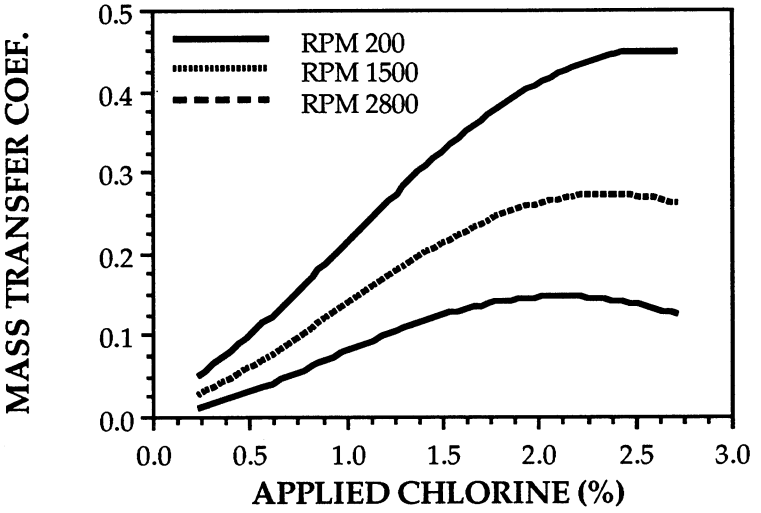

Figure 29. Predicted mass transfer coefficient as a function of chlorine charge for an inert medium consistency pulp suspension.

reaction rapidly consumes chlorine, maintaining the liquid phase chlorine concentration at or near zero, thus maximizing the liquid phase chlorine concentration and serving as one point of reference for the rate observed with unbleached pulp. If the chemical reaction leading to disappearance of chlorine in the solid phase were infinitely fast, the average concentration in the liquid phase would be reduced to a low value and the rate of mass transfer considerably enhanced. Thus, comparison of the rate of mass transfer in the presence of unbleached pulp with the corresponding reference rates (inert system and fast liquid phase reaction) allows assessment of the relative importance of chemical reaction and mass transfer in determining the rate of kraft pulp chlorination in medium consistency mixers.

Chlorine Absorption in the Presence of a Fast Liquid Phase Chemical Reaction

In order to determine the relative impact of the solid phase reaction of chlorine and lignin, it was necessary to determine the enhancement to mass transfer of a fast liquid phase reaction. The liquid phase reaction minimized the liquid side resistance to mass transfer and set the upper bound of the mass transfer coefficients in the system. For the case with a liquid side reaction, the chlorine was reacted with sodium hydroxide to form sodium hypochlorite according to the following equation:

$$Cl_2 + NaOH \rightarrow NaOCl + NaCl \qquad (45)$$

Because of the fast reaction of chlorine with sodium hydroxide ($K_{OH} = 6.82 \times 10^{16}$ l mole^{-1}) (60), the concentration of molecular chlorine in the suspension was maintained near zero. In the absence of liquid phase reaction, the chlorine concentration in the suspension created a resistance for further chlorine absorption. With a fast liquid phase reaction, the resistance to chlorine absorption due to liquid phase chlorine concentration was minimized thereby increasing the amount of chlorine transferred. The total amount of chlorine absorbed by the liquid phase was the sum of any free molecular chlorine and that which was consumed by the reaction. It was expected that the liquid phase reaction would change the form of the regression equation for both chlorine absorption and mass transfer coefficient.

Prediction of Chlorine Absorption in the Presence of a Fast Liquid Phase Reaction

Table 17 summarizes the quantity of chlorine measured in the liquid phase. Since the chlorine concentration was measured iodometrically, the value listed for chlorine concentration is the sum of the amount of chlorine as sodium hypochlorite plus that as molecular chlorine in solution. On average the amount of chlorine absorbed was 89% of the maximum available for absorption. This was twice that absorbed in the first case. The most likely reason that all the applied chlorine was not absorbed by the liquid phase, was that there was not enough retention time in the mixer. Other possible explanations were:

1) local depletion of NaOH, which could cause an increase in the local concentration of chlorine increasing the liquid phase resistance to mass transfer (mixing not fast enough),

2) as the chlorine was depleted in the gas phase, the gas driving force may have been reduced, or

3) the reaction itself was not fast enough to prevent local chlorine concentration buildup. It is most probable that the retention time had the biggest impact on the amount of absorbed chlorine.

Linear Regression analysis of the data resulted in the following equation for the amount of absorbed chlorine:

$$\sqrt{C_{Cl}} = 1.147 + 0.453\,K + 0.0968\,K\,R - 0.295\,K^2 \qquad (46)$$

The analysis of variance for the regression is shown in Table 18.

Table 17. Absorption of Chlorine into an Inert Pulp Suspension with a Fast Liquid Phase Chemical Reaction.

Applied Chlorine (%)	RPM	Block	Actual Temp. (°C)	Equil. Solubility (g/l)(58)	Absorbed Chlorine (g/l)	Predicted Chlorine (g/l)
2.70	2800	1	40.0	4.77	2.38	1.97
2.70	1500	1	47.0	4.28	1.19	1.71
2.70	1500	1	22.0	6.99	1.31	1.71
2.70	200	1	35.0	5.28	1.34	1.46
1.47	2800	1	30.0	4.07	1.29	1.32
1.47	2800	1	23.0	6.84	1.32	1.32
1.47	1500	1	37.0	5.08	1.18	1.32
1.47	1500	1	37.0	5.08	1.16	1.32
1.47	1500	1	36.0	5.18	1.35	1.32
1.47	200	1	41.0	4.70	1.30	1.32
1.47	200	1	22.0	6.99	1.30	1.32
0.24	2800	1	37.0	5.08	0.09	0.248
0.24	1500	1	49.0	4.14	0.16	0.161
0.24	1500	1	24.0	6.69	0.20	0.161
0.24	200	1	31.0	5.70	0.20	0.093
2.70	2800	2	235.0	5.28	2.04	1.97
2.70	1500	2	50.0	4.07	1.87	1.71
2.70	1500	2	19.0	7.53	2.19	1.71
2.70	200	2	33.0	5.49	1.57	1.46
1.47	2800	2	45.0	4.42	1.35	1.32
1.47	2800	2	21.0	7.14	1.54	1.32
1.47	1500	2	35.0	5.28	1.60	1.32
1.47	1500	2	35.0	5.28	1.42	1.32
1.47	1500	2	37.0	5.08	1.47	1.32
1.47	200	2	41.0	4.70	1.39	1.32
1.47	200	2	21.0	7.14	0.91	1.32
0.24	2800	2	36.0	5.18	0.17	0.248
0.24	1500	2	51.0	4.02	0.07	0.161
0.24	1500	2	21.0	7.14	0.21	0.161
0.24	200	2	30.0	5.80	0.23	0.093

Table 18. Analysis of Variance for the Equation Predicting the Amount of Chlorine Absorbed with a Fast Liquid Side Reaction.

$$\sqrt{C_{Cl}} = 1.147 + 0.453\,K + 0.0968\,K\,R - 0.295\,K^2$$

Source	Degrees of Freedom	Sum of Squares	Mean Square	F-ratio
Regression	3	3.964	1.3213	115.6*
Residual				
Lack of Fit	8	0.0390	0.004869	0.494**
Pure Error	21	0.207	0.00986	
	26	0.297	0.01143	
Total	29	4.261		

$$* \text{ F-ratio} = \frac{MS_{REG}}{MS_{RES}} \qquad ** \text{ F-ratio} = \frac{MS_{LOF}}{MS_{PE}}$$

Coded Applied Chlorine K = (Applied Chlorine - 1.47)/1.23
Coded Rotor Speed R = (Rotor Speed - 1500)/1300

95% Confidence Interval for the K Coefficient = 0.4534 ± 0.0534
95% Confidence Interval for the K^2 Coefficient = -0.295 ± 0.0782
95% Confidence Interval for the R Coefficient = 0.0968 ± 0.0138

$R^2 = 0.942$

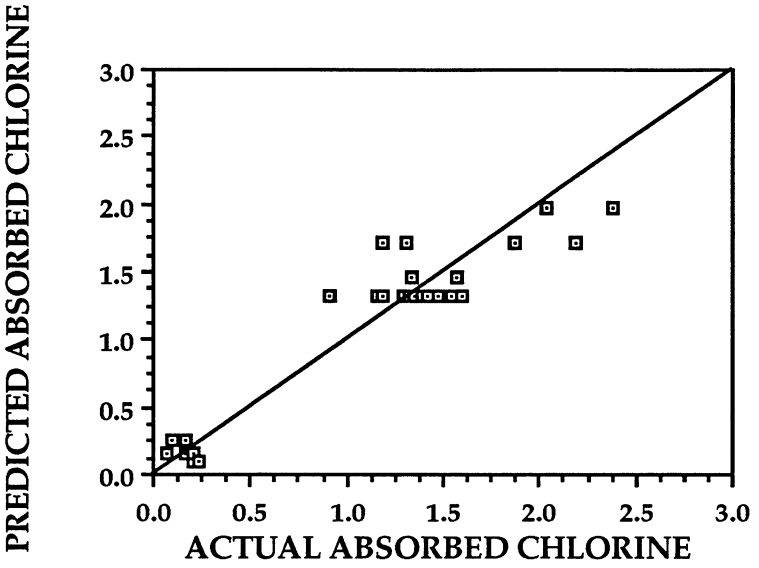

Figure 30. The predicted versus actual absorbed chlorine concentration for the quantity of chlorine absorbed by a pulp suspension with a fast liquid phase reaction.

In this experiment, the two experimental blocks were run on consecutive days so that the impact of the blocking variable was not significant.

Figure 30 is a plot of the predicted versus the actual absorbed chlorine concentration. The line drawn represents the points where the predicted equals the actual. In this Figure, the regression slightly under-predicts the highest level of absorbed chlorine, but there is no significant lack of fit (based on the lack of fit test in the Table (61)).

Figure 31 is a plot of the predicted amount of absorbed chlorine versus the applied chlorine. In Figure 31, the effect of increasing the chlorine charge can be readily seen. At all levels of rotor speed, the amount of chlorine absorbed increased with increasing chlorine charge until it reached the maximum amount of absorbed chlorine. Beyond the maximum increasing

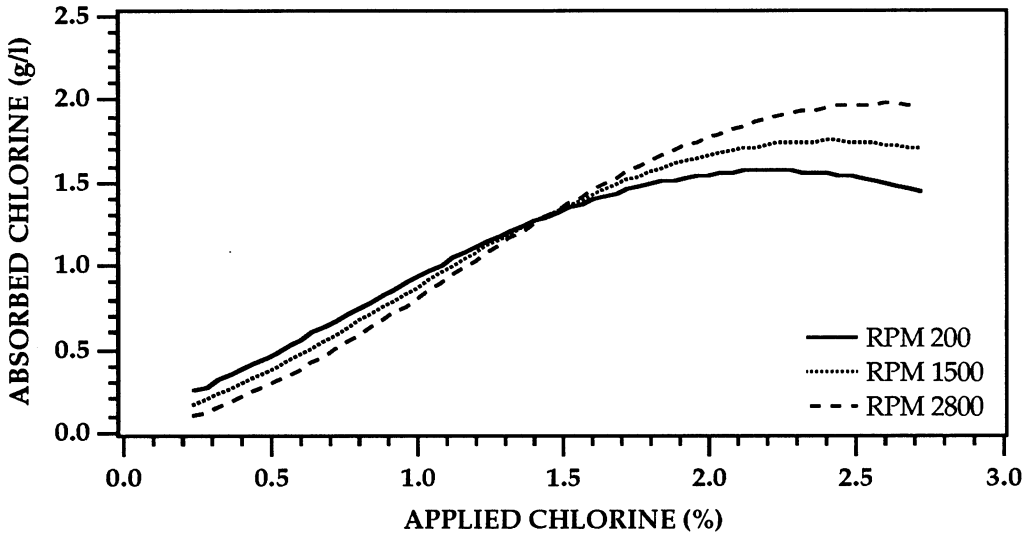

Figure 31. Predicted absorbed chlorine as a function of applied chlorine for the absorption of chlorine by a pulp suspension with a fast liquid phase reaction.

the amount of applied chlorine did not increase the amount of absorbed chlorine. The shape of the curve in Figure 31 is similar to the curve for the case without any reaction shown in Figure 29.

Increasing the rotor speed did not directly increase the amount of chlorine absorbed. The corresponding regression coefficient was expressed as the interaction between the chlorine charge and the rotor speed instead of a main effect as when there was no reaction. The difference is due to the reduction in the liquid phase mass transfer resistance due to the reaction of chlorine with sodium hydroxide. Chemical reaction prevented chlorine from building up in the boundary layer where it would inhibit other chlorine molecules from entering the liquid phase. Because the resistance to mass transfer of chlorine in the boundary layer was minimized, convective

transport of chlorine was not as important as in the case with no liquid phase reaction.

Prediction of the Mass Transfer Coefficient in the Presence of a Fast Liquid Phase Reaction.

The mass transfer coefficient was calculated using Equation 24 and the values obtained are summarized in Table 19. The equilibrium solubility concentration of chlorine at the mixer temperature was used as the value for the interfacial chlorine concentration. Because of the liquid phase reaction, the concentration of chlorine in the bulk liquid did not increase and the concentration gradient driving force for mass transfer did not diminish during the retention time in the mixer. Therefore, the mass transfer coefficient for a system with a liquid phase reaction will be larger than the mass transfer coefficient for an analogous system without reaction.

Regression analysis of the mass transfer coefficients gave the following equation:

$$\sqrt{k_l a} = 0.759 + 0.344\,K - 0.19\,K^2 + 0.0549\,R + 0.0961\,K\,R + 0.108\,T + 0.0844\,K\,T \qquad (47)$$

The analysis of variance for Equation 47 is shown in Table 20 along with the 95% confidence interval for its coefficients. Figure 32 is the plot of the predicted mass transfer coefficient versus the actual coefficients. Although there was some scatter in the data at the higher values of $k_l a$, there was not any significant lack of fit (Table 20).

Figure 33 shows the mass transfer coefficient as a function of

Table 19. Mass Transfer Coefficient for Absorption of Chlorine into a Pulp Suspension with a Fast Liquid Phase Reaction.

Applied Chlorine (%)	RPM	Block	Temp. (°C)	$k_l a$	Pred. $k_l a$
2.70	2800	1	40.0	1.66	1.274
2.70	1500	1	47.0	0.642	1.14
2.70	1500	1	22.0	0.384	0.558
2.70	200	1	35.0	0.567	0.582
1.47	2800	1	30.0	0.773	0.607
1.47	2800	1	23.0	0.398	0.531
1.47	1500	1	37.0	0.504	0.600
1.47	1500	1	37.0	0.493	0.600
1.47	1500	1	36.0	0.587	0.589
1.47	200	1	41.0	0.637	0.560
1.47	200	1	22.0	0.381	0.374
0.24	2800	1	37.0	0.030	0.0353
0.24	1500	1	49.0	0.0670	0.0615
0.24	1500	1	24.0	0.0514	0.0436
0.24	200	1	31.0	0.0606	0.0632
2.70	2800	2	35.0	1.049	1.134
2.70	1500	2	50.0	1.417	1.224
2.70	1500	2	19.0	0.684	0.502
2.70	200	2	33.0	0.668	0.544
1.47	2800	2	45.0	0.733	0.787
1.47	2800	2	21.0	0.458	0.510
1.47	1500	2	35.0	0.725	0.578
1.47	1500	2	35.0	0.613	0.578
1.47	1500	2	37.0	0.679	0.600
1.47	200	2	41.0	0.700	0.560
1.47	200	2	21.0	0.243	0.365
0.24	2800	2	36.0	0.0566	0.0347
0.24	1500	2	51.0	0.0295	0.0631
0.24	1500	2	21.0	0.0505	0.0416
0.24	200	2	30.0	0.0688	0.0535

Table 20. Analysis of Variance for the Mass Transfer Coefficient for the Case with Liquid Side Reaction

$$\sqrt{k_l a} = 0.759 + 0.344\,K - 0.19\,K^2 + 0.0549\,R + 0.0961\,K\,R + 0.108\,T + 0.0844\,K\,T$$

Source	Degrees of Freedom	Sum of Squares	Mean Square	F-ratio
Regression	6	2.455	0.4092	43.2*
Residual				
Lack of Fit	6	0.053	0.00888	0.91**
Pure Error	17	0.165	0.00971	
	23	0.2176	0.00946	
Total	29	2.6726		

$$* \text{ F-ratio} = \frac{MS_{REG}}{MS_{RES}} \qquad ** \text{ F-ratio} = \frac{MS_{LOF}}{MS_{PE}}$$

Coded Applied Chlorine	K=(Applied Chlorine - 1.47)/1.23
Coded Rotor Speed	R = (Rotor Speed - 1500)/1300
Coded Temperature	T = (Temperature - 35)/15

95% Confidence Interval for the Coefficients
95% Confidence Interval for the K Coefficient = 0.344 ± 0.0488
95% Confidence Interval for the R Coefficient = 0.0549 ± 0.0488
95% Confidence Interval for the T Coefficient = 0.0108 ± 0.0586
95% Confidence Interval for the K^2 Coefficient = -0.19 ± 0.0717
95% Confidence Interval for the K R Coefficient = 0.0961 ± 0.0698
95% Confidence Interval for the K T Coefficient = 0.0844 ± 0.0732

$R^2 = 0.918$

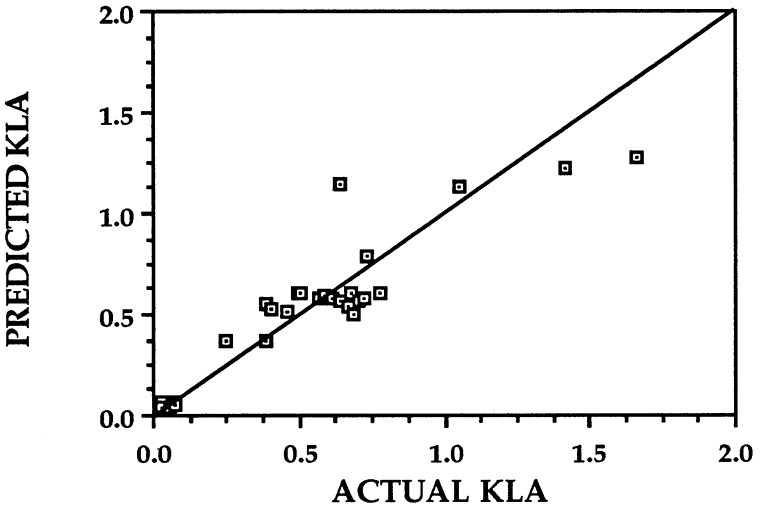

Figure 32. Predicted mass transfer coefficient versus actual mass transfer coefficient for the absorption of chlorine by a pulp suspension with a fast liquid phase reaction.

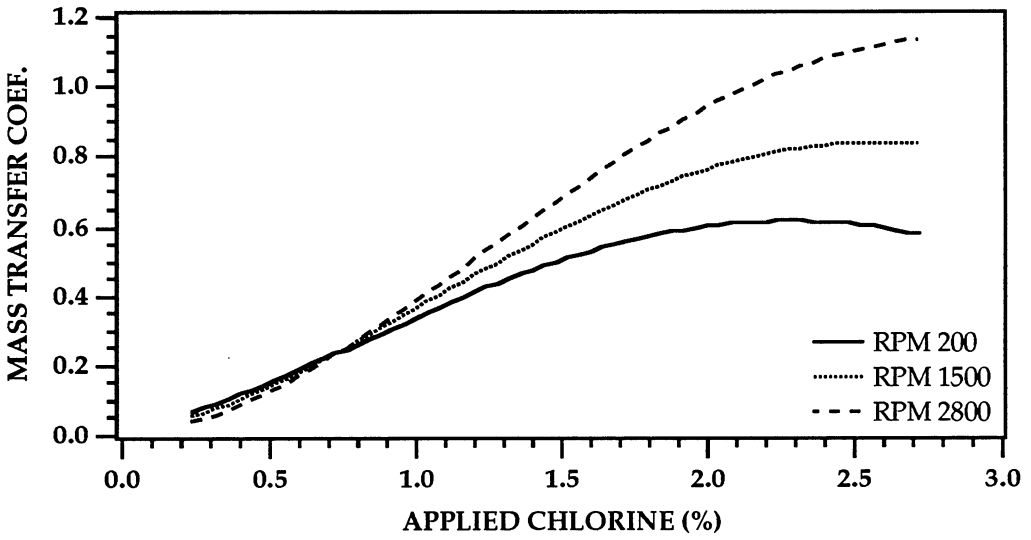

Figure 33. Predicted mass transfer coefficient as a function of chlorine charge for the absorption of chlorine by a pulp suspension with a fast liquid phase reaction.

chlorine charge at the midpoint of the temperature range (35 °C). The shape of the curve is similar to that for the case without reaction with the maximum mass transfer coefficient for the low level of rotor speed occurring at approximately the same chlorine charge.

Although rotor speed did not have a large impact on the amount of absorbed chlorine, it did affect the mass transfer coefficient. At the highest level of chlorine charge increasing the rotor speed from 200 to 2800 rpm doubled the mass transfer coefficient. One could speculate that increasing the rotor speed decreased the bubble size which increased the area available for mass transfer. At the same time, the increase in rotor speed will increase the number of turbulent eddies which will minimize the impact of local NaOH depletions.

Absorption of Chlorine in the Presence of Solid Phase Reaction

In the third experimental phase, the effect of a solid phase reaction on the mass transfer rate was measured. The solid phase reaction studied was the reaction of chlorine with kraft residual lignin according to Equation 48:

$$a\ Cl_2 + \text{lignin} \rightarrow \text{Products} \qquad (48)$$

In this system the applied chlorine can have one of three fates:

1) it can be dissolved by the liquid phase and react with the solid;

2) it can be dissolved by the liquid phase and stay in solution; or

3) it can remain in the gaseous phase.

Preliminary Flow Through Mixer Chlorination Experiments

Prior to investigating the effect of the solid phase reaction on the mass transfer coefficient, a preliminary set of experiments was run to measure how the chlorinated kappa number varied with changing mixer parameters. Three replicates were run of a 2^3 factorial design where the chlorine dosage, rotor speed, and temperature were the parameters of interest. This experiment is described in more detail in Appendix VI.

The total amount of chlorine absorbed by the liquid phase was the sum of the chlorine in solution at the end of the experiment (measured iodometrically) plus the amount of chlorine that had reacted with the lignin in the solid phase. The amount of chlorine that reacted with the lignin was calculated from the change in residual lignin content times the stoichiometric coefficient for chlorine in Equation 48. Analysis of the data using analysis of variance indicated that the chlorine dosage, rotor speed, and temperature had a significant impact on the total amount of absorbed chlorine.

Prediction of the Quantity of Lignin Consumed by Chlorine in the Flow Through Mixer Experiments

After completion of the preliminary experiments, several questions remained concerning the dependence of the extent of reaction, the amount of chlorine absorbed, and the mass transfer coefficient on mixer variables. To generate the data necessary to answer these questions, two replicates of a Box-Behnken incomplete factorial design were run. The data were analyzed so that the effects of the independent variables could be calculated. These independent variable effects were determined by changes in

the initial chlorinated-extracted kappa number (K_{CEi}), the chlorinated-extracted kappa number after an additional 10 minute reaction time (K_{CE10}), the total amount of chlorine absorbed by the pulp suspension, and the mass transfer coefficient for the system.

The K_{CEi} number was a measure of the residual lignin content when the chlorination reaction was stopped at the flow through mixer outlet by quenching the reaction with an acidified potassium iodide solution. Comparison of the K_{CEi} to the initial lignin content is an estimate of the overall reaction rate for the initial phase of the chlorination reaction. The overall reaction rate is a function of the reaction's impedances such as the resistance to mass transfer of chlorine, the resistance to diffusion of chlorine through the pulp suspension, and the intrinsic reaction rate constant.

The K_{CEi}'s for the experiment are summarized in Table 21. The amount of lignin that remained in the fiber when the reaction was stopped can be predicted by Equation 42:

$$K_{CEi} = 9.35 - 0.6\,K - 0.738\,R \qquad (42)$$

Figure 34 is the plot of predicted initial CE Kappa Number versus the observed value. There is some scatter in the data, but overall the regression equation predicts the value of the initial CE Kappa number throughout the experimental space investigated. The analysis of variance for the Equation is summarized in Table 22. The predicted values for the initial CE Kappa number are also listed in Table 21.

Figure 35 is a plot of the predicted initial CE kappa number as a function of applied chlorine. Since there was not an interaction between the

Table 21. Lignin Conversion for the Chlorine-Lignin Reaction where the Chlorinated Extracted Kappa Number Was Used as a Measure of Lignin Content

Applied Chlorine (%)	RPM	Block	Actual Temp. (°C)	K_{CEi}	K_{CEi} Pred	K_{CE10}	K_{CE10} Pred
2.070	2800	1	32.0	7.5	8.01	7.0	6.59
2.70	1500	1	34.0	9.4	8.75	7.3	7.08
2.70	1500	1	20.0	8.7	8.75	7.2	7.08
2.70	200	1	31.0	9.4	9.49	8.4	8.40
1.47	2800	1	37.0	8.9	8.61	7.5	7.59
1.47	2800	1	21.0	8.1	8.61	8.1	7.59
1.47	1500	1	35.0	9.2	9.35	6.8	7.45
1.47	1500	1	31.0	9.0	9.35	6.7	7.45
1.47	1500	1	34.0	9.3	9.35	8.0	7.45
1.47	200	1	30.0	7.9	10.09	8.1	8.15
1.47	200	1	18.0	11.8	10.09	7.8	8.15
0.24	2800	1	31.0	9.5	9.21	9.8	9.80
0.24	1500	1	36.0	9.9	9.95	9.4	9.02
0.24	1500	1	20.0	9.3	9.95	9.9	9.02
0.24	200	1	31.0	12.0	10.69	9.3	9.10
2.70	2800	2	35.0	8.5	8.01	6.1	6.59
2.70	1500	2	39.0	8.7	8.75	7.2	7.08
2.70	1500	2	22.0	9.1	8.75	7.0	7.08
2.70	200	2	32.0	9.6	9.49	8.1	8.40
1.47	2800	2	37.0	9.2	8.61	7.5	7.59
1.47	2800	2	22.0	7.0	8.61	7.2	7.59
1.47	1500	2	3.4.0	9.8	9.35	7.3	7.45
1.47	1500	2	36.0	9.5	9.35	7.8	7.45
1.47	1500	2	37.0	8.9	9.35	7.8	7.45
1.47	200	2	41.0	9.5	10.09	8.3	8.15
1.47	200	2	20.0	11.0	10.09	8.8	8.15
0.24	2800	2	32.0	10.5	9.21	9.9	9.80
0.24	1500	2	34.0	9.7	9.95	7.9	9.02
0.24	1500	2	30.0	9.8	9.95	8.8	9.02
0.24	200	2	33.0	9.8	10.69	8.8	9.10

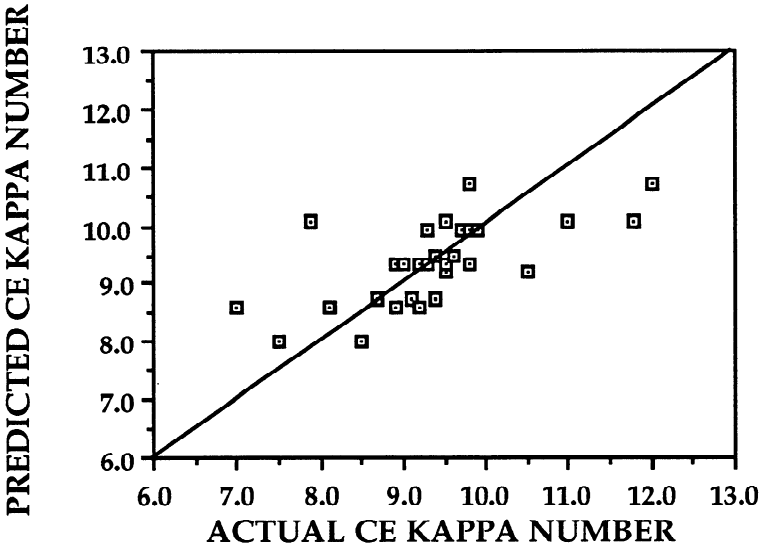

Figure 34. Predicted versus actual K_{CEi} for the reaction of chlorine with the solid phase in the flow through mixer.

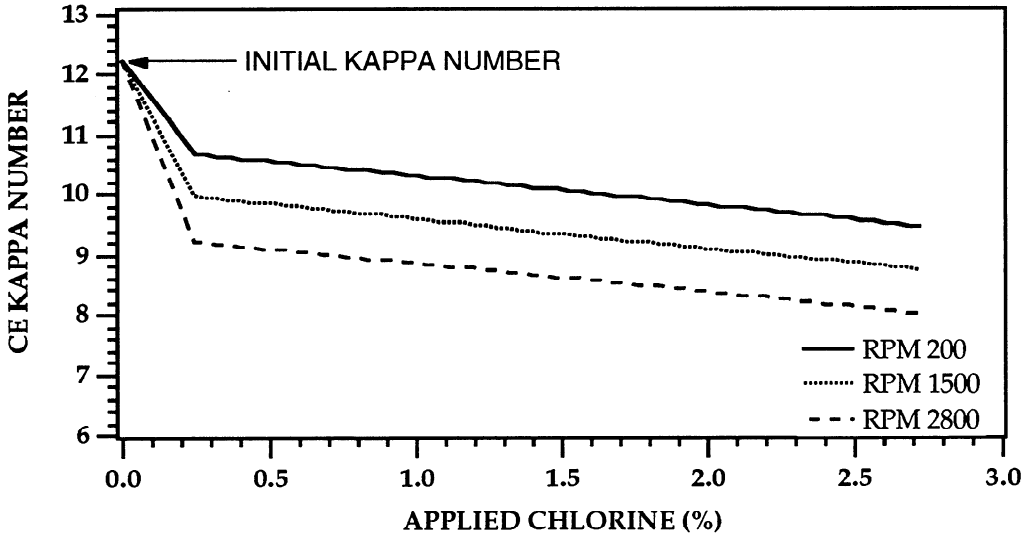

Figure 35. Predicted K_{CEi} as a function of applied chlorine.

Table 22. Analysis of Variance Table for the Prediction of the K_{CEi}.

$$K_{CEi} = 9.35 - 0.6\,K - 0.738\,R$$

Source	Degrees of Freedom	Sum of Squares	Mean Square	F-ratio
Regression	2	14.463	7.231	10.501*
Residual				
Lack of Fit	6	4.017	0.670	0.964**
Pure Error	21	14.576	0.694	
	27	18.593	0.689	
Total	29	33.055		

Coded Applied Chlorine K = (Applied Chlorine - 1.47)/1.23
Coded Rotor Speed R = (Rotor Speed - 1500)/1300

$$* \text{ F-ratio} = \frac{MS_{REG}}{MS_{RES}} \qquad ** \text{ F-ratio} = \frac{MS_{LOF}}{MS_{PE}}$$

95% Confidence Interval for the Coefficients
95% Confidence Interval for the K Coefficient = - 0.6 ± 0.414
95% Confidence Interval for the R Coefficient = - 0.738 ± 0.414

$R^2 = 0.438$

applied chlorine and rotor speed, the Figure shows a family of parallel lines where the distance between the lines is the effect of the rotor speed. In the figure, the initial kappa number of the pulp was 12.25 and has been connected to the family of curves by the dotted lines.

The overall impact of increasing the applied chlorine from 0.24 to 2.7% chlorine on pulp was to reduce the CE Kappa number by 1.2 units. This was the result of more chlorine in the liquid phase being available for reaction.

The overall impact of increasing the rotor speed from 200 to 2800 was to reduce the CE Kappa number by 1.47 units. This was the result of increased convective diffusion of chlorine from the gas-liquid interface to the fiber so that more chlorine molecules were available at the fiber wall for reaction. In this case the rotor speed had a slightly greater effect than the applied chlorine.

Table 23 summarizes the values used in Equation 43 below to calculate the reaction rate constant for the experiments. For experiments where the bulk chlorine concentration was zero, the reaction rate constant was calculated using the bulk chlorine concentration based on the applied chlorine.

$$k_c = \frac{n_l^o - n_l}{\left(C_{Cl} C_L\right) V_r} \qquad (50)$$

For a system where more than one process can contribute to the overall rate of reaction, the inverse overall reaction rate is the sum of the inverses of the coefficients of the individual processes. The dependence of the

overall reaction rate on the individual processes is similar to the sum of electrical resistances in parallel (62). Thus if one process is much slower than the others, it controls the overall rate of reaction.

For a system that is controlled only by the mass transfer coefficient, the reaction rate is expected to double for every fifty degree temperature increase (62). In other words, a mild temperature dependence is expected within the temperature range used in the experiment. For a system that is controlled only by the intrinsic chemical reaction rate, the overall reaction rate is expected to be highly dependent on temperature. For such a system, the reaction rate might, for example, double for every 10 degree increase in temperature. The calculated reaction rate for this experiment was independent of temperature as shown in Equation 51:

$$\ln\left|k_c\right| = -2.266 - 0.39\,K + 0.33\,R \qquad (51)$$

The analysis of variance for the regression is summarized in Table 24. A plot of the predicted values for the reaction rate constant versus the measured values is shown in Figure 36. There is some scatter in the data and the regression under predicts the value for the reaction rate constant at high values of the observed constant, however there was not significant lack of fit as shown in Table 24.

Figure 37 shows the relationship between the reaction rate constant and the applied chlorine and the rotor speed. For the short reaction time, 0.6 s, the reaction rate constant decreases with increasing amount of applied chlorine. This is probably due to the small change in initial CE Kappa

Table 23. Estimation of the Reaction Rate Constant for the Reaction of Chlorine with Hardwood Kraft Lignin.

Applied Cl_2 (%)	RPM	Temp. (°C)	Lignin (gmol/ m^3)	Lignin (gmol/s x 10^3)	Cl_2 (gmol/ m^3)	k_c	Pred. k_c
2.70	2800	32.0	4.64	1.060	8.71	0.121	0.0977
2.70	1500	34.0	5.81	1.327	6.29	0.0807	0.0702
2.70	1500	20.0	5.38	1.228	18.71	0.0365	0.0702
2.70	200	31.0	5.81	1.327	4.71	0.108	0.0505
1.47	2800	37.0	5.50	1.256	4.86	0.130	0.144
1.47	2800	21.0	5.01	1.144	4.29	0.199	0.144
1.47	1500	35.0	5.69	1.299	5.00	0.110	0.104
1.47	1500	31.0	5.57	1.272	4.71	0.128	0.104
1.47	1500	34.0	5.75	1.313	4.43	0.120	0.104
1.47	200	30.0	4.89	1.117	6.57	0.140	0.0746
1.47	200	18.0	7.30	1.667	2.57	0.0249	0.0746
0.24	2800	31.0	5.88	1.343	3.00	0.160	0.213
0.24	1500	36.0	6.12	1.397	3.00	0.133	0.153
0.24	1500	20.0	5.75	1.313	1.14	0.0465	0.153
0.24	200	31.0	7.42	1.694	1.00	0.0364	0.110
2.70	2800	35.0	5.26	1.201	8.00	0.0919	0.0977
2.70	1500	39.0	5.38	1.228	14.71	0.0464	0.0702
2.70	1500	22.0	5.63	1.286	7.29	0.0791	0.0702
2.70	200	32.0	5.94	1.356	18.29	0.0252	0.0505
1.47	2800	37.0	5.69	1.299	8.14	0.0681	0.144
1.47	2800	22.0	4.33	0.989	4.71	0.266	0.144
1.47	1500	34.0	6.06	1.384	3.57	0.117	0.104
1.47	1500	36.0	5.88	1.343	5.00	0.0963	0.104
1.47	1500	37.0	5.50	1.256	3.57	0.176	0.104
1.47	200	41.0	5.88	1.343	3.43	0.140	0.0746
1.47	200	20.0	6.80	1.553	2.71	0.0705	0.0746
0.24	2800	32.0	6.49	1.482	3.00	0.0934	0.213
0.24	1500	34.0	6.00	1.370	1.43	0.307	0.153
0.24	150.0	30.0	6.06	1.384	3.00	0.139	0.153
0.24	200	33.0	6.06	1.384	3.57	0.117	0.110

Table 24. Analysis of Variance Table for the Prediction of the Reaction Rate Constant

$$\ln (k_c) = -2.266 - 0.39\ K + 0.33\ R$$

Source	Degrees of Freedom	Sum of Squares	Mean Square	F-ratio
Regression	2	4.173	2.087	6.328*
Residual				
Lack of Fit	6	2.127	0.354	1.098**
Pure Error	21	6.776	0.323	
	27	8.903	0.33	
Total	29	13.076		

$$* \text{ F-ratio} = \frac{MS_{REG}}{MS_{RES}} \qquad ** \text{ F-ratio} = \frac{MS_{LOF}}{MS_{PE}}$$

Coded Applied Chlorine K = (Applied Chlorine - 1.47)/1.23
Coded Rotor Speed R = (Rotor Speed - 1500)/1300

95% Confidence Interval for the Coefficients
95% Confidence Interval for the K Coefficient = - 0.39 ± 0.288
95% Confidence Interval for the R Coefficient = 0.33 ± 0.288
$R^2 = 0.32$

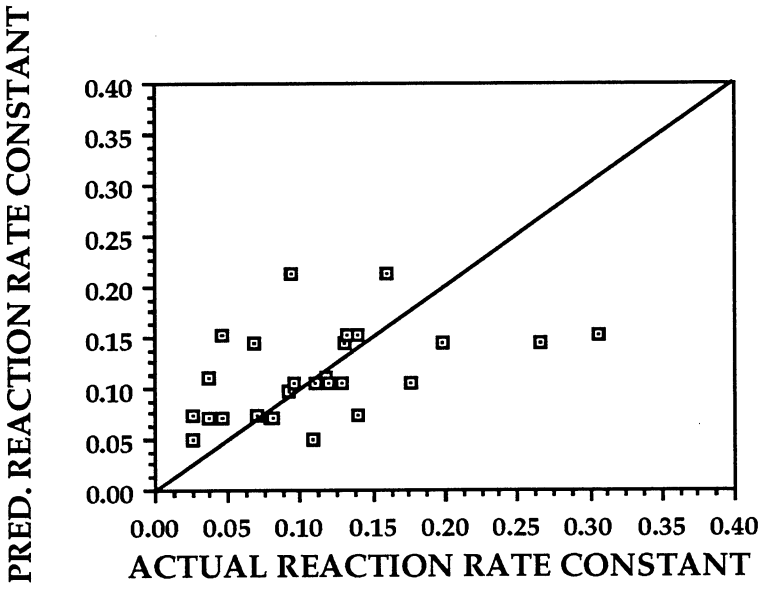

Figure 36. Predicted versus actual reaction rate constant of the chlorine-lignin reaction in the flow-through reactor.

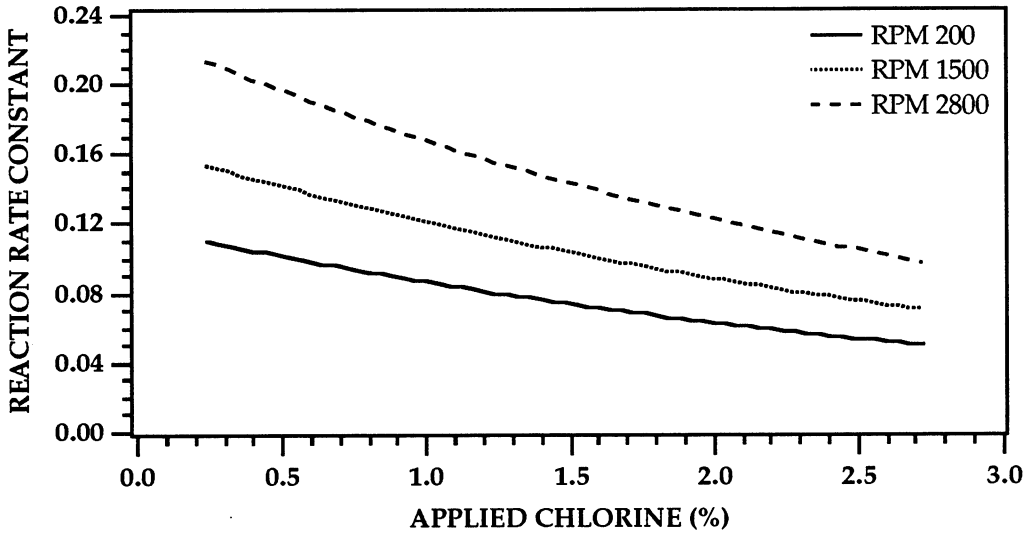

Figure 37. The overall reaction rate constant as a function of applied chlorine and rotor speed for the initial phase of chlorination.

number over the range of chlorine used, and the inverse relationship between the chlorine concentration and the reaction rate constant in Equation 51.

Because the temperature effect was not significant, it is unlikely that the intrinsic reaction rate controlled the extent of reaction for the initial phase of chlorination in the equipment used. It is likely that the mass transfer of chlorine from the gas to the liquid phase or the rate of chlorine diffusion through the bulk liquid controlled the reaction rate.

Samples were also taken at the reactor outlet, and allowed to react in a water bath for ten minutes at the desired temperature. The quantity of residual lignin at the end of ten minutes is summarized for each experiment in Table 21.

When the flow through mixer's 10 minute CE kappa numbers were compared to the CE kappa numbers for the low consistency chlorinations summarized in Table 3, the low consistency CE kappa numbers were consistently lower. The difference in performance between the batch system and the flow through system was due to the actual amount of chlorine available for each reaction. In the low consistency system, all the applied chlorine was added to the system in a solution and was available for reaction as the system was sealed after the addition of chlorine. For the flow-through system, although the same mass of chlorine was applied, only the chlorine gas that was transferred to the liquid phase was available for reaction.

The amount of lignin remaining in the medium consistency pulp at the end of 10 minutes can be described as follows:

$$K_{CE10} = 7.454 - 0.967\,K - 0.281\,R + 0.593\,K^2 - 0.625\,K\,R + 0.418\,R^2 \quad (52)$$

The analysis of variance for this Equation 52 is shown in Table 25. Note that at the end of ten minutes, the residual lignin content is dependent on the same variables that determine the amount of chlorine absorbed into the pulp suspension without a liquid phase reaction. One additional term is also included which is the square of the rotor speed. This is due to the dependence of the reaction on the amount of chlorine in solution.

Figure 38 shows the predicted residual lignin at the end of ten minutes of retention time versus the observed residual lignin content. There is some scatter in the data, but no evidence of any lack of fit. Figure 39 shows the residual CE lignin content as a function of applied chlorine and rotor speed.

Table 25. Analysis of Variance Table for the Prediction of the K_{CE10} for the flow through mixer

$$K_{CE10} = 7.454 - 0.967\,K - 0.281\,R + 0.593\,K^2 - 0.625\,K\,R + 0.418\,R^2$$

Source	Degrees of Freedom	Sum of Squares	Mean Square	F-ratio
Regression	5	23.0759	4.6152	20.13*
Residual				
Lack of Fit	3	0.1573	0.0524	0.199**
Pure Error	21	5.346	0.264	
	24	5.5028	0.2293	
Total	29	28.5787		

$$* \text{ F-ratio} = \frac{MS_{REG}}{MS_{RES}} \qquad ** \text{ F-ratio} = \frac{MS_{LOF}}{MS_{PE}}$$

Coded Applied Chlorine K = (Applied Chlorine - 1.47)/1.23
Coded Rotor Speed R = (Rotor Speed - 1500)/1300

95% Confidence Interval for the Coefficients
95% Confidence Interval for the K Coefficient = -0.9688 ± 0.2394
95% Confidence Interval for the R Coefficient = -0.2812 ± 0.2394
95% Confidence Interval for the K^2 Coefficient = 0.5933 ± 0.3514
95% Confidence Interval for the K R Coefficient = -0.625 ± 0.3386
95% Confidence Interval for the R^2 Coefficient = 0.418 ± 0.3514

$R^2 = 0.810$

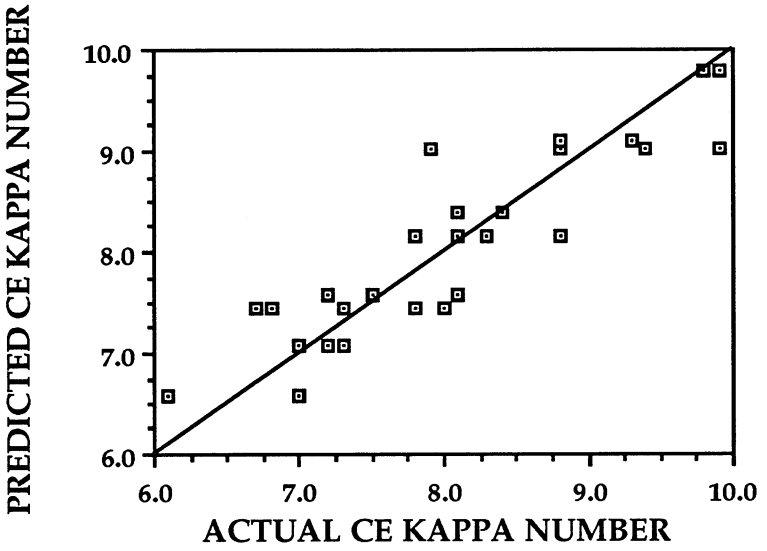

Figure 38. Predicted versus actual amount of lignin remaining at the end of 10 minutes reaction time.

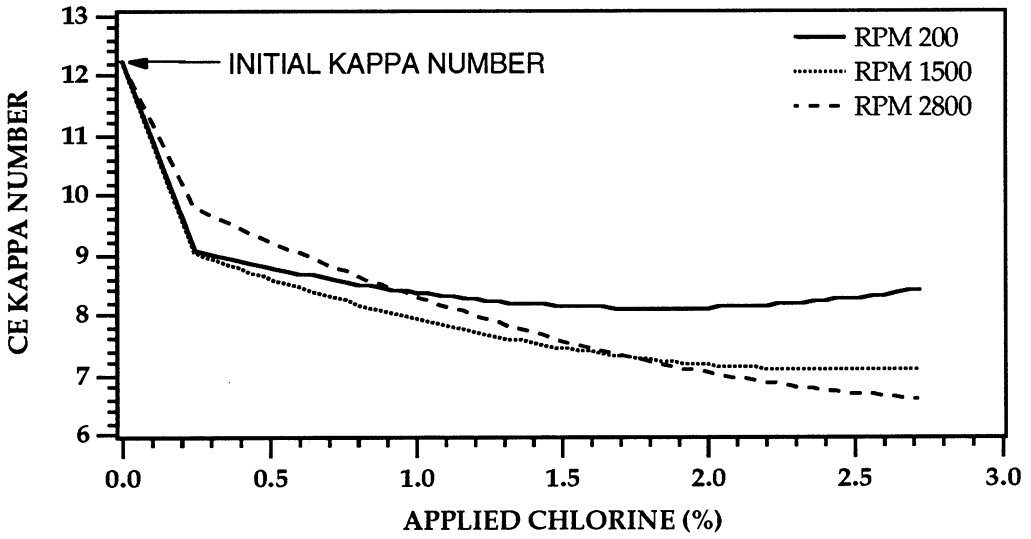

Figure 39. Chlorinated-extracted kappa number as a function of applied chlorine and rotor speed after ten minutes of retention time.

Comparison of Figures 35 and 39, at the low level of chlorine charge shows that at the high level of rotor speed all the absorbed chlorine reacted with the lignin while the pulp was still in the reactor, and no further delignification took place during the external ten minute retention time. At the middle and low level of rotor speed, further delignification occurred during the 10 minute retention time (the kappa number dropped from 10.7 to 9.0 and from 10.0 to 9.0 at the low and middle levels of rotor speed, respectively).

Therefore, when the system was severely underchlorinated, high rates of rotor speed facilitated the consumption of chlorine, but not all of the chlorine was consumed by delignification reactions. For the same chlorine charge and slower mixing rates, the chlorine may not have been consumed as quickly as in the case of high rotor speed, but ultimately more lignin was removed as chlorine molecules remained in the bulk liquid for longer periods of time.

As the chlorine charge was increased, the effect of higher the rotor speeds was seen by greater amounts of the delignification. Increasing the rotor speed, facilitated replenishment of the chlorine molecules at the boundary layer surrounding the fiber.

Prediction of the Amount of Chlorine Absorbed in the Presence of Solid Phase Chemical Reaction

The total amount of chlorine that was absorbed by the pulp suspension was the sum of the chlorine in solution at the mixer outlet plus the chlorine which reacted with the lignin. The amount of chlorine in

solution was measured by titration with 0.1N sodium thiosulfate. The amount of chlorine that was consumed by the lignin was equal to the amount of lignin consumed times the stoichiometric ratio for chlorine as in the Equation:

$$C_{LCl} = \left(12.25 - K_{CEi}\right) 0.133 \qquad (53)$$

For the low level of applied chlorine (Chlorine Charge = 0.24%), the value of the stoichiometric coefficient used was 1.67. The stoichiometric coefficient used for the middle and high level of applied chlorine was 2.67. The same value was used for the higher two levels of chlorine charge, because the amount of chlorine available in the liquid phase for reaction was less than that applied. The total amount of chlorine absorbed by the pulp suspension is summarized in Table 26. On average, the amount of chlorine absorbed was 1.28 times that absorbed in the case with no reaction.

Linear regression for the absorbed chlorine data results in Equation 47:

$$\sqrt{C_{Cl}} = 0.79 + 0.262\,K + 0.094\,R \qquad (54)$$

The analysis of variance for Equation 54 is shown in Table 27. The plot of the predicted absorbed chlorine versus the measured values is shown in Figure 40. There was some scatter in the data, but there is not an appreciable lack of fit.

The unique feature of Equation 54 is that there is not a quadratic term for the applied chlorine. Because of this, the curves in Figure 41 do not pass through a maximum, but continually increase. It was expected that there would be a difference in the equations because of the difference in the

Table 26. Absorption of Chlorine into a Pulp Suspension with a Solid Phase Chemical Reaction.

Cl_2 Charge (%)	RPM	Block	Actual Temp. (^0C)	Equil. Sol. (g/l)	Absorb. Cl_2 (g/l)	React. Cl_2 (g/l)	Total Cl_2 (g/l)	Pred. Cl_2 (g/l)
2.70	2800	1	32.0	5.58	0.61	0.63	1.24	1.31
2.70	1500	1	34.0	5.36	0.44	0.38	0.82	1.10
2.70	1500	1	20.0	7.29	1.31	0.47	1.78	1.10
2.70	200	1	31.0	5.69	0.33	0.38	0.71	0.92
1.47	2800	1	37.0	5.08	0.34	0.44	0.78	0.78
1.47	2800	1	21.0	7.14	0.30	0.55	0.85	0.78
1.47	1500	1	35.0	5.28	0.35	0.40	0.75	0.62
1.47	1500	1	31.0	5.69	0.33	0.43	0.76	0.62
1.47	1500	1	34.0	5.36	0.31	0.39	0.70	0.62
1.47	200	1	30.0	5.80	0.46	0.58	1.04	0.48
1.47	200	1	18.0	7.79	0.18	0.26	0.24	0.48
0.24	2800	1	31.0	5.69	0.00	0.22	0.22	0.39
0.24	1500	1	36.0	5.14	0.00	0.19	0.19	0.28
0.24	1500	1	20.0	7.29	0.08	0.24	0.32	0.28
0.24	200	1	31.0	5.69	0.07	0.19	0.26	0.19
2.70	2800	2	35.0	5.28	0.56	0.50	1.06	1.31
2.70	1500	2	39.0	4.69	1.03	0.47	1.50	1.10
2.70	1500	2	22.0	6.99	0.51	0.42	0.93	1.10
2.70	200	2	32.0	5.56	0.00	0.35	0.35	0.92
1.47	2800	2	37.0	5.08	0.57	0.40	0.97	0.78
1.47	2800	2	22.0	6.99	0.33	0.70	1.03	0.78
1.47	1500	2	34.0	5.36	0.25	0.32	0.57	0.62
1.47	1500	2	36.0	5.14	0.35	0.36	0.71	0.62
1.47	1500	2	37.0	5.08	0.25	0.78	1.03	0.62
1.47	200	2	41.0	4.70	0.24	0.36	0.60	0.48
1.47	200	2	20.0	7.29	0.19	0.17	0.36	0.48
0.24	2800	2	32.0	5.28	0.00	0.14	0.14	0.39
0.24	1500	2	34.0	5.36	0.10	0.21	0.31	0.28
0.24	1500	2	30.0	5.80	0.00	0.20	0.20	0.28
0.24	200	2	33.0	5.47	0.25	0.20	0.45	0.19

Table 27. Analysis of Variance Table for the Regression Equation Describing the Total Amount of Chlorine Absorbed by a Pulp Suspension with a Solid Phase Reaction.

$$\sqrt{C_{Cl}} = 0.79 + 0.262\,K + 0.094\,R$$

Source	Degrees of Freedom	Sum of Squares	Mean Square	F-ratio
Regression	2	1.236	0.618	22.631*
Residual				
Lack of Fit	6	0.332	0.0553	2.86**
Pure Error	21	0.406	0.0193	
	27	0.738	0.027	
Total	29	1.974		

$$* \text{ F-ratio} = \frac{MS_{REG}}{MS_{RES}} \qquad ** \text{ F-ratio} = \frac{MS_{LOF}}{MS_{PE}}$$

Coded Applied Chlorine K = (Applied Chlorine - 1.47)/1.23
Coded Rotor Speed R = (Rotor Speed - 1500)/1300

95% Confidence Interval for the Coefficients
95% Confidence Interval for the K Coefficient = 0.262 ± 0.082
95% Confidence Interval for the R Coefficient = 0.094 ± 0.041

$R^2 = 0.626$

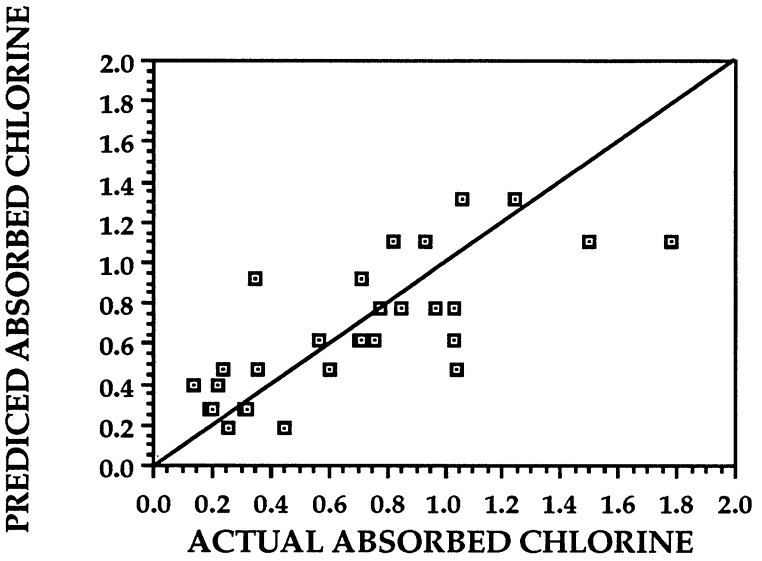

Figure 40. Predicted absorbed chlorine versus the measured values for the absorption of chlorine with a solid phase reaction.

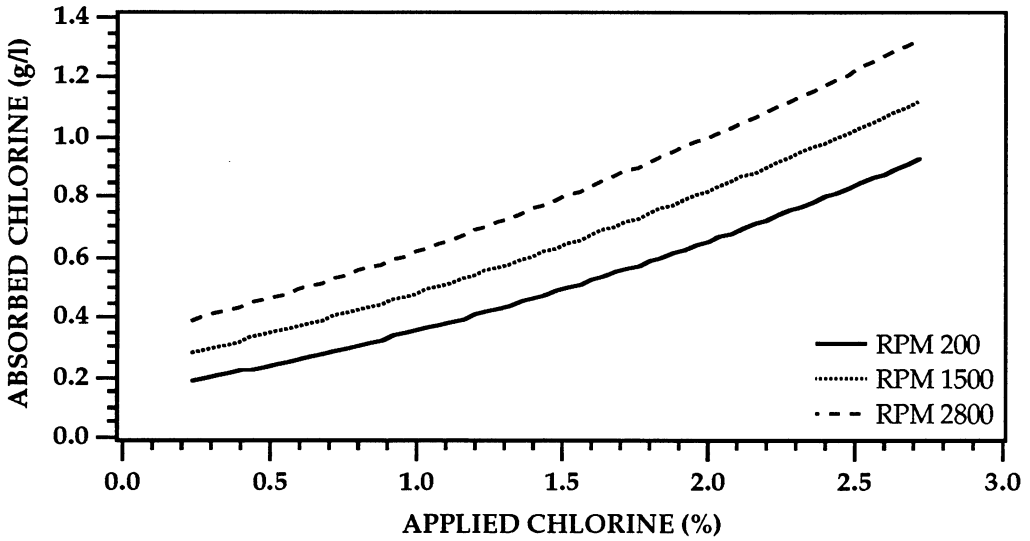

Figure 41. Predicted absorbed chlorine as a function of applied chlorine for the absorption of chlorine by a pulp suspension with a solid phase reaction.

chlorine concentration profiles for the three cases. Figure 42 depicts the three chlorine concentration profiles.

For first and second case, the gradient across the gas-liquid boundary layer controls the mass transfer. For case 3, the gas-liquid boundary layer gradient plus the liquid-solid boundary layer gradients control the mass transfer. The bulk chlorine concentration in the third case depended on the relative speed at which the chlorine diffused to the fiber surface when compared to the rate at which it was consumed at the fiber surface. At one extreme if the reaction rate was slower than the diffusion rate, the bulk chlorine concentration would increase, so that case 3 would be analogous to case 1. At the other extreme, if the reaction rate was so fast that the diffusion rate across the bulk fluid was the limiting step in the process, then case three would be analogous to case 2. The main difference between case 3 and case 2 would be that the point of zero chlorine concentration for case 3 would be at the fiber surface instead of at the edge of the gas-liquid boundary layer. In other words for case 3, there would be a constant chlorine concentration gradient across the fluid layer surrounding the fiber.

In this experiment, case 3 lay between the two extreme cases as the total amount of absorbed chlorine lay between that measured for the other two cases.

Prediction of the Mass Transfer Coefficient in the Presence of Solid Phase Reaction

The mass transfer coefficient was calculated using Equation 24. The interfacial concentration of chlorine used for the calculation was the

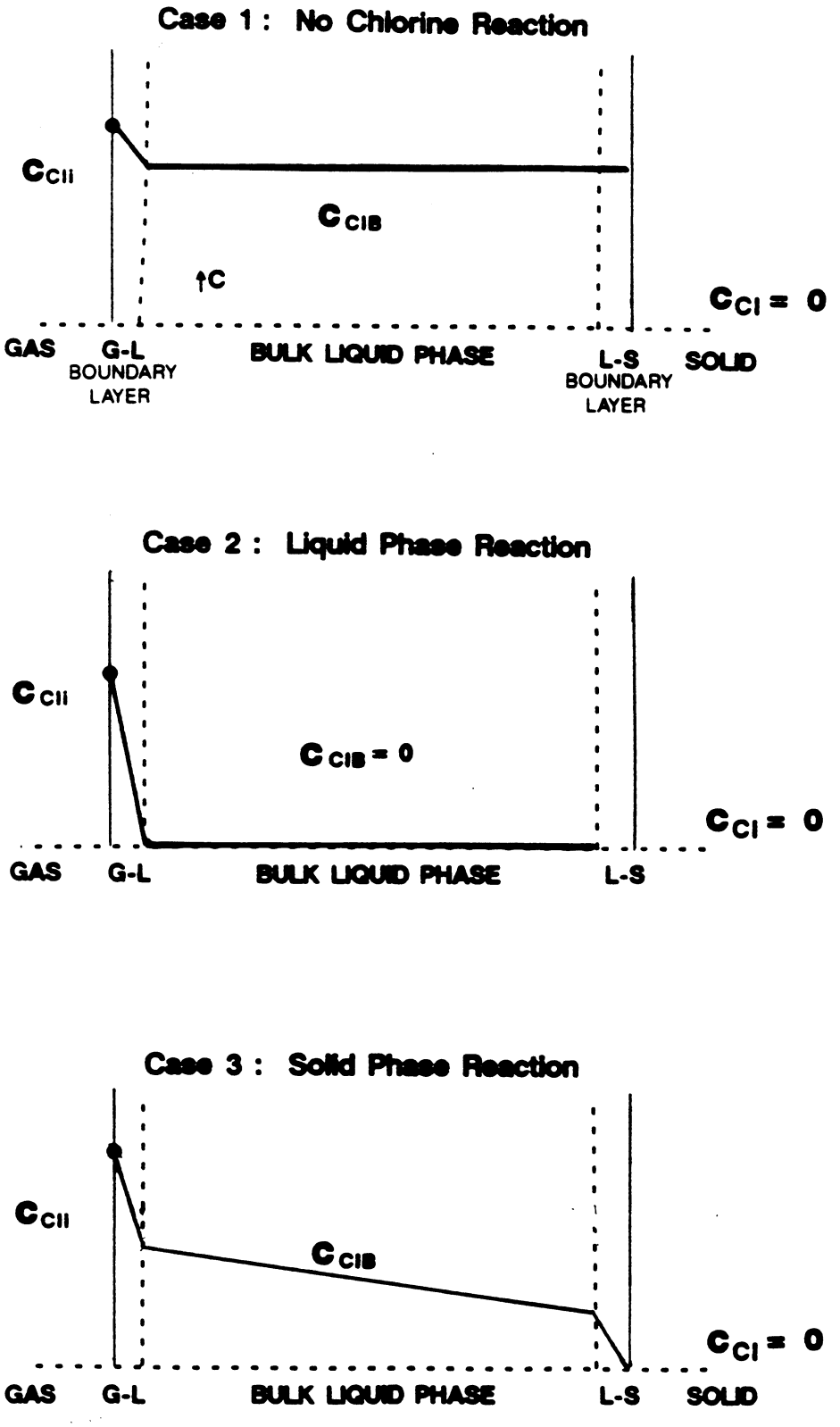

Figure 42. Concentration profiles for the three experimental cases.

equilibrium solubility concentration for the temperature of the experiment. The calculated values of mass transfer are summarized in Table 28.

For the liquid phase reaction, the interfacial resistance to mass transfer was minimized due to the ability of chlorine to react with sodium hydroxide in the boundary layer surrounding the gas bubbles. Because the reaction of chlorine with the lignin occurred within the fiber wall, chlorine molecules had to diffuse through the bulk liquid to reach a fiber. Assuming that the reaction rate was fast when compared to the diffusion and mass transfer rates, the concentration of chlorine in the fluid envelope around the fiber was zero. Since the fiber was a chlorine sink, the slope of the overall chlorine gradient remained constant and was determined by the rate of chlorine diffusion from the gas-liquid interface to the fiber. (As shown in Figure 42.)

The mass transfer coefficient was dependent on the chlorine charge, the rotor speed, the temperature, and the chlorine charge-rotor speed interaction as shown in Equation 55:

$$\sqrt{k_l a} = 0.496 + 0.163\ K + 0.0505\ R + 0.0843\ K\ R + 0.105\ T \qquad (55)$$

The analysis of variance for the regression is shown in Table 29. Figure 43 shows the predicted versus actual mass transfer coefficient for the case with solid phase reaction. In this figure, there is some scatter in the data at the higher levels of mass transfer coefficient, however there was no significant lack of fit as shown in Table 29.

Table 28. Mass Transfer Coefficient for the Absorption of Chlorine into a Pulp Suspension with a Solid Phase Reaction.

Cl_2 Charge (%)	RPM	Block	Temp. (°C)	k_la	Pred. k_la
2.70	2800	1	32.0	0.476	0.597
2.70	1500	1	34.0	0.301	0.425
2.70	1500	1	20.0	0.538	0.307
2.70	200	1	31.0	0.238	0.246
1.47	2800	1	37.0	0.302	0.314
1.47	2800	1	21.0	0.225	0.200
1.47	1500	1	35.0	0.276	0.246
1.47	1500	1	31.0	0.257	0.219
1.47	1500	1	34.0	0.250	0.239
1.47	200	1	30.0	0.364	0.169
1.47	200	1	18.0	0.0530	0.107
0.24	2800	1	31.0	0.0670	0.0739
0.24	1500	1	36.0	0.0640	0.116
0.24	1500	1	20.0	0.0765	0.0520
0.24	200	1	31.0	0.0798	0.0648
2.70	2800	2	35.0	0.419	0.630
2.70	1500	2	39.0	0.784	0.472
2.70	1500	2	22.0	0.256	0.322
2.70	200	2	32.0	0.112	0.253
1.47	2800	2	37.0	0.393	0.314
1.47	2800	2	22.0	0.288	0.207
1.47	1500	2	34.0	0.199	0.239
1.47	1500	2	36.0	0.267	0.253
1.47	1500	2	37.0	0.429	0.260
1.47	200	2	41.0	0.244	0.238
1.47	200	2	20.0	0.0866	0.116
0.24	2800	2	32.0	0.0454	0.0774
0.24	1500	2	34.0	0.102	0.106
0.24	1500	2	30.0	0.0595	0.0890
0.24	200	2	33.0	0.149	0.124

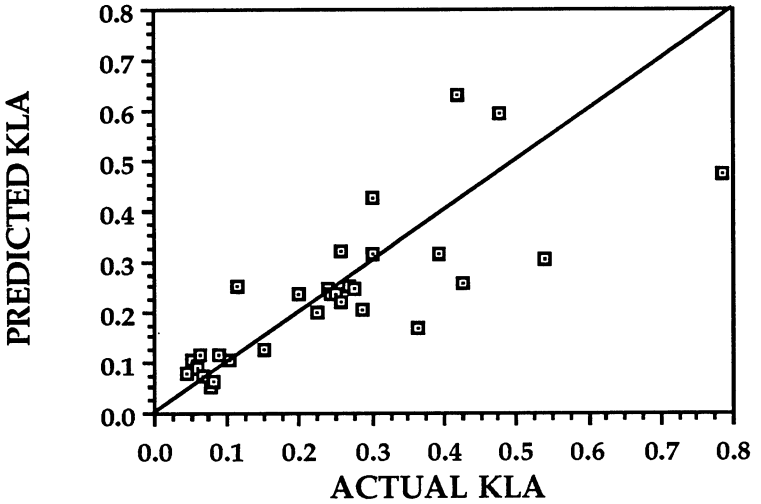

Figure 43. Predicted versus actual mass transfer coefficient for the absorption of chlorine by a pulp suspension with solid phase reaction.

Table 29. Analysis of Variance Table for the Regression Equation Describing the Mass Transfer Coefficient for a Pulp Suspension with a Solid Phase Reaction.

$$\sqrt{k_1 a} = 0.496 + 0.163\,K + 0.0505\,R + 0.0843\,K\,R + 0.105\,T$$

Source	Degrees of Freedom	Sum of Squares	Mean Square	F-ratio
Regression	4	0.5919	0.1480	14.83*
Residual				
Lack of Fit	8	0.0932	0.01165	1.268**
Pure Error	17	0.1562	0.00919	
	25	0.2494	0.00998	
Total	29	0.8413		

$$* \text{ F-ratio} = \frac{MS_{REG}}{MS_{RES}} \qquad ** \text{ F-ratio} = \frac{MS_{LOF}}{MS_{PE}}$$

Coded Applied Chlorine K = (Applied Chlorine - 1.47)/1.23
Coded Rotor Speed R = (Rotor Speed - 1500)/1300
Coded Temperature T = (Temperature - 35)/15

95% Confidence Interval for the Coefficients
95% Confidence Interval for the K Coefficient = 0.163 ± 0.0499
95% Confidence Interval for the T Coefficient = 0.0105 ± 0.0872
95% Confidence Interval for the R Coefficient = 0.0505 ± 0.0500
95% Confidence Interval for the K R Coefficient = 0.0843 ± 0.0707
$R^2 = 0.703$

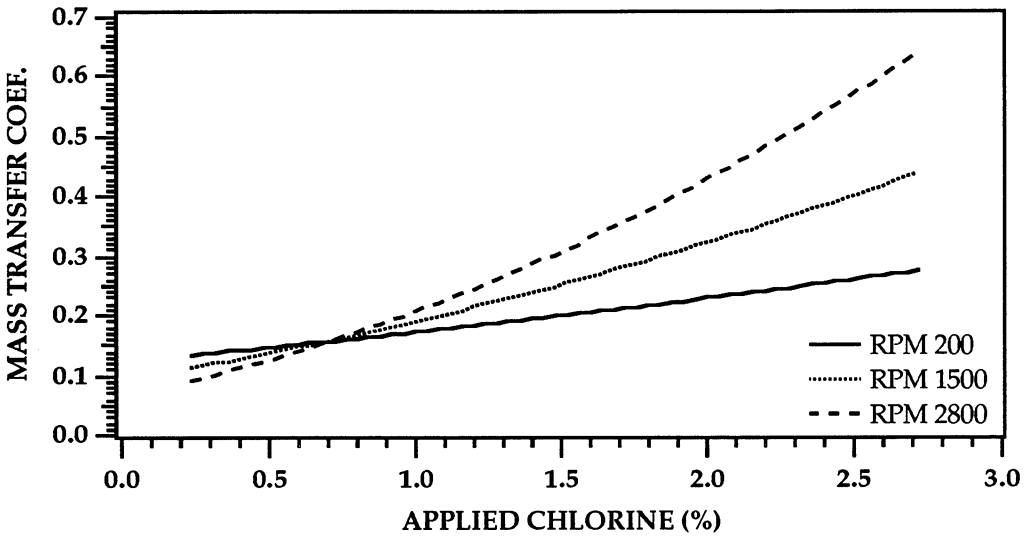

Figure 44. Predicted mass transfer coefficient as a function of applied chlorine for the absorption of chlorine by a pulp suspension with a solid phase reaction.

Figure 44 shows the shape of the predicted mass transfer coefficient curve as a function of applied chlorine and rotor speed at 35 °C. The mass transfer curve appears to be an increasing function of chlorine charge and rotor speed. Comparison of Figure 44 with Figure 33 shows that the mass transfer coefficient for the case of solid phase reaction does not go through a maximum. In addition, the values for the mass transfer coefficient are much lower for the case with solid phase reaction than for the case with liquid phase reaction. They are, however, higher than the mass transfer coefficients for the case with no reaction.

The three equations for prediction of the mass transfer coefficient are listed in Table 30. As one can see, the equation for the solid phase reaction lacks the quadratic term for the applied chlorine. The quadratic

Table 30. The Coefficients for the Equation Predicting the Square Root of the Mass Transfer Coefficient for the Flow Through Reactor.

Case No.	Constant	Applied Chlorine	RPM	Temp.	Applied Chlorine sq.	Ap. Cl. X RPM	Ap. Cl. X Temp.	RPM X Temp.
1	0.562	0.174	0.0746	0.0431	-0.122	0.0488		0.0344
2	0.760	0.344	0.0549	0.108	-0.190	0.0961	0.0844	
3	0.496	0.163	0.0505	0.105		0.0843		

term causes the inflection in the curves of case 1 and 2 which results in the maximum values of mass transfer coefficient.

The effect of temperature on the mass transfer coefficient is slightly larger that what would be expected based on the transport properties of the system. For a ten degree increase in temperature (25 ^{o}C to 35 ^{o}C), the ratio of the mass transfer coefficient at 35 ^{o}C to that at 25 ^{o}C is 1.36. The ratio predicted based on the transport properties is 1.32. The temperature affect lies between that for the cases of liquid phase reaction and no reaction. For comparison the temperature ratio for the case with liquid side reaction is 1.29 and that for no reaction is 1.17.

The dependence of the mass transfer coefficient on the rotor speed can be described as the ratio of the mass transfer coefficient at the high level of rotor speed to that at the low level of rotor speed. The ratio for the case with no reaction was 2.47. The ratio for the case with a liquid phase reaction was 1.95. The ratio for the solid phase reaction case was 2.29.

The system without a reaction is highly dependent on the rotor speed, because the turbulence generated by increasing the shear rate enhances the diffusion on chlorine away from the gas liquid interface into the bulk fluid. The system with the liquid phase reaction is only slightly dependent of the shear rate, because the chlorine can react with the reactive species in the gas-liquid boundary layer. Increasing the shear rate replenishes the reactive species to prevent local depletion of the reactive species in the gas-liquid boundary layer.

For the system with a solid phase reaction, the mass transfer dependence on the shear rate is halfway between the two extreme cases. Increasing the shear rate enhances the diffusion away from the gas-liquid interface to the bulk fluid, and it enhances the movement of chlorine molecules away from the bulk fluid to the solid surface. The convective diffusion is also accompanied by natural diffusion from the gas-liquid interface to the solid surface due to the concentration gradient.

CONCLUSIONS

1. On the basis of the relative mass transfer coefficients and quantities of absorbed chlorine, it may be concluded that the diffusion of chlorine away from the gas-liquid interface controls the rate of reaction of chlorine with medium consistency kraft pulp.

Of the cases examined, that of rapid liquid phase reaction resulted in absorption of the most chlorine, with 90% of the applied chlorine transferred to the liquid phase. In the absence of chemical reaction, only 45% of the applied chlorine was absorbed. The quantity of chlorine absorbed by the unbleached pulp suspension was 58% of the available chlorine. The reaction of chlorine with lignin reduced the liquid phase chlorine concentration and maintained a steeper chlorine concentration gradient than in the case without reaction.

2 The mass transfer coefficients for the case with liquid phase reaction were the largest, indicating that the reaction of chlorine with sodium hydroxide minimized the liquid side mass transfer resistance.

The coefficients for the case with a solid phase reaction were slightly greater than those for the case without reaction. For these experiments, the reaction of chlorine with lignin did not reduce the liquid phase mass transfer resistance to the same extent as that for the case with a fast liquid phase reaction.

3. The amount of chlorine charged to the system had the largest impact on the mass transfer coefficient. The effect of increasing the chlorine charge from 0.24 to 2.7% on pulp for the case with no reaction was to increase the

mass transfer coefficient 7 times. The coefficient increased 16 times for the case with a fast liquid reaction while it increased only 4 times for the case with a solid phase reaction.

4. The effect of the rotor speed on the mass transfer coefficient was to increase it 2.5 times for the case with no reaction. For the case with a liquid phase reaction, the coefficient increased 1.95 times while that for the case with a solid phase reaction was 2.29 times. The rotor speed had the biggest impact on the case without a reaction, because higher levels of turbulence will aid in the removal of chlorine from the gas-liquid interface to the bulk fluid.

5. The effect of temperature on the mass transfer coefficient was to increase the coefficient 1.5 times for the case without a reaction. The temperature effect for the case with a liquid phase reaction increased the coefficient 1.77 times. The temperature effect for the case of reaction with unbleached pulp increased the coefficient 2.36 times. The positive effects of increased temperature on the system's transport properties had the biggest impact on the solid reaction case.

6. For chlorine-lignin reaction in this system, the reaction rate constant was independent of temperature indicating that a physical process controlled the overall reaction rate.

7. The flow through reactor used for this thesis could be described as a continuous stirred tank reactor. The reactor volume available for flow was smaller than anticipated, because of pulp build-up around the stationary baffles.

RECOMMENDATIONS

1. Modify the flow-through mixer so that sufficient back pressure is maintained in the reactor to simulate actual mill conditions.

2. Modify the reactor to reduce the dead volume in the mixing chamber.

ACKNOWLEDGEMENTS

The author would like to thank the Institute of Paper Science and Technology and the Member Companies for the support necessary to complete this thesis. I would like to thank my thesis committee members present and past, who over the years have provided the technical guidance necessary to bring it to fruition: Dr. T. McDonough, Dr. E. Malcolm, Dr. J. Lindsay, Dr. J. Cameron, Dr. T. Farrington, and Dr. D. Wahren. I would especially like to thank Dr. McDonough whose confidence in me never wavered.

The author would like to acknowledge the support and patience of Scott Paper Company in that they gave my equipment a home during the transition. I would also like to thank the staff at Scott especially Dr. P. Yiannos who constantly prodded me into finishing this piece of work.

Lastly, I would like to show my never ending gratitude to my family. James, Annie, and Daniel this is for you.

NOMENCLATURE

A - Area available for mass transfer, (m^2)

A_C - Chapnerkar's empirical constant, (dimensionless)

a - Empirical constant for determining the disruptive shear stress of a pulp suspension, (dimensionless)

a - Interfacial area in reactor volume, (m^2)

a_i - Interfacial area between the gas and liquid phases, (m^2)

a_s - Interfacial area between the solid and liquid phases, (m^2)

B - Block number, (dimensionless)

B_c - Chapnerkar's empirical constant, (dimensionless)

b - Empirical constant for determining the disruptive shear stress of a pulp suspension, (dimensionless)

C - Tracer concentration, (moles m^{-3})

C_{ClB} - Concentration of chlorine in the bulk liquid phase, (moles m^{-3})

C_{Cli} - Concentration of chlorine at the gas interface, (moles m^{-3})

C_{Clout} - Concentration of chlorine at the reactor outlet, (moles m^{-3})

C_{Cls} - Liquid phase concentration of chlorine at the solid-liquid interface, (moles m^{-3})

C_L - Concentration of lignin, (moles m^{-3})

C_{LCl} - Concentration of chlorine consumed by the reaction with lignin, (moles m^{-3})

C_m - Pulp consistency, (%)

C_o - Liquid phase chlorine concentration, (moles cm^{-3})

C_0 - Tracer concentration of the step input zone, (moles m^{-3})

C_1 - Concentration of reacting gas, (kg m^{-3})

C_1^0 - Concentration of reacting gas at the tarnish's outer surface, (kg m^{-3})

D_1 - Diffusion coefficient of reacting gas, (m^2 s^{-1})

D_{25} - Diffusion coefficient of chlorine at 25 °C, (m^2 s^{-1})

D_{35} - Diffusion coefficient of chlorine at 35 °C, (m^2 s^{-1})

G - Gas flow rate, (cm^3 s^{-1})

H - Henry's constant for chlorine, (N m $mole^{-1}$)

K - Coded applied chlorine, (dimensionless)

K_{CEi} - Initial chlorinated-extracted kappa number, (dimensionless)

NOMENCLATURE CONTINUED

K_{CE10} - Chlorinated-extracted kappa number after 10 minutes of chlorination time, (dimensionless)

k_c - Reaction rate constant for the lignin-chlorine reaction (s^{-1})

k_{c2} - Reaction rate constant for second order reaction, (m^3 $moles^{-1}$ s^{-1})

k_c' - Pseudo-first order reaction rate constant (s^{-1})

$k_{g\,Cl}$ - Gas side mass transfer coefficient, (moles N^{-1} m^{-3} s^{-1})

k_l - Liquid side mass transfer coefficient, (m^2 s^{-1})

$k_{l\,Cl}$ - Liquid-side mass transfer coefficient, (m^2 s^{-1})

$k_{l\,Cl}'$ - Liquid-side mass transfer coefficient for mass transfer to the solid phase, (m^2 s^{-1})

k_1 - Rate constant for Chapnerkar's fast reaction, (s^{-1})

k_2 - Rate constant for Chapnerkar's slow reaction, (s^{-1})

k_{25} - Mass transfer coefficient at 25 °C, (m^2 s^{-1})

k_{35} - Mass transfer coefficient at 35 °C, (m^2 s^{-1})

L - Stirrer length, (m)

L - Lignin content corrected for the fraction that reacts instantaneously, (kg m^{-3})

N_{Cl} - Flux of chlorine into the liquid phase, (moles m^{-2} s^{-1})

n_c - Chlorine outlet flow rate in the liquid phase, (moles s^{-1})

n_{co} - Chlorine inlet flow rate in the liquid phase, (moles s^{-1})

n_g - Chlorine outlet flow rate in the gas phase, (moles s^{-1})

n_{go} - Chlorine inlet flow rate in the gas phase, (moles s^{-1})

n_1 - Mass flow rate of lignin at the reactor outlet, (moles s^{-1})

n_1^o - Mass flow rate of lignin entering the reactor, (moles s^{-1})

P - Pulp flow rate, (cm^3 s^{-1})

P/V - Power/unit volume, (W m^{-3})

P_c - Coded pulp flow rate, (dimensionless)

p_{Cl} - Partial pressure of chlorine in the gas phase, (N m^{-2})

p_{Cli} - Partial pressure of chlorine in the gas phase at the gas-liquid interface, (N m^{-2})

R - reactor's rotor speed, (rev min^{-1})

R - Coded reactor's rotor speed, (dimensionless)

R - Universal gas constant, (KJ $mole^{-1}$), (cm^3 atm $moles^{-1}$ K^{-1})

NOMENCLATURE CONTINUED

r_1 - Rate of reaction for the chlorine lignin reaction, (moles m^{-3} s^{-1})
r_{Cl} - Reaction rate in Equation 8, (moles m^{-3} s^{-1}).
T - Coded temperature in the reactor, (dimensionless)
T - Temperature, (^oC)
T_K - Absolute temperature, (K)
$T_{OVERALL}$ - Time elapsed from the start of the experiment, (s)
T_{PF} - Time required for the step change to reach the reactor, (s)
t - Time, (s)
THETA - Time elapsed / total run time, (dimensionless)
V_l - Gas volume, (m^3)
V_l - Liquid volume, (m^3)
V_r - Volume of reactor, (cm^3)
v_o - Inlet volumetric flow rate, (cm^3 s^{-1})
x_1 - Tarnish thickness, (m)
z - Distance from outer surface of the tarnish, (m)

Symbol
α - Intermediate variable of the error function, (dimensionless)
ε - Power dissipation / unit volume (W m^{-3})
μ - Viscosity of water, (kg m s^{-1})
μ_{20} - Viscosity at 20 ^oC, (kg m s^{-1})
μ_{25} - Viscosity at 25 ^oC, (kg m s^{-1})
μ_{35} - Viscosity at 35 ^oC, (kg m^{-1} s^{-1})
ν - Kinematic viscosity, (m^2 s^{-1})
ρ - Bulk density of the tarnish, (kg m^{-3})
ρ_{25} - Fluid density at 25^oC, (kg m^{-3})
ρ_{35} - Fluid density at 35^oC, (kg m^{-3})
τ - mean space time of the reactor, (s)
τ_d - power dissipation capacity, (s^{-1})
τ_s - Disruptive shear stress, (Pa)
ω - Mass fraction of gaseous component in tarnish, (dimensionless)

REFERENCES

1. Berry, R. M.; Fleming, B. I. Why does Chlorination and Extraction Fail to Delignify Unbleached Kraft Pulp Completely? Int'l Symp. on Wood and Pulping Chemistry. CPPA/Tappi, 1985:71-78.

2. Rydholm. S. A. Pulping Process. Interscience Publishers, 1965:917.

3. Reeve, D. W.; Earl, P. F. Mixing Gases, Water, and Pulp in Bleaching. Tappi 69(7): 84-88(1986).

4. Paterson, A. H. J.: Kerekes, R. J. Fundamentals of Mixing in Pulp Suspensions: Measurements of Microscale Mixing in Mill Chlorination Mixers. J. of Pulp and Paper Science 12(3):J78-J83(1986).

5. Paterson, A. H. J.; Kerekes, R. J. Fundamentals of Mixing in Pulp Suspensions: Measurement of Microscale Mixing of Chlorine. J. of Pulp and Paper Science 11(4):J108-J113(1985).

6. Gullichsen, J.; Harkonen, E. Medium Consistency Technology 1. Fundamental Data. Tappi 64(6): 69-72(1981).

7. Danckwerts, P. V. Appl. Sci. Res. Sect. A (3):279-296(1950).

8. Liebergott, N.; Trinh, D. T.; Poirer, N; Crotogin, R. H. Chlorination of pulp - The effect of mixing intensity, chlorine concentration, and reaction temperature. Part 1: Chlorine water - pulp system. 1984 Pulping Conference. Tappi Press, 1984:359-368.

9. Reeve, D. W.; Earl, P. F. Studies with a High Intensity Medium Consistency Laboratory Pulp Mixer. 1985 Medium Consistency Mixing Seminar, Tappi Press, 1985:19-23.

10. Bennington, C. P. J.; Kerekes, R. J.; Grace, J. R. Mixing in Pulp Bleaching. J. of Pulp and Paper Science 15(5):J186-J195(1989).

REFERENCES CONTINUED

11. Tribbling, P. Medium Consistency Chlorination: Studies in a High Intensity Laboratory Mixer. 1988 Int'l Pulp Bleaching Conf. CPPA/Tappi 1988:127-137.

12. Wahren, D. Fiber Network Structures in Papermaking Operations. Proc. Conf. Paper Science and Tech. - The Cutting Edge. Appleton, WI, The Institute of Paper Science and Technology, 1979:112-129.

13. Kerekes, R. J.; Soszynski, R. M.; Tam Doo, P. A. The Flocculation of Pulp Fibers. Papermaking Raw Materials and Their Interaction with the Production Process and their effect on Paper Properties. Trans. of the 8th Fundamental Research Symp held at Oxford: Sept. 1985. London, Mechanical Engineering Publications Ltd, 1985:265-310.

14. Duffy, G. G. APPITA 28(5):309(1975).

15. Mills, D. B.; Bar, R.; Kerwan, D. J. Effect of Solids on Oxygen Transfer in Agitated Three-Phase Systems. AIChE J 33(9):1542-1549(1987).

16. Hsu, C. L.; Hsieh, J. S. Gas-Liquid Mass Transfer and Pressure Drop in Pulp Bed with Flexible Fibers as Solid Supports. AIChE J 32(10):1710-1715 (1986).

17. Wong, B. M.; Reeve, D. W. Diffusion in Fibre Beds Part I: Fundamentals. 1988 Annual Meeting Technical Section. CPPA, 1988:A223-A228.

18. Wong, B. M.; Reeve, D. W. Diffusion in Fibre Beds Part II. Bleaching Chemicals. 1988 International Pulp Bleaching Conf. CPPA/Tappi, 1988:151-159.

19. Danckwerts, P. V. Unsteady-state Diffusion or Heat Conduction with Moving Boundary. Transactions of Faraday Society (46):701-712(1950).

20. Annau, D. R. The Effect of Forced Convection on the Dissolution of Single Chlorine Bubbles in Suspensions of Unbleached Pulp. BaSc. Thesis Vancouver, BC, University of British Columbia, 1984.

REFERENCES CONTINUED

21. Bennington, C. P. J. Mixing of Pulp Suspensions. Doctoral Dissertation. Vancouver, BC, University of British Columbia, 1988.

22. Dence, C. W.; Annegren, G. Chlorination. The Bleaching of Pulp. 3rd ed. Atlanta, GA, TAPPI Press, 1979:29-80.

23. Kempf, A. W.; Dence, C. W. Structure and Reactivity of Chlorolignin II. Alkaline Hydrolysis of Chlorinated Kraft Pulp. Tappi 53(5):864-873(1970).

24. Ni, Y.Mechanism and Kinetics of Demethylation During Kraft Pulp Chlorination. J. of Pulp and Paper Science 16(1):J13-J19(1990).

25. Sarkanen, K. V.; Strauss, R. W. Demethylation of Lignin and Lignin Models by Aqueous Chlorine Solution I. Softwood Lignins. Tappi 44(7):459-464(1961).

26. Singh, A. Mechanisms of Reactions of Chlorine, Chlorine Dioxide, and Nitrogen Dioxide. 1988 International Pulp Bleaching Conf. CPPA/Tappi, 1988:85-90.

27. Grangaard, D. H. Beaching I. The Chlorination of Pulp. Tappi 39(5):270-276 (1956).

28. Lindstrom, K.; Nordin, J.; Osterberg, F. Advances in the Identification and Analysis of Organic Pollutants in Water, Vol. 2. Ann Arbor Science, 1981:1039-1058.

29. Osterberg, F.; Lindstrom, K. Characterization of the High Molecular Chlorinated Matter in Spent Bleach Liquors (SBL) Part II. Acidic SBL. Holzforschung 39(3):149-158(1985).

30. Lindstrom, K.; Osterberg, F. Chlorinated Carboxylic Acids in Softwood Kraft Pulp Spent Bleach Liquors. Environ. Sci. Technol. 20(2):133-138 (1986).

REFERENCES CONTINUED

31. Goring, D. A. I. Physicochemical Aspects of Lignin Removal in Pulp Washing. Pulp Washing 1983 An Int'l Symp on the Fundamentals and Practice of Pulp Washing. CPPA, 1983:19-25.

32. Karter, E. M. The Role of Physico-Chemical Rate Phenomena in Wood Pulp Chlorination. Doctoral Dissertation. Orono, ME, University of Maine, 1968.

33. Pugliese, S. C.; McDonough, T. J. Kraft Pulp Chlorination: A New Mechanistic Description. Tappi 72(3):159-167(1989).

34. Kuang, S.-J.; Saka. S.; Goring, D. A. I. The Distribution of Chlorine in Chlorinated Kraft Pulp Fibers From Spruce Wood as Determined by TEM-EDX. J. of Wood Chem and Tech. 4(2):163-169(1984).

35. Pugliese, S. C. Kinetics and Mass Transfer in the Chlorination of Kraft Pulp Fibers. Doctoral Dissertation. Appleton, WI, The Institute of Paper Science and Technology, 1988.

36. Berry, R. M.; Fleming, B. I. Hot Water Treatment of Chlorinated Pulp - Part I. 1984 Pulping Conference. Tappi Press, 1984:169-171.

37. Berry, R. M.; Fleming, B. I. Hot Water Treatment of Chlorinated Pulp - Part II. J. of Pulp and Paper Science 11(5):J141-J144(1985).

38. Chapnekar, V. D. A Kinetic Study of the Chlorination of Unbleached Kraft Pulp. Doctoral Dissertation. Gainesville, Fl, University of Florida, 1961.

39. Levenspiel, O. Chemical Reaction Engineering, 2nd ed. New York, NY, John Wiley and Sons, 1972.

40. Holland, C. D.; Anthony, R. G. Fundamental of Chemical Reaction Engineering. Englewood Cliffs, NJ, Prentice-Hall, Inc, 1979.

41. Chaudhari, R.; Ramachandian, P. AIChE J 26(2):117-201(1980).

REFERENCES CONTINUED

42. Rapson, W. H.; Anderson, C. B..Dynamic Bleaching: Continuous Movement of Pulp Through Liquor Increases Bleaching Rate. Tappi 49(8):329-334 (1966).

43. Ackert, J. E.; Koch, D. D.; Edwards, L. I. Displacement Chlorination of Kraft Pulps: 1. An Experimental Study and Comparison of Models. 1975 Annual Meeting. Tappi Press, 1975:151-155.

44. Hinrichs, D. D. Gas Phase Chlorination of Kraft Pulp. Tappi 45(10):765-770 (1962).

45. Liebergott, N.; Yorston, F. H. Experiments in Rapid High Density Bleaching. Tappi 48(1):20-24(1965).

46. Liebergott, N.; Barclay, H. G.; Merka, J.; Pounds, D. P. W.; Bolker, H. I.; Clayton, D. W. 1973 Int'l Pulp Bleaching Conf. CPPA/Tappi, 1973:177-190.

47. Yagi, S.; and Kunii, D. T. 5th Symp Int'l on Combustion. 1955:231-244.

48. Hartman, M.; Coughlin, R. Reaction of Sulfur Dioxide with Limestone and the Grain Model. AIChE J 22(3):490(1976).

49. Russell, N. The Initial Phase of Aqueous Chlorination of Kraft Pulp Meals. Tappi 49(9):418(1966).

50. Cussler, E. L. Diffusion Mass Transfer in fluid systems. Cambridge, Cambridge University Press, 1984:240-248.

51. Danckwerts, P.V. Gas - Liquid Reactions. New York, McGraw - Hill, 1970:18.

52. Box, G. E. P.; Behnken, D. W.; Some New Three Level Designs for the Study of Quantitative Variables. Technometrics. 2(4):455-475(1960).

53. Burns, B. J. Laboratory Fluidization of Pulp. Masters Thesis. Appleton, WI, The Institute of Paper Science and Technology, 1986.

REFERENCES CONTINUED

54. Weast, R. C. CRC Handbook of Chemistry and Physics, 59th ed. West Palm Beach, FL, CRC Press, Inc., 1978:A37-A43.

55. Tappi Test Methods. Atlanta, GA, TAPPI Press, 1992:T236:1-3.

56. Dence, C. W.; Meyer, J. A.; Unger, K.; Sadowski, J. Steric Effects in the Dealkylation of Phenol Ethers with Aqueous Chlorine. Tappi 48(3):148-157(1965).

57. Ostle, B.; Mensing, R. W. Statistics in Research Ames, IA, Iowa State University Press, 1975:431-434.

58. Perry, R. H.; Chilton, C. H. Chemical Engineer's Handbook. New York, NY, McGraw-Hill Book Co., 1973:3-97.

59. Cussler, E. L. Diffusion Mass Transfer in fluid systems. Cambridge, Cambridge University Press, 1984:230.

60. Lahiri, R. N.; Yadav, G. D.; Sharma, M. M. Absorption of Chlorine in Aqueous Solutions of Sodium Hydroxide. Chemical Engineering Science 38(7):1119-1133(1983).

61. Draper, N,; Smith, H. Applied Regression Analysis, 2nd ed. New York, NY, John Wiley & Sons, 1966:33-40.

62. Cussler, E. L. Diffusion Mass Transfer in fluid systems. Cambridge, Cambridge University Press, 1984:330.

63. Teledyne-Hastings. Mass-flowmeter Information Sheet. (1986)

APPENDIX I. MEDIUM CONSISTENCY MIXER DESIGN CALCULATIONS

Mixer Design:

Two constraints were placed on the equipment design: 1) the power density in the mixing zone must exceed 2.5 x 10^7 W m^{-3} (this energy density is within the range of commercial equipment for the processing of medium consistency pulp suspensions (12)), and 2) continuous flow of pulp through the mixing zone must be maintained. The free volume of the mixer was determined by the desired energy density, and the drive motor size.

Energy density input = 2.506 x 10^7 w/m^3

Chamber free volume = 3.99 x 10^{-8} m^3 /w x 747 w = 2.98 x 10^{-4} m^3

Chamber cross sectional area: chamber height 5.1 cm.

Free area	58.3 cm^2
Rotor	35.48 cm^2
Baffles	6.45 cm^2
Cross sectional area	100.23 cm^2
Vessel diameter	11.30 cm

APPENDIX II. CALIBRATION

TRANSERA VOLTAGE CARD CALIBRATION AND THERMOCOUPLE CALIBRATION

The voltage card was calibrated by applying a known voltage to the card inputs and subsequently recording the measured voltage. The voltage applied was generated by a regulated voltage source. The input voltage was varied by changing the setting on the voltage regulator. The resulting data for the A3 board - A1 channel is shown in Figure 45 where the measured voltage is plotted versus the applied voltage. In Figure 45, regression analysis of the data points produces a line that has a slope of 0.9879 and an intercept of -0.00148 with an R^2 of 1.00. Since the slope of the channel's regression line was not significantly different from one it was assumed that the TransEra is recording the applied voltage correctly.

The thermocouple used was an Omega J-type thermocouple. The signal was corrected for the ice point reference by the thermocouple board in the TransEra. The thermocouple was calibrated by submersion in water of varying temperatures. The thermocouple was allowed to equilibrate with the water prior to reading the temperature. The temperature was also measured using a standard laboratory thermometer (Fisher Scientific Number IF1185 Test No. 137038). Figure 46 is the schematic for this experiment. The thermocouple reading recorded by the TransEra is plotted versus the temperature measured by the thermometer, in Figure 47. The regression line for the data has a slope of 1.003 and an intercept of -2.389 ^{o}C. The slope is not significantly different from one, however, the intercept is significantly

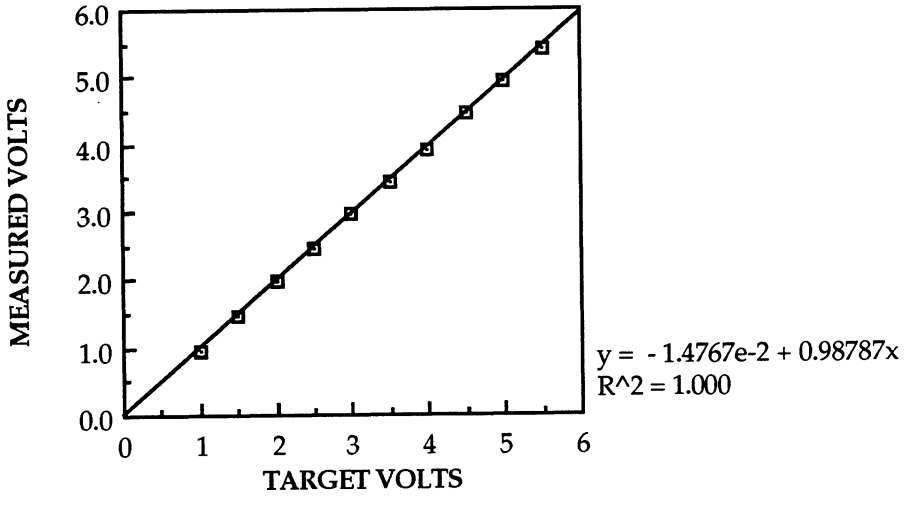

Figure 45. Measured versus applied voltage for the A3 - A1 channel of the TransEra Data Acquisition System.

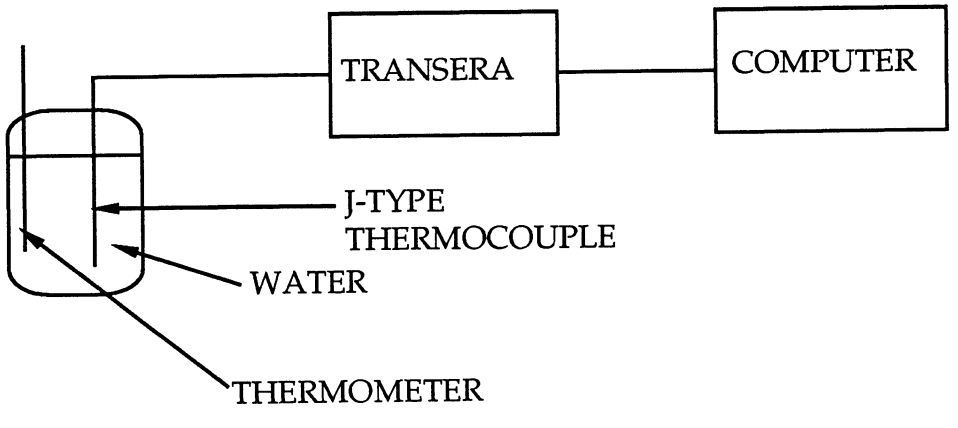

Figure 46. Schematic for the temperature calibration.

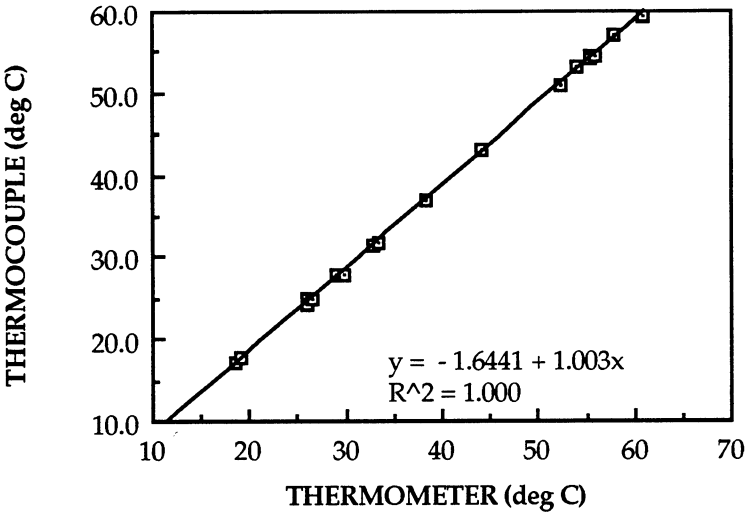

Figure 47. Temperature calibration of the flow-through mixer's thermocouple.

different from zero. Thus the results indicate that the thermocouple - thermocouple card has a -2 ^{o}C offset. The R^2 of the regression is 0.998. The readings listed in the experimental section have been corrected for the temperature offset.

TELEDYNE-HASTINGS FLOWMETER CALIBRATION

The Teledyne-Hastings mass flowmeter (Model No. CSH-50KGR) was calibrated using a Sprague Wet Test Meter (Textron #T - 195697). The meter was calibrated using nitrogen and argon as test gases. Two gases were used to ensure that the calibration was gas independent. Chlorine could not be used, because the chlorine-water solution would be corrosive to the wet test meter.

The two meters were connected in series, and the wet test meter was saturated by the test gas prior to calibration measurements. The data recorded was the time required for one cubic foot of gas to pass through the wet test meter. Other data recorded were the mass flowmeter reading (as standard cubic centimeters per second as chlorine), and the barometric pressure. Standard conditions for the mass flowmeter were zero degrees Centigrade and one atmosphere of pressure. The mass flowmeter reading was corrected for the differences in molecular weights according to the factors provided by the factory. The actual flow for nitrogen was 1.2 times the flow meter value, the actual flow for argon was 1.68 times the flow meter value. The measured flows are summarized in Table 31. All the data were corrected for water vapor entrainment as determined from psychometric charts. The humidity correction factor used was 0.011 kg water/kg gas.

Figure 48 is the plot of the corrected Teledyne-Hastings flow versus the corrected wet test meter flow for nitrogen. Linear regression of the data gives a line whose slope is 0.902 with as R^2 of 1.0. The 95% confidence interval for the slope does not include one, thus the slope is statistically different from one. Figure 49 is a plot of the corrected Teledyne-Hastings flow versus corrected wet test meter flow for argon. Linear regression of the data gives a line whose slope is 0.878 with an R^2 of 0.998. Its 95% confidence interval does not include one either.

The slope's deviation from one for both gases is probably due to a slight error introduced from the conversion factors supplied by the manufacturer. The conversion factor for chlorine unlike those for argon and nitrogen was not determined experimentally but was estimated from

Table 31. Calibration Data for the Teledyne-Hastings Flowmeter.

Nitrogen		Argon	
T-H Flow (sccs)	Wet Test Meter Flow (sccs)	T-H Flow (sccs)	Wet Test Meter Flow (sccs)
84	79.0	117.6	116.8
84	79.5	117.6	117.7
84	79.7	117.6	116.2
84	79.9	117.6	116.7
168	157.8	235.2	232.4
168	158.7	235.2	234.6
168	159.5	235.2	233.3
168	159.6	235.2	231.0
252	233.9	352.8	330.6
252	236.7	352.8	347.9
252	237.2	352.8	348.9
252	237.6	352.8	346.9
336	309.0	470.4	441.6
336	310.7	470.4	444.9
336	311.5	470.4	445.7
336	311.5	470.4	445.7
420	386.6	558.0	551.5
420	387.9	588.0	554.0
420	389.2	588.0	551.5
420	389.2	588.0	549.0
504	465.1	705.6	648.6
504	465.7	705.6	664.9
504	466.7	705.6	663.0
504	466.0	705.6	659.4
588	536.8	823.2	748.0
588	536.8	823.2	750.3
588	541.6	823.2	748.0
588	544.2	823.2	748.0
672	604.7	940.8	842.8
672	611.9	940.8	854.8

(Teledyne-Hastings Flowmeter Calibration Continued)

NITROGEN		ARGON	
T-H Flow (sccs)	Wet Test Meter Flow (sccs)	T-H Flow (sccs)	Wet Test Meter Flow (sccs)
672	613.7	940.8	851.8
672	618.4	940.8	883.2
756	687.1	1058.4	949.8
756	689.1	1058.4	942.3
756	691.0	1058.4	942.3
756	691.0	1176.0	942.3
840	756.2	1176.0	1040.6
840	758.6	1176.0	1040.6
840	763.4	1176.0	1036.2
840	770.7	1176.0	1036.2

LINEAR REGRESSION	N_2	AR	N_2/AR
X Coefficient	0.902	0.857	0.889
Constant	7.56	37.6	16.7
R^2	1.0	1.0	1.0
No. Observations	40	40	40
Degrees of Freedom	38	38	38

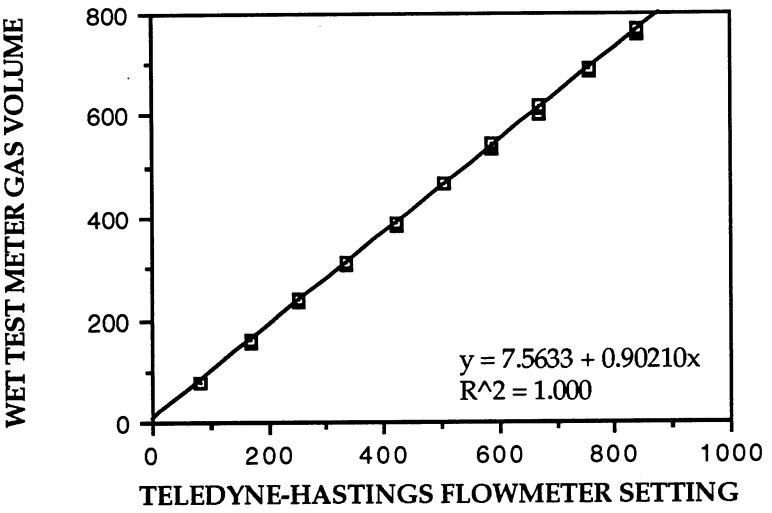

Figure 48. Mass flowmeter calibration curve for nitrogen.

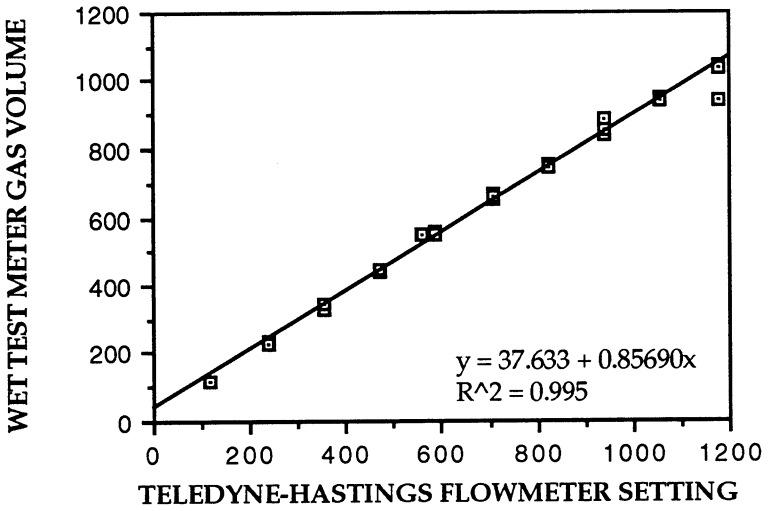

Figure 49. Mass flowmeter calibration curve for argon.

generalized equations (63). The objectives for this work were to determine if the response of the flowmeter was 1) gas independent and 2) linear over the desired flow range. Both of these objectives were met in addition the measured flow is gas independent when the proper correction factors are used.

This flowmeter was used only for the early flow-through mixer work. The flowmeter corroded due to the corrosivity of the chlorine gas.

PISTON CALIBRATION

In order to determine the pulp flow rate, the piston descent rate was measured for various hydraulic fluid flow controller valve settings. The period of time required for the piston to travel 0.46 m was measured. The calibration curve is shown in Figure 50. As you can see, the curve is linear, but does not pass through zero, i.e. the piston does not move with a finite control valve setting. The repeatability of piston travel rate for a given control valve setting was surprising considering the lack of precision of the valve dial.

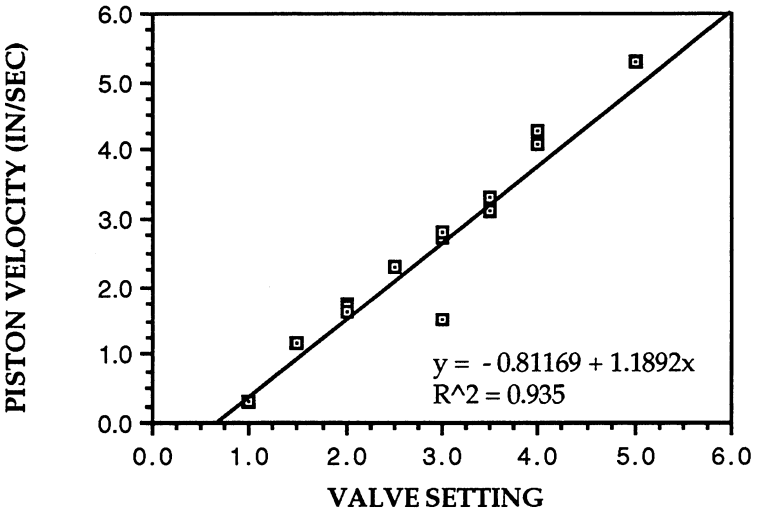

Figure 50. Calibration curve for the piston stroke velocity.

APPENDIX III. TRANSERA DATA ACQUISITION PROGRAM

```
100!        Chlorination Trials
110!        Transera Data Acquisition Program
120!        Written by Barbara J. Burns 5/5/88
130!
140!        This program collects data from the high mixing device
150!        Using the TransEra and written in Tbasic
160!        Signals collected are Reflectance (ave. and RMS), and
170!        Temperature
180         Clear
190!        Defining File size and data arrays
200!        REFL = Reflectance values
210!        RMS = Calculated RMS array
220!        RAVE = average reflectance array
230!        TEMP = Temperature array
240!        TEMPA = average temperature array
250!
260         Print "Setting Program Parameters..."
270!
280         DIM Rms[60], Rave[60], Refl[3600], Temp[600], Tempa[60]
290         Rms = 0 ! Rave = 0 ! Refl = 0 ! Temp = 0 ! Tempa = 0
300         Mflag = 0
310         Firstflag = 0
320         Wrtflag = 1
330!
340!        Open communication port to TransEra
350!
360         ON ERROR GOTO Errsub
370         OPEN #1:"com1,f"
380         Print "Attempting communications with TransEra.."
390!        Sending message to TransEra to insure proper communications
400         Errcnt = 0
410         PRINT #1:"ge;"
420!        Setting error number to zero
430         INPUT #1:Te_err
440!        Receiving error number which should be zero if not the
            program goes to the error subroutine after the second try.
450         IF Te_err = 0 THEN GOTO 520
460!        If no error occurs then the program continues
470         Errcnt = Errcnt + 1
480!        If communications fail the first time then it is retried
490         IF Errcnt < 2 THEN GOTO 410
500         Print "Error in TransEra->";Te_err
```

```
510         STOP
520         Print "Communications are functional."
530!
540!        Data Handling
550!
560!        Setting up data buffers in the TransEra
570!
580         Print "Defining system."
590!
600!        Define Buffers to receive data
610!        Buffer 1 is the reflectance buffer which holds 60 data points
            /cycle
620!        Buffer 2 is the temperature buffer which holds 10 data
            points/cycle
630!        Buffer 64 is the TransEra internal program buffer
640!
650         PRINT #1:"dfn 1 60 4 2 10 4 64 2000 5;"
660!
670!        Defining data channels
680!        Channel A1 is the reflectance channel;"
690!        Channel A12 is the temperature channel;"
700!
710         PRINT #1:"dfnc A1 0 1;"
720         PRINT #1:"dfnc A12 2;"
730!
740!        Menu Subroutine
750!
760!        This subroutine gives the user different options for program
            operation
770!
780         Clear
790!
800         Menu:
810!
820         Myflag = 0
830         PRINT "Select One"
840         PRINT
850         PRINT "     1. Collect Data and Calculate Values"
860         PRINT "     2. View raw data"
870         PRINT "     3. Copy data to disk"
880         PRINT "     4. Exit the program"
890         PRINT
900         INPUT KEY WAIT Rsp$
910!        Program waits for keyboard response. Sets value to Rsp$
920         IF Rsp$="1" THEN GOTO Analogin
930         IF Rsp$="2" THEN GOTO Scrnprt
```

```
940         IF Rsp$="3" THEN GOTO Dskwrt
950         IF Rsp$<>"4" THEN GOTO 900
960         IF Wrtflag=0 THEN GOTO 1000
970         PRINT ! PRINT ! PRINT
980         PRINT "Program has been terminated"
990         END
1000!
1010        PRINT "Last data file not written to disk!"
1020        PRINT ! PRINT
1030        PRINT "You have one more chance"
1040        PRINT
1050        PRINT "Press the number of your choice..."
1060        Wrtflag = 1
1070        GOTO 900
1080!       sends you back to keyboard for input
1090!
1100!       Analogin Subroutine
1110!
1120!       This subroutine collects the data and stores it in the TransEra
1130!
1140        Analogin:
1150!
1160        OPEN #1:"com1","f"      !Opens the communication port to
            TransEra
1170        If Wrtflag=0 THEN GOTO 1000
1180!       This prevents you from writing over unsaved data"
1190!
1200        Firstflag = 0
1210        Clear
1220        PRINT "Press <ANY KEY> when ready to collect data"
1230        INPUT KEY WAIT Rsp$
1240!
1250!       Setup for analog input from the channels
1260!       Data will be taken in the following manner: the reflectance
            channel
1270!       will be sampled every 1.6e-6 sec for 60 data points then the
            temperature
1280!       channel will be sampled every 3e-6 sec for 10 data points. The
            sequence
1290!       will be repeated 60 times.
1300!
1310!       Load the program buffer with the data aquisition instructions
1320!
1330        PRINT #1:"load 64;"
1340!       Set the period and sample the reflectance
1350        PRINT #1:"per 1.6 e-6;"
```

```
1360        PRINT #1:"ai 60 A1 1 1;"
1370        Set the period and sample the temperature
1380        PRINT #1:"per 3 e-6 ;"
1390        PRINT #1:"ai 10 A12 2 1;"
1400        PRINT #1:"end;"
1410!
1420!       Tell the TransEra to start collecting data and then dump to the
1430!       computer
1440!       Repeat 60 times
1450!
1460        B=60
1470        FOR X = 1 TO B
1480              PRINT #1:"run 64;"
1490              PRINT #1:"ge;"
1500              INPUT #1: Rsp$
1510!       Down load reflectance data
1520              PRINT #1:"wr 1;"
1530              INPUT #1:N
1540              FOR Y = 1 TO N
1550                    Z = Y + (X-1)*60
1560                    INPUT #1:Refl[Z]
1570              NEXT Y
1580!       Down load temperature data
1590              PRINT #1:"wr 2;"
1600              INPUT #1:N
1610              FOR Y = 1 TO N
1620                    Z = Y + (X-1)*10
1630                    INPUT #1:Temp[Z]
1640              NEXT Y
1650              PRINT X
1660        NEXT X
1670!
1680!       Calculate the ave. reflectance and RMS for each reflectance buffer
            value
1690!       RMS = {[Sum(Value-Rave)**2]/N}**0.5 where N=no. of samples
1700!       Average values for each set of temperature buffers is also
            calculated
1710!
1720!       Reflectance Average
1730!
1740        PRINT "Calculating Average Values"
1750        FOR X = 1 TO B
1760              Esumrum = 0
1770              FOR Y = 1 TO 60
1780                    Z = (X-1)*60 + Y
1790                    Esumrum = Esumrum + Refl[Z]
```

```
1800            Next Y
1810            Rave[X] = Esumrum/B
1820!       Calculate RMS
1830            Rmsx = 0
1840            For Y = 1 TO 60
1840                Z = (X-1)*60 + Y
1850                Rmsx = Rmsx + (Refl[Z]-Rave[X])**2
1860            Next Y
1870!
1880!       Calculate averages for each set of temperature data
1890!
1900        FOR X = 1 TO B
1910            Tempx = 0
1920            FOR Y = 1 TO 10
1930                Z = (X-1)*10 + Y
1940                Tempx = Tempx + Temp[Z[
1950            NEXT Y
1960            Tempa[X] = Tempx/10
1970        NEXT X
1980!
1990        Wrtflag = 0
2000        GOTO Menu
2010!
2020!       Screen Print Subroutine
2030!
2040        Scrnprt:
2050!
2060        CLEAR
2070        PRINT | PRINT
2080        PRINT "Press <ANY KEY> to Look at the Data."
2090        INPUT KEY WAIT Rsp$
2100        CLEAR
2110        SLEEP 2
2120!       Causes the program to pause for 2 seconds
2130        CLEAR
2140        PRINT AT 1,1:"AVE REFL       RMS  AVE TEMP"
2150        PRINT
2160        FOR X = 1 TO B
2170            PRI USI "6d.3d,5x,6d.3d,3x,6d.3d" Rave[X],Rms[X],Temp[X]
2180        NEXT X
2190        GOTO Menu
2200!
2210!       Disk Write Subroutine
2220!
2230        Dskwrt:
2240!
```

```
2250        CLEAR
2260        PRINT ! PRINT
2270        INP PROMPT "Enter the Name for the First Data File->":
            Filnam$
2280        Filnama$ = Filnam$
2290        OPEN #2:Filnama$,"w"
2300        PRINT "Now Writing Data to Disk.."
2310        PRINT #2:3600
2320        Bb = 60*B
2330        FOR X = 1 to Bb
2340              PRINT #2 USING "10d.3d":Refl[X]
2350        NEXT X
2360        FOR X = 1 TO 600
2370              PRINT #2 USING "10d.3d":Temp[X]
2380        NEXT X
2390        CLOSE #2
2400        PRINT ! PRINT
2410        INP PROMPT "Enter the Name for the 2nd Data File->":
            Filnam$
2420        Filnama$ = Filnam$
2430        OPEN #3:Filnama$,"w"
2440        PRINT "Now Writing Data to Disk.."
2450        FOR X = 1 TO B
2460              PRI # 2 USI
            "10d.3d,1x,10d.3d,1x,10d.3d":Refla[X],Rms[X],Temp[X]
2470        NEXT X
2480        CLOSE #3
2490        Wrtflag = 1
2500        GOTO Menu
2510!
2520!       Error Subroutine
2530!
2540        Errsub:
2550!
2560        IF Ern = 6 THEN GOTO 2640
2570        CLOSE
2580        PRINT
2590        PRINT "Error #";Ern;"Has occurred at line";Erl;
2600        PRINT
2610        PRINT "This run may still be salvagable.";
2620        PRINT
2630        PRINT "Program aborted."
2640        END
```

APPENDIX IV. OMEGA CONDUCTIVITY PROBE CALIBRATION

A conductivity probe and signal conditioner (Omega Model No. CDCN - 83) was used to measure the conductivity of a KCl spiked pulp solution. KCl was used, because it was readily available and gave a strong conductivity signal at low concentrations. The KCl solution was used to measure the residence time distribution of the mixer. The probe was calibrated using KCl solutions of varying strength. The resulting calibration curve for a probe whose cell constant, K, is 1.08 is shown in Figure 51. (The data is shown in Table 32.)

Once the probe was calibrated, a series of tests were made to determine the probe's response to changes in both pulp consistency and conductivity. The purpose of these tests was to determine if adsorption of KCl onto the fibers would significantly change the solution's measured conductivity. In these experiments, the KCl concentration in the pulp suspension was increased from zero to thirteen weight percent KCl. The KCl concentration was calculated as follows:

$$wt\% = \frac{wt\ KCl}{wt\ H_2O + wt\ KCl} \qquad (56)$$

regardless of the pulp concentration. For a given KCl concentration the mixture was mixed and then the conductivity was measured. The conductivity of the suspension was the probe's output after it was stable for ten seconds. This allowed for the KCl to adsorb onto the pulp. Figure 52 shows the resulting data for pulp suspensions whose consistencies vary from zero to ten percent consistency. In this figure, the measured conductivity is not significantly affected by the presence of pulp fibers (Table 33).

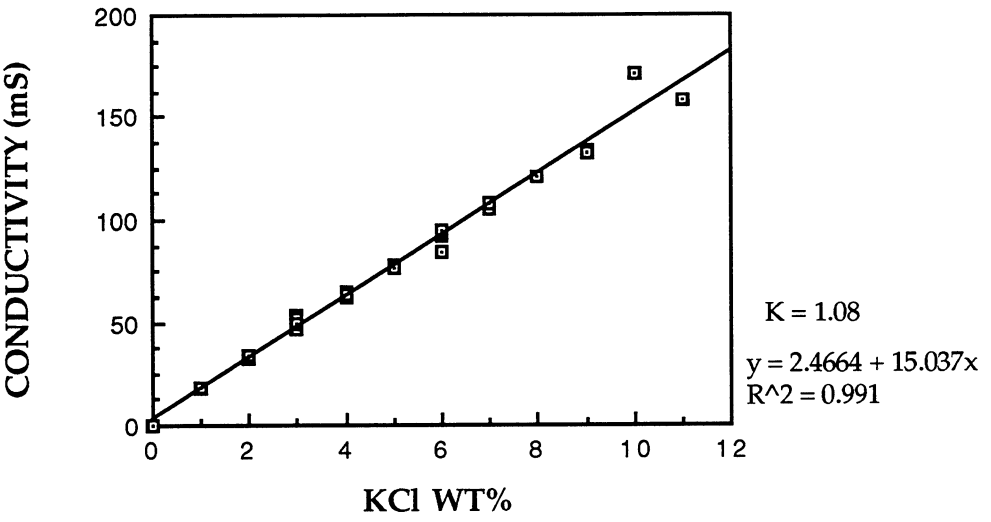

Figure 51. Calibration of Conductivity Probe, K=1.08.

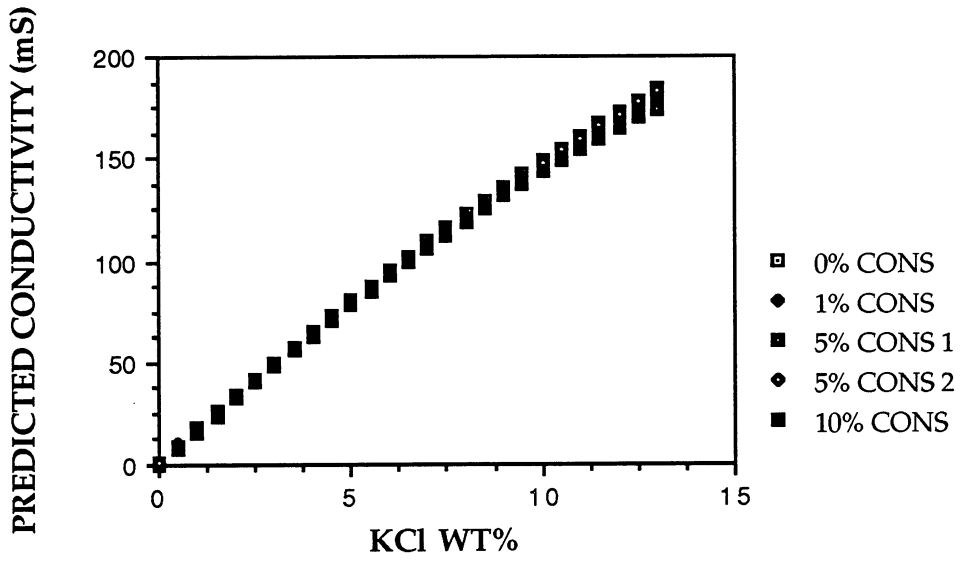

Figure 52. Conductivity of pulp suspensions of varying consistency.

Table 32. Calibration data for the Omega Conductivity Probe using a KC1 Solution in Water (Cell Constant K = 1.08).

Weight % KCL	Meter Reading (mS)
0	03.
0	03.
0	03.
0	0.3
1	17.9
1	17'7
1	17'8
1	17.9
2	33'9
2	32'2
3	46'8
3	52'8
3	46'5
3	48'1
3	51.4
3	49'0
4	65'0
4	62'6
4	63'6
4	63'5
5	76.9
5	76'7
5	78'1
5	77'8
6	95’4
6	95'2
6	91.7
6	92'9
6	95'0
6	84'7
7	105.3
7	107'8
8	120'7
9	134'0
9	132’1
10	171'0
11	159.0.

LINEAR REGRESSION	
X Coefficient	15.04
Constant	2.47
R^2	0.991

Table 33. Calibration Of Omega Conductivity Probe As A Function Of Pulp Consistency.

Cell Constant K = 1.04 Consistency - 0%

	Conductivity (mS)			
KC1 WT%	Trial 1	Trial 2	Trial 3	Trial 4
0.0	0.20	0.21	0.21	0.21
05	9.32	9.02	9.15	9.33
0'99	17.7	17.2	17.3	17.7
1.48	25.9	25.2	25.5	25.7
1.96	33.9	32.9	33.5	33.6
2'44	41.8	40.5	41.3	41.2
2'91	49.3	47.9	48.8	48.5
3'38	56.7	55.2	56.2	55.9
3.85	64.1	62.3	63.4	63.2
4.31	71.2	69.4	70.7	70.3
4'76	78.2	76.2	77.8	77.2
5'21	84.8	82.5	84.5	84.1
5.66	91.1	89.3	90.9	90.6
6.10	97.3	95.3	97.0	96.6
6'54	103.1	101.3	103.0	102.7
6'98	109.2	107.1	109.1	108.7
7'41	115.1	112.3	114.9	114.6
7'83	121.1	118.8	121.0	120.6
8'26	126.9	124.6	126.9	126.5
8'68	132.6	130.2	130.2	132.3
9'09	138.1	135.8	138.2	137.9
9'50	143.3	141.1	143.4	143.1
9.91	148.0	145.8	148.3	148.0
10.3	152.8	150.5	152.9	152.7
10.7	157.4	155	157.8	157.5
11.1	162.4	159.6	162.6	162.6
11.5	167.7	164.6	168.5	168.3

Consistency - 1.0%

KCl WT%	Trial 1	Trial 2	Trial 3	Trial 4
0.0	0.21	0.20	0.15	0.19
0.5	9.22	8.50	9.20	9.32
1.0	17.6	17.5	17.7	17.8
1.5	25.7	25.2	26.0	26.0
2.0		28.8	33.9	33.9
2.5	41.1	32.2	41.6	41.6
3.0	48.4		49.2	49.0
3.5	55.6	56.6	56.6	56.4
4.0	62.6	63.5	64.0	63.9
4.5	69.3	69.9	71.1	71.0
5.0		77.0	75.1	77.8
5.5	82.9	83.4	83.6	84.4
6.0	89.5	89.6	89.6	90.6
6.5	95.2	95.6	95.3	96.9
7.0	102.0	101.9	100.9	102.7
7.5	107.6	107.8	106.8	108.7
8.0	113.2	113.7	112.4	113.6
8.5	118.9	118.9	117.7	118.8
9.0	124.8	124.4	123.1	123.8
9.5	130.4	129.7	127.9	129.0
10.0	136.4	135.1	139.6	136.9
10.5	141.6		144.1	141.4
11.0	146.9	145.0	149.2	145.9
11.5	150.7	149.5	153.4	150.2
12.0	155.1	155.7	158.3	154.4
12.5	159.5	159.3	163.2	158.6
13.0	164.0	164.2	168.3	164.1

Consistency - 5%

KC1 WT%	Trial 1	Trial 2	Trial 3	Trial 4
0.0	0.04	0.07	0.067	0.05
0.5	9.32	9.00	10.26	13.31
1.0	18.60	18.64	20.1	17.80
1.5	27.1	26.5	27.3	26.0
2.0	37.0	34.1	34.6	34.1
2.5	43.7	42.8	44.2	42.5
3.0	51.8	51.1	50.1	49.8
3.5	58.3	57.9	58.8	57.4
4.0	65.1	65.6	67.6	65.7
4.5	71.9	72.1	72.7	69.1
5.0	81.1	80.3	80.7	80.2
5.5	89.0	88.2	86.5	88.3
6.0	95.0	95.8	92.5	94.7
6.5	102.2	101.4	99.6	101.9
7.0	108.8	108.0	108.8	107.8
7.5	113.9	115.3	116.7	115.7
8.0	121.4	122.2	122.7	123.7
8.5	128.9	128.9	126.7	128.3
9.0	133.3	134.8	132.9	136.6
9.5	142.3	140.5	139.8	142.9
10.0	147.5	146.9	144.4	149.3
10.5	155.6	153.3	151.1	154.5
11.0	159.7	159.0	156.6	161.0
11.5	164.8	164.1	162.2	166.5
12'0	169.5	171.3	173.3	180.1
12'5	178.4	176.7	173.3	180.1
13'0	182.2	184.0	181.2	191.9

Consistency - 10%

KC1 WT%	Trial 1	Trial 2	Trial 3
0.0	0.03	0.05	0.05
0.5	9.53	9.14	8.17
1.0	14.3	16.8	15.5
1.5	26.9	23.5	26.8
2.0	27.7	30.1	35.1
2.5	29.8	34.1	40.8
3.0	44.4	40.3	46.3
3.5	60.6	52.3	57.7
4.0	65.5	63.3	66.7
4.5	75.4	67.3	70.3
5.0	83.1	76.0	75.7
5.5	86.6	87.9	81.6
6.0	95.6	95.0	94.1
6.5	101.8	98.1	100.3
7.0	107.8	106.8	104.7
7.5	115.8	112.6	112.3
8.0	122.9	117.8	118.0
8.5	127.8	124.9	124.5
9.0	135.9	131.4	127.9
9 5	143.4	138.9	137.7
10.0	146.4	143.4	145.2
10.5	151.0	149.8	149.1
11.0	153.5	155.7	152.8
11.5	163.5	158.5	155.4
12'0	170.3	165.0	165.9
12.5	173.9	170.2	170.2
13.0	188.3	177.6	177.4

Regression Equations

Consistency	Constant	Cond Coef.	$Cond^2$ Coef.	R^2
0	0.645	17.17	-0.237	1.00
1	0.612	17.09	-0.25	0.999
5	1.650	16.80	-0.22	0.999
10	-1.154	17.14	-0.26	0.997

APPENDIX V. RTD EXPERIMENTS DATA

Below are the F-curves for the residence time distribution studies. The normalized conductivity values are the actual conductivity value divided by the maximum value for the experiment so that all the values are between zero and one. Theta is the time elapsed when a sample was obtained divided by the total time for the entire run.

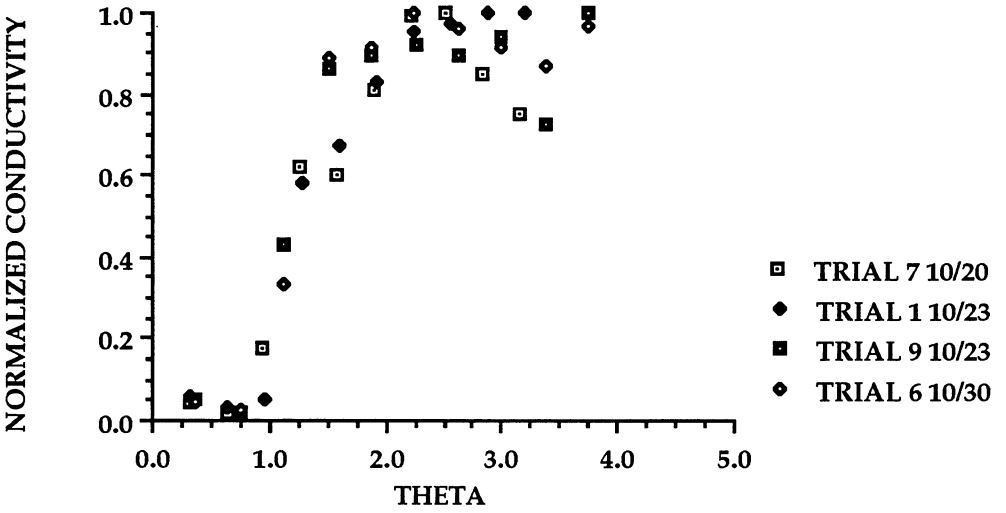

Figure 53. F-curve for the high levels of RPM, piston rate and gas flow rate.

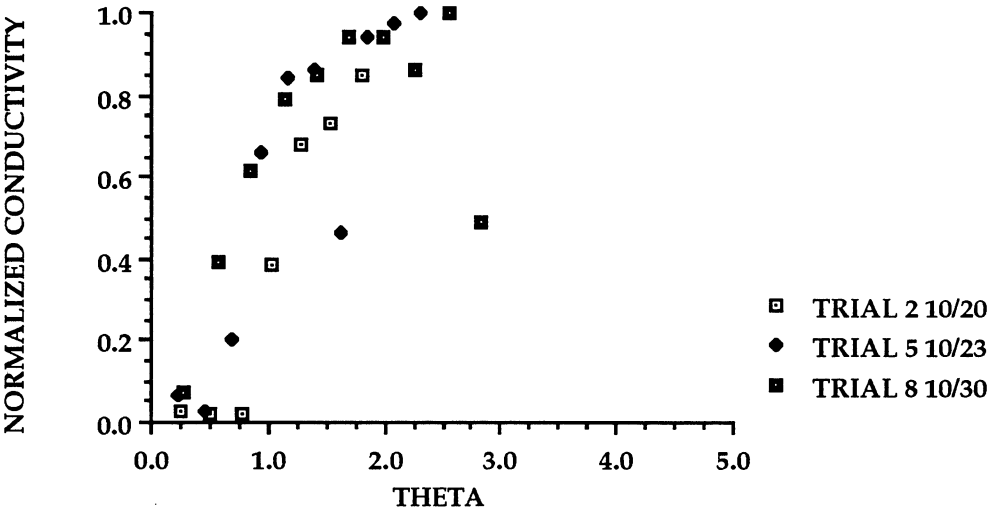

Figure 54. F-curve for high levels of RPM and Gas flow rate- low level of piston.

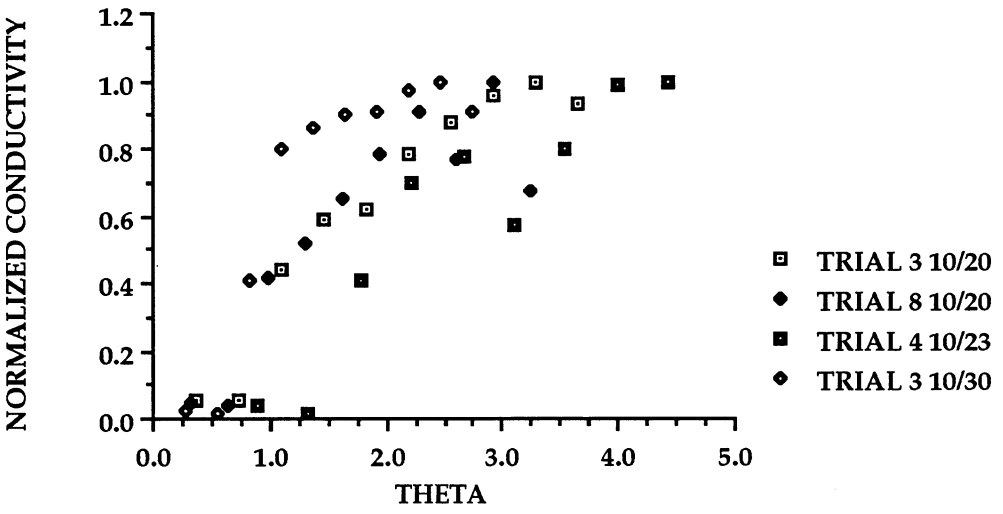

Figure 55. F-curve for high levels of RPM, and piston - low level of gas.

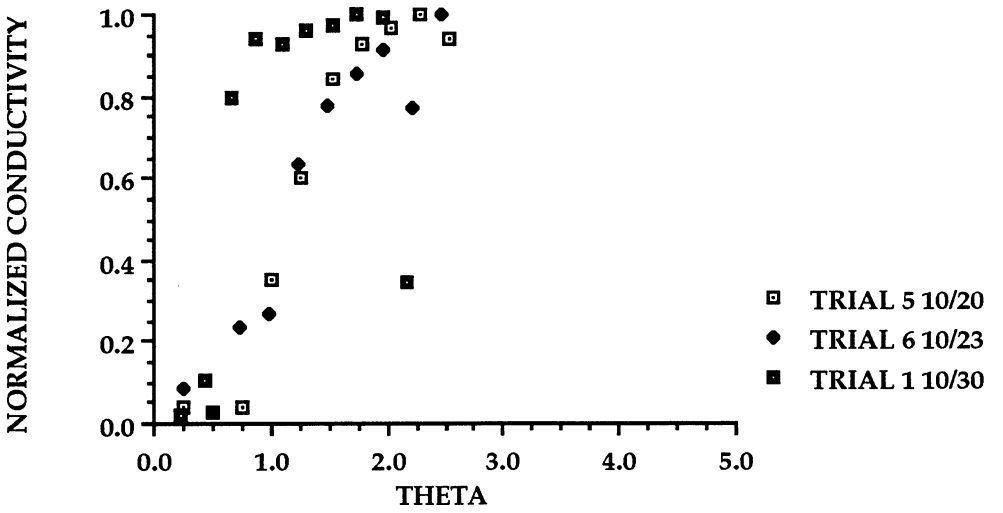

Figure 56. F-curve for high level of RPM - low level of gas and piston.

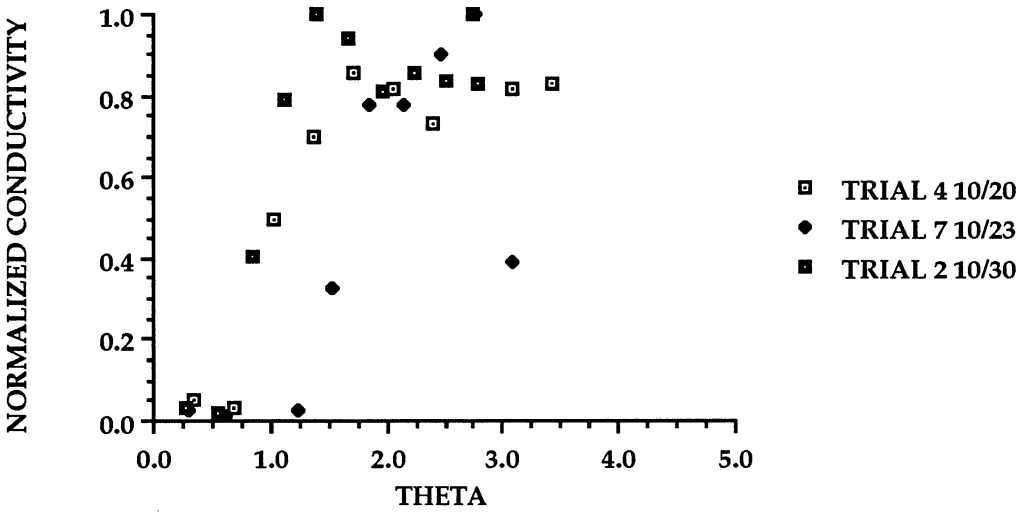

Figure 57. F-curve for low level of RPM - high levels of gas and piston.

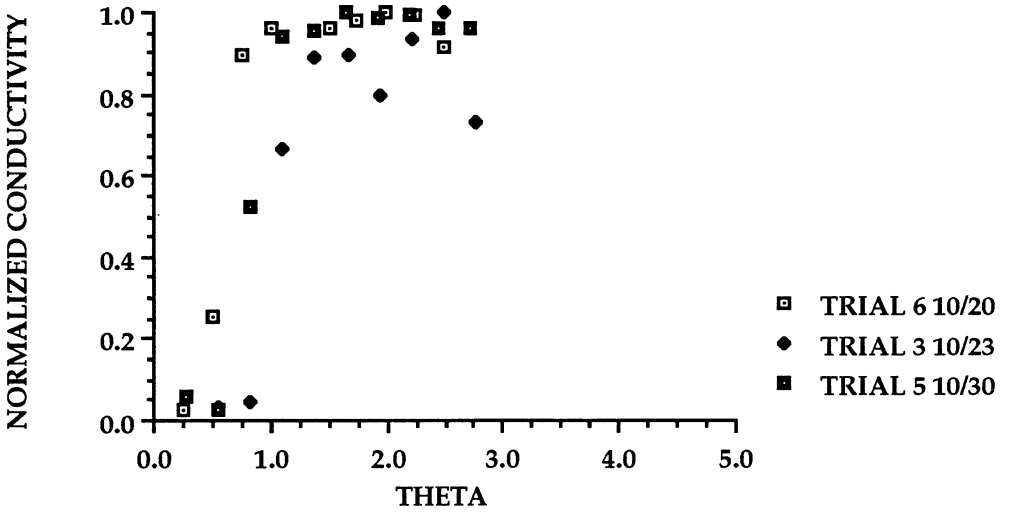

Figure 58. F-curve for low level of RPM and piston - high level of gas.

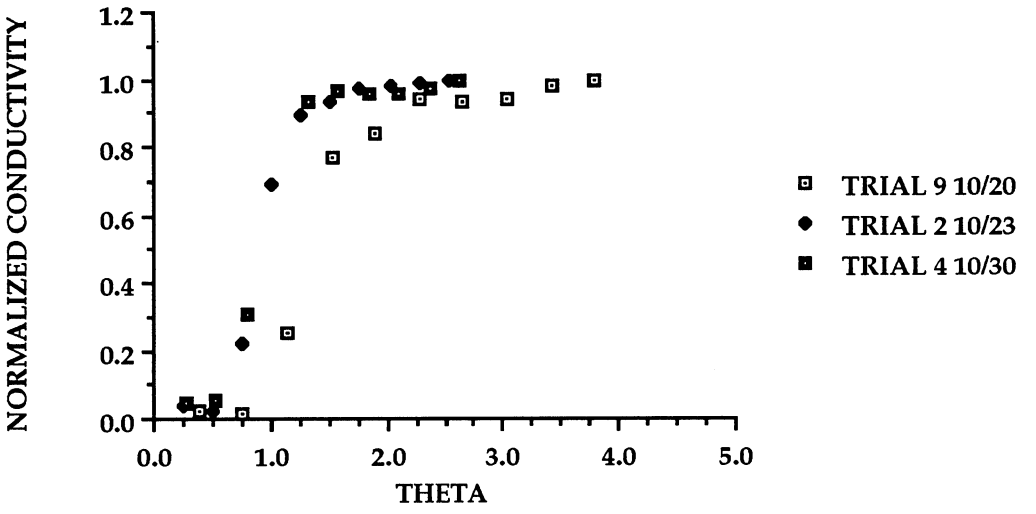

Figure 59. F-curve for low levels of RPM and gas - high level of piston.

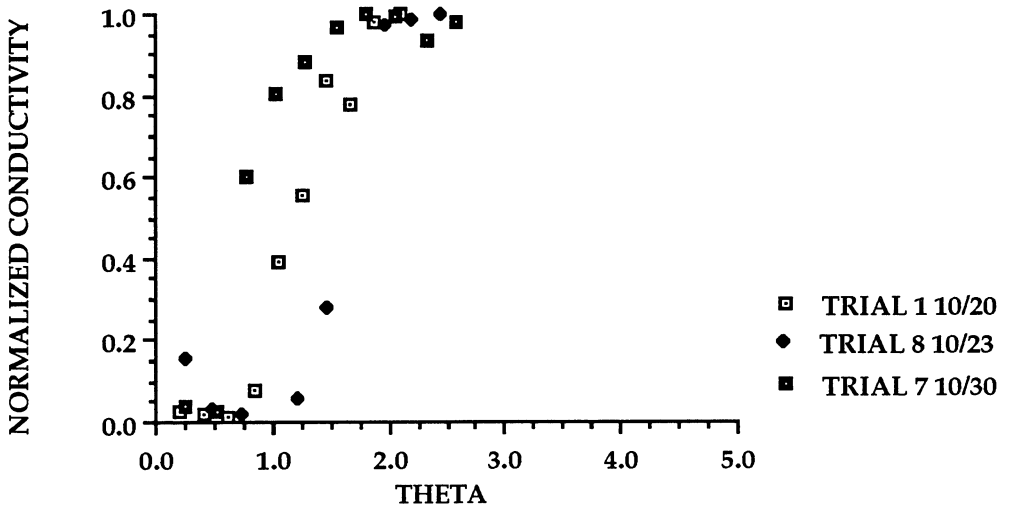

Figure 60. F-curve for low levels of RPM, gas and piston.

APPENDIX VI. PRELIMINARY FLOW THROUGH MIXER CHLORINATION EXPERIMENTS

The purpose of these preliminary experiments was to develop the experimental techniques which were used in subsequent experiments. The main technique developed was the pulp sample treatment of the samples obtained at the mixer outlet. For each mixer run, two pulp samples were taken. The first sample was caught in a container containing acidified potassium iodide solution to quench the chlorine in solution. The sampling container was open to the atmosphere so that the chlorine not absorbed by the pulp-water suspension was vented. The amount of chlorine in absorbed by the liquid phase was determined by titration with sodium thiosulfate. After the amount of chlorine in the liquid phase was determined, the pulp was thoroughly washed, extracted with sodium hydroxide, and tested for residual lignin content.

The second sample was caught in a gas tight plastic bag, and placed in a water bath at the target temperature for ten minutes. At the end of ten minutes the pulp was washed and then extracted. The filtrate was tested for chlorine residual iodometrically. After extraction both pulp samples were tested for residual lignin content using Tappi Standard Method T236 (55).

For the preliminary set of experiments, a 2^3 factorial design was used. The variables chosen were the applied chlorine dosage (% on pulp), the mixer rotor speed (rpm), and the pulp temperature. Three replicates of the design were run so that the experimental error could be measured directly. The experimental conditions used are listed in Table 34. The residual lignin after extraction, and the measured chlorine in solution for the quenched

Table 34. Preliminary Flow Through Mixer Chlorinations Experimental Design.

Conditions	Chlorination	Extraction
Consistency (%)	8.0	10.0
Applied Chlorine (%)	1.35	*
	2.70	
Target Temperature (^{o}C)	23.0	70.0
	60.0	
Rotor Speed (RPM)	1500.0	
	2500.0	
Time (min)		60.0

Initial Kappa Number 12.25

* Enough Caustic was added to raise the initial pH to 11.5. All final pH's were greater than 10.0.

samples are shown in Table 35. The residual lignin in the extracted samples for the second set of samples are shown in Table 36. For the chlorinations in Table 35, all the chlorine was consumed as trace amounts of chlorine were measured during the residual test.

For two treatments in Table 36, one of the three kappa number determinations for the sample was very different from the other two. Outliers were determined as those data points which were outside the 95% confidence interval for the treatment mean. The 95% confidence interval for each treatment mean was constructed using the overall experimental variance. The confidence interval was the treatment mean ± two times the experimental standard deviation.

Table 35. Preliminary Flow-Through Mixer Chlorinations Experimental Data - KI Quenched Samples.

Cl_2 Charge (%)	RPM	Temp. (Act. Temp) (°C)	CE Ka 1	CE Ka 2	CE Ka 3	CE Ka Ave.	Cl_2 RES. (g/l)	TOT. Cl_2* (g/l)
2.70	2500	60	8.58	8.55	8.74	8.62	0.46	0.94
2.70	2500	60	7.38	8.09	8.57	8.01	0.41	0.97
2.70	2500	60 (43.5)	6.94	7.13	6.94	7.06	0.88	1.57
2.70	1500	23	8.72	8.42	8.54	8.56	1.31	1.80
2.70	1500	23	7.18	6.59	6.33	6.70	1.02	1.76
2.70	1500	23 (22.5)	7.85	7.03	8.14	7.66	0.61	1.22
2.70	2500	23	8.35	9.48	9.30	9.04	0.50	0.93
2.70	2500	23 (18.0)	7.84	7.75	7.60	7.73	0.39	0.99
2.70	2500	23 (25.2)	8.82	8.82	8.54	8.73	1.34	1.81
2.70	1500	23	9.83	9.61	9.15	9.53	0.52	0.88
2.70	1500	23	7.85	8.05	7.17	7.69	0.48	1.08
2.70	1500	23 (23.8)	11.02	9.62	9.22	9.95	0.96	1.26
1.35	2500	60	8.40	7.15	7.54	7.70	0.12	0.72
1.35	2500	60 (42.3)					1.56	
1.35	2500	60 (40.0)	8.14	7.92	7.87	7.98	0.12	0.69
1.35	1500	60	10.05	9.13	8.86	9.35	0.77	1.16
1.35	1500	60 (44.5)	7.56	7.63	7.42	7.54	0.18	1.34
1.35	1500	60 (43.5)	9.12	8.08	7.82	8.34	0.74	1.26
1.35	2500	60 (43.4)					0.00	
1.35	2500	60	7.71	7.33	8.00	7.68	0.18	0.79
1.35	2500	60 (37.5)	9.50	9.42	9.40	9.44	2.30	2.67
1.35	1500	23	8.37	8.25	8.04	8.22	1.04	1.58
1.35	1500	23 (21.6)	8.48	8.10	9.01	8.53	0.91	1.40
1.35	1500	23 (23.4)	8.27	9.25	10.80	9.44	0.79	1.16

* Total Transferred Chlorine = the chlorine in solution plus that which reacted with the lignin according to the following equation:

$$\text{Chlorine} = (12.25 - K_{CEi}) \times 0.0015 \times 100 \text{ g pulp} \times 2.67 \times 70 / 211$$

Table 36. Preliminary Flow-Through Mixer Chlorinations Experimental Data - 10 min Samples.

Cl_2 Charge (%)	RPM	Temp. (Act. Temp) (°C)	CE Ka 1	CE Ka 2	CE Ka 3	CE Ka Ave.
2.70	2500	60	7.83	7.62	8.29	7.91
2.70	2500	60	6.92	7.06	6.77	6.92
2.70	2500	60 (43.5)	7.10	7.29	7.22	7.20
2.70	1500	23	7.76	8.31	7.67	7.91
2.70	1500	23	5.66	5.81	5.43	5.63
2.70	1500	23 (22.5)	8.17	8.21	8.14	8.17
2.70	2500	23	6.99	7.18	7.05	7.07
2.70	2500	23 (18.0)	6.82	6.87	6.91	6.87
2.70	2500	23 (25.2)	8.58	7.22	7.29	7.70
2.70	1500	23	8.72	8.82	9.82	9.12
2.70	1500	23	5.99	6.74	7.44	6.72
2.70	1500	23 (23.8)	8.98	7.64	9.05	8.56
1.35	2500	60	9.17	8.15	8.44	8.59
1.35	2500	60 (42.3)	7.79	7.80	7.44	7.68
1.35	2500	60 (40.0)	7.03	7.02	7.00	7.02
1.35	1500	60	8.19	8.42	8.29	8.30
1.35	1500	60 (44.5)	6.30*	8.62	9.17	8.03
1.35	1500	60 (43.5)	7.50	7.80	8.86	8.05
1.35	2500	60 (43.4)	7.92	8.38	8.07	8.12
1.35	2500	60	7.60	5.20"	7.58	6.79
1.35	2500	60 (37.5)	7.54	8.49	7.46	7.83
1.35	1500	23	8.93	8.96	8.92	8.94
1.35	1500	23 (21.6)	8.00	7.22	7.00	7.41
1.35	1500	23 (23.4)	6.69	7.95	6.55	7.06

* Outlier - A data point outside the 95% confidence interval around sample mean, x-bar $\pm$ 2s where the overall experimental variance $s^2 = 0.268$, and $s = 0.52$.

The experimental variance was calculated from an analysis of variance where each set of reactor conditions was treated as a separate treatment. The experimental variance is equal to the mean square error in the analysis of variance. For this set of reactor runs the kappa number determination experimental variance was equal to 0.268.

Using this method to construct the 95% confidence interval around a sample mean, it was determined that the two questionable kappa number determinations were in fact outliers. In Table 36, the outliers are indicated by asterisks and are replaced by the sample average during subsequent calculations.

Comparison of the two average sample kappa numbers for a given run shows that the pulp loses on average 0.66 kappa number units during the ten minutes retention time. In this set of experiments, the effect of increasing the amount of applied chlorine, the mixer's rotor speed, and the system temperature on the residual lignin and the amount of chlorine absorbed were investigated. The two measured responses were interdependent as the concentration of chlorine in solution affected the reaction rate. Conversely, the amount of chlorine absorbed in the solution was dependent on the amount of chlorine consumed by the reaction.

For this experiment, the amount of residual lignin after extraction was not significantly affected by the independent variables. The analysis of variance for the K_{CEi} is shown in Table 37. This result was most likely due to the narrow experimental space used. For subsequent experiments, the experimental space was widened.

Table 37. K_{CEi} Analysis of Variance Table.

Source	Degrees of Freedom	Mean Square	F-Ratio
Applied Chlorine (K)	1	0.0665	0.0860
Rotor Speed (R)	1	0.3605	0.466
Temperature (T)	1	0.4907	0.634
Interactions			
K x R	1	0.0645	0.08341
K x T	1	0.0570	0.07361
R x T	1	0.3201	0.4138
K x R x T	1	3.121	4.0343
ERROR	14	0.7734	

The analysis of variance for the ten minute samples gave similar results as the KI quenched samples as shown in Table 38.

The amount of chlorine transferred to the liquid phase was equal to the chlorine which reacted with the lignin plus the amount of chlorine which remained in solution. Converting the amount of lignin consumed into consumed chlorine according to Equation 57 allowed calculation of the total amount of chlorine transferred to the liquid phase.

$$\text{Chlorine (g/l)} = \{[12.25 - K_{CEi}] \times 0.0015 \times 100 \times 70 \times 2.67\} / 211 \qquad (57)$$

The maximum possible chlorine concentration of chlorine in solution is 2.34 g/l at the 2.70% applied chlorine level. For the 1.35 applied chlorine level the maximum chlorine concentration is 1.17 g/l. Two of the twelve observations for the 1.35% chlorine on pulp were higher than the

Table 38. K_{CE10} Analysis of Variance Table

Source	Degrees of Freedom	Mean Square	F-Ratio
Applied Chlorine (K)	1	0.6801	0.890
Rotor Speed (R)	1	0.735	0.962
Temperature (T)	1	0.510	0.668
Interactions			
K x R	1	0.0193	0.0252
K x T	1	0.2948	0.385
R x T	1	0.608	0.796
K x R x T	1	0.0254	0.0332
ERROR	16	0.764	

maximum possible. The most likely explanation for this anomaly was a chlorine control valve malfunction.

After this set of experiments the control valve was found to be corroded and was replaced. This was the only set of flow through mixer experiments in which the Teledyne-Hastings Mass flowmeter and control valve were used. In the other experiments, a corrosion resistant rotameter and control valve were used for controlling the chlorine flow.

Analysis of variance resulted in the same conclusion as the residual lignin analysis as shown in Table 39.

In order to test the theory of a too narrow experimental space for the applied chlorine and rotor speed, two, one variable at a time experiments were run. In the first experiment, the chlorine charge was varied from zero to 1.35% chlorine on pulp at a constant rotor speed and temperature. In the

Table 39. Total Absorbed Chlorine Analysis of Variance Table.

Source	Degrees of Freedom	Mean Square	F-Ratio
Applied Chlorine (K)	1	9.67×10^{-7}	4.48×10^{-6}
Rotor Speed (R)	1	0.07105	0.344
Temperature (T)	1	0.02901	0.1405
Interactions			
K x R	1	0.00141	0.00682
K x T	1	0.7517	3.640
R x T	1	0.8409	4.072
K x R x T	1	0.1704	0.825
ERROR	14	0.2065	

second experiment, the rotor speed was varied from 500 rpm to 2000 rpm at a constant applied chlorine and temperature. These two experiments are described in the next two subsections.

LOW CHLORINE CHARGE STUDY

The purpose of the low chlorine charge study was to investigate the relationship between applied chlorine and lignin removed for the flow-through reactor. In addition the relationship for the flow through system was compared to the comparable low consistency batch system. The experimental procedure for this series of chlorinations was the same as that for the previous section. The experimental conditions were as follows: temperature, 25 ^{o}C; rotor speed, 2500 rpm; and chlorine charge, 0.0, 0.24, 0.61, 0.98, 1.35% on pulp. The 0.0% applied chlorine treatments were run as true blanks where the

pulp was run through the mixer and then extracted for one hour. This series of experiments was run in duplicate.

The average kappa number results are summarized in Table 40 and Figure 61. For the three smallest chlorine factors, there was not any detectable chlorine residual at the mixer outlet. There was, however, chlorine available to react with lignin in the fiber wall. This is evidenced by the drop in Kappa number after ten minutes reaction time, which may indicate that at low concentration of chlorine in the solution, diffusion to a reaction site within the fiber wall may be rate limiting.

At the highest two level of applied chlorine, 0.98 and 1.35% applied chlorine, additional amounts of available chlorine did not increase the amount of lignin removed. After 10 minutes of reaction time, there was a slight decrease in the average extracted kappa number (K_{CE10}), but it was not significant. When the chlorine residuals are taken into account, the same amount of chlorine was transferred in both cases. The excess chlorine in the 1.35% chlorine on pulp case must have remained in the gaseous phase.

Comparison of the K_{CE10} to those measured for the batch experiments shows that the flow through mixer was not as efficient as the batch system (Table 40). The differences between the two systems increase with increasing amount of applied chlorine.

The difference in efficiencies between the two systems was probably due to the different method of applying the chlorine. Because the batch system was low consistency all the chlorine was added to the system in a solution which removed one mass transfer step for the chlorine. Because the

Table 40. Average Kappa Number for the Low Level of Applied Chlorine Experiments - 2500 RPM - 25 °C.

CHLORINE CHARGE	CHLORINE RESIDUAL	K_{CEi} AVERAGE	K_{CE10} AVERAGE	BATCH AVE KAPPA
0.0	0.0	10.2	10.7	
0.0	0.0	11.2	11.6	
0.24	0.0	10.5	10.6	9.25
0.24	0.03	11.1	9.9	9.45
0.61	0.0	10.3	9.1	7.33
0.61	0.11	10.5	9.1	7.99
0.98	0.22	9.1	7.2	4.36
0.98	0.38	8.4	9.1	5.43
1.35	0.35	8.4	8.4	5.72
1.35	0.26	9.3	7.1	4.97

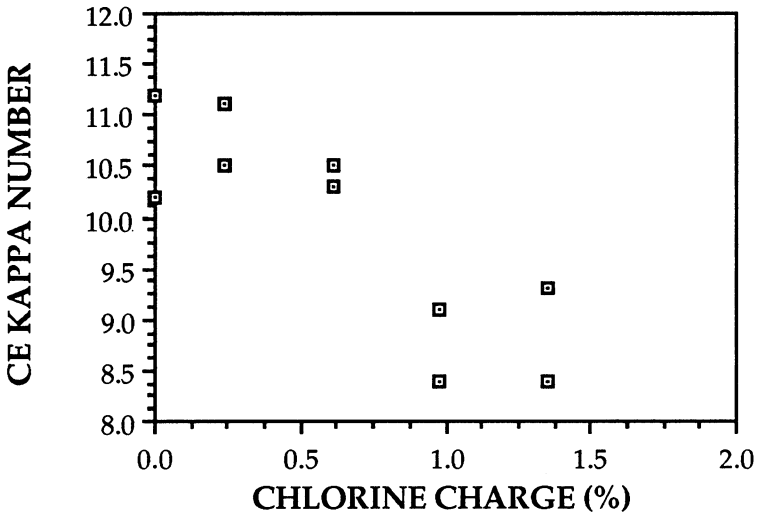

Figure 61. K_{CEi} versus chlorination dosage for the low chlorine charge study.

flow through mixer system was medium consistency, only the chlorine absorbed by the liquid phase was available for reaction.

FLOW THROUGH MIXER TURBULENCE LEVEL STUDY

In the preliminary chlorination study, the amount of residual lignin was independent of the rotor speed. It was expected that as the turbulence level increased, the rotor speed, the amount of chlorine available for reaction in the liquid phase would increase. Increased agitation should increase the gas-liquid interfacial area by reducing the gas bubble size. Increased agitation should also increase the diffusion rate of chlorine away from the interface into the bulk fluid due to turbulent eddies.

This set of experiments was designed to investigate the effect of the turbulence field (rotor speed) on the chlorine-lignin reaction. The experimental conditions were chosen as follows: applied chlorine, 0.98% on pulp; temperature, 28 ^{o}C; the rotor speed, 500, 1000, 1500, and 2000 rpm.

The pulp samples were handled as in the previous experiments: one sample was quenched at the mixer outlet with acidified potassium iodide, and the other was reacted for ten minutes. Both were extracted and then tested for residual lignin. The liquid phase from the potassium iodide quenched sample was tested for residual chlorine. The experimental data is shown in Table 41 and Figure 62. Included in both is the equivalent data for the 2500 rpm - 0.98 % chlorine on pulp cases from Table 35 for comparison.

For this set of data, there also was not a significant effect of rotor speed on the kappa number reduction. There was not a significant effect on the residual chlorine in solution either. The maximum amount of total

Table 41. Final Kappa Number From the RPM Single Variable Study Applied Chlorine - 0.98 Temperature - 28 °C.

ROTOR SPEED	CHLORINE RESIDUAL	K_{CEi} AVERAGE	K_{CE10} AVERAGE
500	0.21	9.8	8.6
500	0.15	8.9	8.0
1000	0.11	9.5	8.8
1000	0.30	9.5	8.0
1500	0.23	9.2	7.7
1500	0.21	8.9	8.0
2000	0.24	9.7	8.5
2000	0.25	8.8	8.0
2500*	0.22	9.1	7.2
2500*	0.38	8.4	9.1

* Data from Table 35.

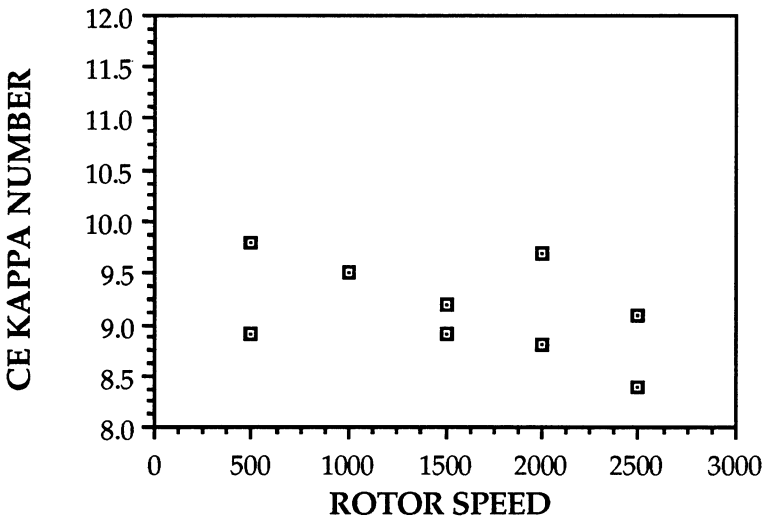

Figure 62. K_{CEi} versus flow-through mixer rotor speed for the flow-through mixer turbulence level study.

chlorine in solution that could be measured for the 0.98% chlorine charge was 0.85 g/l. The average chlorine residual for this experiment was 0.23 g/l with an average KI quenched kappa number of 9.2.

Even though a significant amount of chlorine was left in the gaseous phase, increasing the rotor speed from 500 to 2000 rpm did not significantly affect the amount of chlorine transferred into the liquid phase. This observation suggests that the rotor speed did not affect the mass transfer rate alone, but it possibly has an affect in conjunction with the amount of applied chlorine and/or the reaction temperature.